# TRIP13 IS A CRITICAL REGULATOR OF MITOTIC DURATION AND PROLIFERATION IN MAD2-OVEREXPRESSING CELLS

by

Daniel H. Marks

A Dissertation

Presented to the Faculty of the Louis V. Gerstner, Jr.

Graduate School of Biomedical Sciences,

Memorial Sloan Kettering Cancer Center

in Partial Fulfillment of the Requirements for the Degree of

Doctor of Philosophy

New York, NY

January, 2017

_____ _____

Robert Benezra, PhD
Dissertation Mentor

Date

## DEDICATION

To my parents, David and Claudia Marks

## ABSTRACT

The mitotic checkpoint ensures proper segregation of chromosomes by delaying anaphase until all kinetochores are bound to microtubules. This inhibitory signal is composed of a complex containing Mad2, which inhibits anaphase progression. The complex can be disassembled by p31comet and TRIP13; however, TRIP13 knockdown has been shown to cause only a mild mitotic delay. Overexpression of checkpoint genes, as well as TRIP13, is correlated with chromosomal instability (CIN) in cancer, but the initial effects of Mad2 overexpression are prolonged mitosis and decreased proliferation. Here we show that TRIP13 overexpression significantly reduced, and TRIP13 reduction significantly exacerbated, the mitotic delay associated with Mad2 overexpression but not that induced by microtubule depolymerization. The combination of Mad2 overexpression and TRIP13 loss reduced the ability of checkpoint complexes to disassemble and significantly inhibited the proliferation of cells in culture and tumor xenografts. These results identify an unexpected dependency on TRIP13 in cells overexpressing Mad2.

## BIOGRAPHICAL SKETCH

Daniel Marks was born and raised in New York City, New York. He graduated from Ethical Culture Fieldston High School in 2005. Following graduation, he attended Yale University, majoring in Molecular, Cellular, and Developmental Biology. He conducted research in the laboratory of Dr. John Roboz at Mount Sinai Hospital in New York City, where he worked to identify novel biomarkers for cancer using mass spectrometry. At Yale, Daniel conducted research identifying anti-cancer compounds produced by endophytic bacteria and fungi in the laboratory of Scott Strobel. He graduated from Yale University with honors in 2009. In July 2009, he returned to New York City to begin the PhD program at the Gerstner Sloan Kettering School of Biomedical Sciences. In 2010, he joined the laboratory of Dr. Robert Benezra in the Department of Cancer Biology.

## ACKNOWLEDGMENTS

I would like to thank my thesis advisor, Dr. Robert Benezra, for his mentorship and support during my time in his laboratory. All the members of the Benezra lab, both past and present, have been incredibly helpful and made the lab a fun place to work. I would like to especially thank Rozario Thomas for helping conduct many of the mouse experiments. Dr. Peter Cook, Yvette Chin, Bina Desai, Riddhi Shah, Dr. Paulina Wojnarowicz, Dr. Bishma Amlani, Dr. Lindy Barrett, Courtney Coker, Dr. Pascal Duijf, Dr. Marta Garcia Cao, Dr. Christine Khoo, Dr. Zvika Granot, Dr. Svetlana Pavlovic, Dr. Marko Stankic, and Dr. Juan Manuel Schvartzman all taught me how to be a scientist and helped me tremendously with my project.

Dr. Andrea Ventura and the members of the Ventura lab have also been wonderful scientists to work alongside, and have provided many helpful comments over the years. Dr. Jose Rodriguez-Rodriguez in Prasad Jallepalli's lab and members of Michael Overholtzer's lab also gave me critical technical advice. My advisory committee members, Dr. Prasad Jallepalli and Dr. Maria Jasin, have provided excellent guidance along the winding road of my work over the years. I would also like to thank Dr. Meng-Fu Tsou for agreeing to Chair my defense and Dr. Matthew O'Connell for agreeing to be the external examiner.

I would like to thank all my classmates in the Gerstner Sloan Kettering Graduate School, especially those in the class of 2009, for their friendship and support. I am also

incredibly grateful for all the support from those in the Gerstner Sloan Kettering office over the years.

Lastly, I would like to thank my family and friends outside of GSK. My friends, especially Yuji and Gil, have helped me learn to take a break and have fun outside of lab. And for my incredible family, especially my mother, Claudia, and my brother, Bobby, there is no way for me to express how grateful I am for their love and support and always being there for me.

## Table of Contents

## LIST OF FIGURES

**Introduction**



**Results**

**Discussion**



**Perspectives and Future Directions**

## LIST OF ABBREVIATIONS

AAA+ ATPase: ATPases Associated with Diverse Cellular Activities

APC/C : Anaphase Promoting Complex or Cyclosome

APC15: Anaphase Promoting Complex Subunit 15

ATP: Adenosine Triphosphate

BBC: Bub3, BubR1, Cdc20 Complex

Bub1: Budding Uninhibited By Benzimidazoles 1

Bub3: Budding Uninhibited By Benzimidazoles 3

BubR1: Mad3 in yeast, Budding Uninhibited By Benzimidazoles Related 1

Cdc20: Cyclin Division Cycle 20

CDE: Cell Cycle-Dependent Element

Cdk1: Cyclin-Dependent Kinase 1

CENP-E: Centromere-Associated Protein E

ChIP: Chromatin Immunoprecipitation

CHR: Cell Cycle Genes Homology Region

CIN: Chromosomal Instability

W-CIN: Whole Chromosomal Instability

S-CIN: Structural Chromosomal Instability

CMT2: Caught by Mad2, Renamed p31comet

D-box: Destruction Box

FISH: Fluorescence *In Situ* Hybridization

Hec1: Highly Expressed in Cancer 1

HORMA Domain: Hop1, Rev7, Mad2 Domain

HORMAD1: Horma Domain-Containing Protein 1

HORMAD2: Horma Domain-Containing Protein 2

Knl1: Kinetochore Scaffold 1

Mad1: Mitotic Arrest Deficient 1

Mad2: Mitotic Arrest Deficient 2

C-Mad2: Mad2 (Closed Conformer)

O-Mad2: Mad2 (Open Conformer)

MCC: Mitotic Checkpoint Complex - Mad2, Bub3, BubR1, Cdc20 complex

MEF: Mouse Embryonic Fibroblast

MELT repeats: Met-Glu-Leu-Thr

Mis12: MIS12 Kinetochore Complex Component

Mps1: Monopolar Spindle 1

Myc: Human Homolog of Avian Myelocytomatosis Viral Oncogene

p53: Tumor Protein p53

PCH2: Pachytene Checkpoint 2, Homolog of TRIP13

PP1: Protein Phosphatase 1

PP2A-B56: Protein Phosphatase 2A B Subunit 56

PTTG/Securin: Pituitary Tumor-Transforming Gene

Rb: Retinoblastoma Protein

Rod: Rough Deal Homolog

RPE2: Retinal Pigment Epithelial Cell Line 2

RPE-M: Inducible Mad2-Overexpressing RPE2 Cells

shT13-1: TRIP13 shRNA #1

shT13-2: TRIP13 shRNA #2

siT13-1: TRIP13 siRNA #1

siT13-2: TRIP13 siRNA #2

T13G: TRIP13-GFP Expressing RPE-M Cells

TKO: Rb, p107, p130 Triple Knockout Mouse Embryonic Fibroblasts

TPR: Translocated Promoter Region, Nuclear Basket Protein

TRIP13: Thyroid Hormone Receptor Interacting Protein 13

ZW10: Zeste White 10 Homolog

CHAPTER 1

# INTRODUCTION

## 1.1 Overview of the Mitotic Checkpoint

The mitotic checkpoint ensures proper segregation of chromosomes during mitosis by generating a diffusible, inhibitory signal to the E3 ubiquitin ligase Anaphase Promoting Complex (APC/C). Inhibition of the APC/C blocks anaphase progression until sister chromatids are properly attached to opposite spindle poles by microtubules bound to their kinetochores. Once the checkpoint signal is quenched, the APC/C, bound to its co-activator Cdc20, can ubiquitinate and degrade key mitotic proteins by recognizing D-box (Glotzer et al., 1991) and KEN-box (Pfleger et al., 2001) motifs in its substrates. The two most prominent APC/C substrates that get degraded are cyclin B1 and securin (Dawson et al., 1995; Schwab et al., 2001). Securin degradation activates separase (Hornig et al., 2002), a protease that cleaves the cohesin rings holding together sister chromatids, and allows their separation in anaphase (Haering et al., 2008; Uhlmann et al., 1999). Cyclin B1 degradation inactivates the key mitotic kinase Cdk1 and allows for mitotic exit (Nurse, 1990).

Kinetochores not bound by microtubules generate the checkpoint signal by templating the conversion of Mad2 from its inactive, open, conformer (O-Mad2), to its closed, active, conformer (C-Mad2) (De Antoni et al., 2005). Together with BubR1, Bub3, and Cdc20, C-Mad2 can form mitotic checkpoint complexes (MCC) that can bind to and inhibit APC/C activity (Sudakin et al., 2001). In addition to the formation of MCC

at unoccupied kinetochores, recent work has shown that Mad1-Mad2 complexes present at nuclear pores during interphase also can induce the formation of MCC prior to mitosis, and that this process is critical for basal mitotic timing (Rodriguez-Bravo et al., 2014).

## 1.2 Production of the Checkpoint Signal

Summarized in Fig 1.1

**Kinetochore Production**

In their famous experiment, Rieder et al. demonstrated that a single unoccupied kinetochore can delay anaphase, and kinetochore ablation relieves checkpoint arrest (Rieder et al., 1995). This suggested that kinetochores are a critical structure for producing this wait-anaphase signal. Essential proteins for the checkpoint, such as Mad1, Mad2, Bub1, Bub3, BubR1, Cdc20, and the kinase Mps1 all get recruited to unattached kinetochores in prometaphase (Howell et al., 2004). The sequential steps for recruiting these components of the MCC, and forming the inhibitory complex, have recently been elucidated.

The KMN network (Knl1-Mis12-Ndc80) is an essential dock at kinetochores for both the recruitment of checkpoint proteins, and for the eventual binding of microtubules (Ciferri et al., 2008; Wei et al., 2007). The kinase Aurora B phosphorylates Ndc80, which facilitates the recruitment of Mps1 (Vigneron et al., 2004; Zhu et al., 2013). Mps1 makes critical phosphorylations on MELT repeats in Knl1, which recruits Bub1:Bub3 complexes to kinetochores (London et al., 2012; Shepperd et al., 2012; Yamagishi et al., 2012). Bub3 can directly bind these phosphorylated repeats (Primorac et al., 2013), but

Bub1 interaction is required for this recruitment (Overlack et al., 2015). The Bub1:Bub3 complex then forms a pseudo-symmetric interaction with a BubR1:Bub3 complex to allow this component of the mitotic checkpoint complex to be recruited to kinetochores (Overlack et al., 2015). Bub3 also aids in bringing Cdc20 to the kinetochore by stimulating its binding to BubR1 (Han et al., 2014).

Bub1 may also play a critical role in recruiting the other critical piece of the mitotic checkpoint complex, Mad2, to kinetochores. Mad2 is recruited to the kinetochore in complex with Mad1, which is necessary for its localization (Luo et al., 2002). Bub1 interacts with Mad1, and is necessary for the initial recruitment of Mad1:Mad2 complexes to unattached kinetochores (Moyle et al., 2014). Mps1 may also play a role in stimulating this interaction by directly phosphorylating Bub1, which is required for its binding to Mad1 (London and Biggins, 2014). The Rod-Zw10-Zwilch complex (RZZ) also recruits the Mad arm of the pathway to kinetochores (Kops et al., 2005). This recruitment of Mad1:Mad2 by the RZZ complex may be Bub1-dependent to misaligned kinetochores (Zhang et al., 2015b), or Bub1-independent to unattached kinetochores (Silió et al., 2015).

One of the critical roles of kinetochores for producing the checkpoint signal is the catalytic activation of Mad2. Mad2 exists in two conformations, inactive O-Mad2, and active C-Mad2 that can bind Cdc20 (Luo et al., 2004). Mad2 can spontaneously convert from O-Mad2 to C-Mad2, although this process is slow, with a reaction lifetime of >9 hours, which is too slow to be responsive to kinetochore attachment status in mitosis

(Luo et al., 2004). Mad2 exists in its open conformation in the cytosol, but is found in its closed conformation when binding to either Mad1, at kinetochores, or its target Cdc20 (Luo et al., 2002). Further, C-Mad2 is constitutively bound to Mad1 at unoccupied kinetochores where it interacts with cytosolic O-Mad2, with this interaction necessary for production of the checkpoint signal (De Antoni et al., 2005). This data suggests a Mad2 template model, where Mad2 can catalyze its own activation through a prion-like process converting O-Mad2 to C-Mad2 at kinetochores (Mapelli et al., 2007).

In addition to being essential for starting the cascade of checkpoint protein recruitment to kinetochores, Aurora B also plays a critical role in correcting improper kinetochore microtubule attachments, such as merotelic (one kinetochore attached to both poles) or syntelic (both kinetochores attached to same pole) attachments (Ditchfield et al., 2003; Hauf et al., 2003). Aurora B can induce disassembly of kinetochore-microtubule fibers and activate the microtubule depolymerase MCAK at sites of improper attachment (Knowlton et al., 2006; Lampson et al., 2004). Aurora B can also phosphorylate Ndc80 of the KMN complex, which decreases Ndc80's ability to bind microtubules *in vitro*, and blocking this phosphorylation by mutating Ndc80 causes defects in error correction (Cheeseman et al., 2006; DeLuca et al., 2006). An intriguing hypothesis for how Aurora B senses improper attachments is that proper biorientation creates tension on kinetochores that spatially inactivates Aurora B by pulling its substrates away from its location at the inner centromere (Liu et al., 2009).

**Figure 1.1. Checkpoint Signaling at the Kinetochore.**

**A**

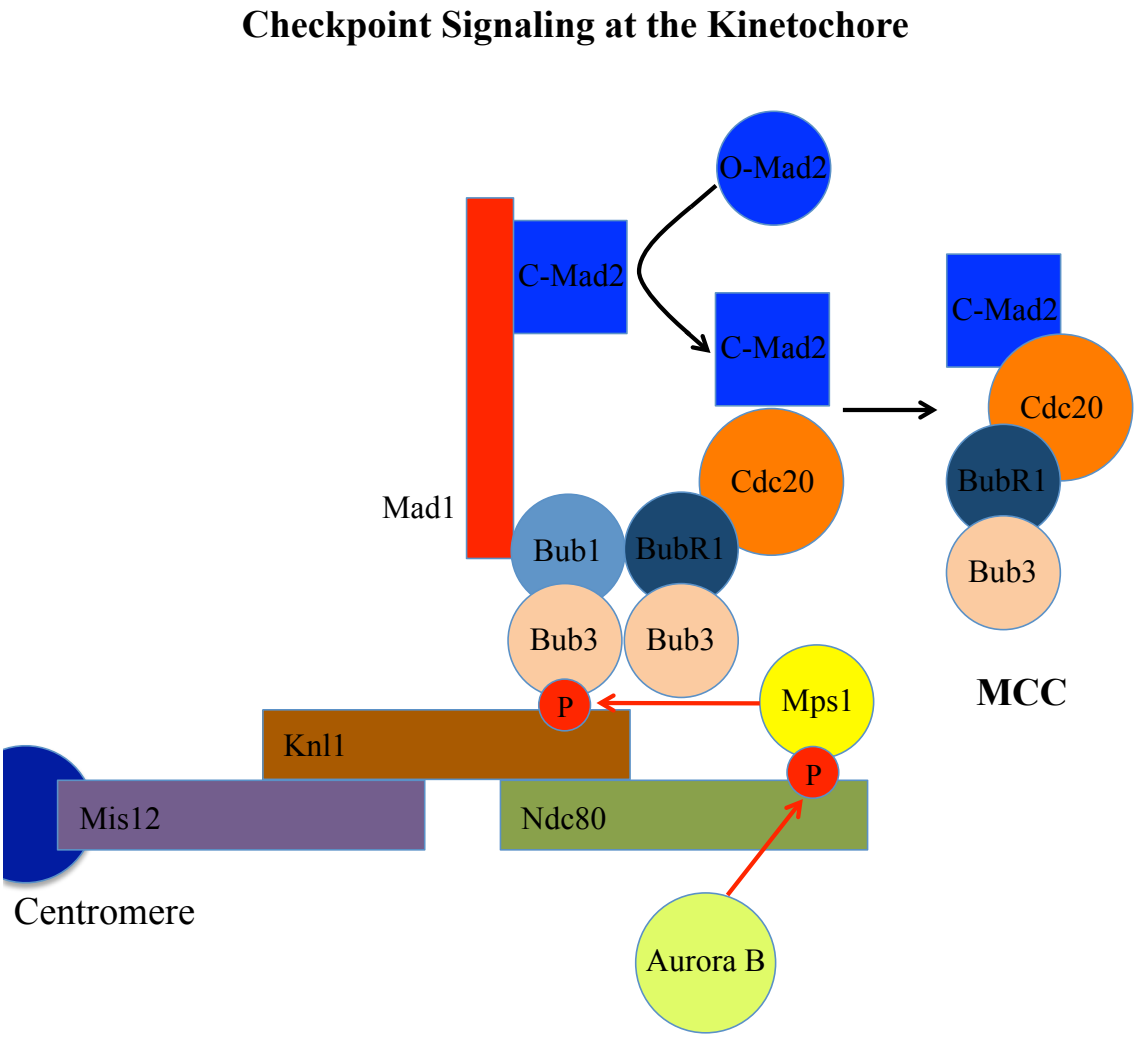


**Figure 1.1. Checkpoint signaling at the kinetochore.**
(**A**) Schematic of recruitment of mitotic checkpoint components to kinetochore with catalytic conversion of O-Mad2 to C-Mad2 and production of the mitotic checkpoint complex (MCC)

**Interphase Production**

In addition to its production in mitosis, it has been noted that MCC is also present at lower levels in interphase (Sudakin et al., 2001). Importantly, in addition to its role in sensing unoccupied kinetochores, basal mitotic timing is specified by a kinetochore-independent role of MCC (Meraldi et al., 2004). Additionally, components of the MCC, such as BubR1, have been shown to be necessary for APC/C-Cdc20 inhibition in interphase to allow accumulation of cyclin B in G2 (Malureanu et al., 2009). The kinase Mps1 has also been shown to be important for both the recruitment of MCC components to kinetochores in mitosis, as well as for the formation of interphase MCC (Maciejowski et al., 2010).

Surprisingly, Mad1 and Mad2 localize to nuclear pores in interphase (Campbell et al., 2001), but the functional relevance of this interaction had been unclear. Recently, depletion of the nuclear pore component Tpr was shown to decrease the strength of the checkpoint (Schweizer et al., 2013). More definitive proof for the importance of nuclear pores came when they were demonstrated to be necessary for production of interphase MCC, with this production critical for control of basal mitotic timing (Rodriguez-Bravo et al., 2014). These studies demonstrate that MCC has dual roles in maintaining proper mitotic timing, with interphase production at nuclear pores essential ensuring a minimum mitotic duration, and mitotic production at kinetochores for responding to attachment status.

## 1.3 The Mitotic Checkpoint Complex

Many of the major components of the mitotic checkpoint, Mad1, Mad2, BubR1, Bub1, and Bub3, were originally discovered in genetic screens in *S. cerevisiae* for mutants that fail to arrest in mitosis when microtubules are disrupted (Hoyt et al., 1991; Li and Murray, 1991). Of these, Mad2, BubR1, and Bub3 join Cdc20 to form the mitotic checkpoint complex (Fraschini et al., 2001; Sudakin et al., 2001). Cdc20 serves dual roles as both a co-activator of APC/C, necessary for its activity and substrate specificity, and also as a crucial component of the inhibitory mitotic checkpoint complex. This apparent paradox was resolved when it was demonstrated that the MCC can contain 2 copies of Cdc20; one copy part of the core inhibitory complex, and one copy bound to APC/C (Izawa and Pines, 2014). This affirmed that the MCC functions not just by sequestering Cdc20 from APC/C but also acts as a direct inhibitor of its activity. Structural studies of the MCC bound to APC/C-Cdc20 confirmed this finding, and demonstrated how the MCC inhibits APC/C activity as a pseudo-substrate (Alfieri et al., 2016; Yamaguchi et al., 2016).

BubR1 contains KEN- and D-boxes implicated in binding this second copy of Cdc20 (Izawa and Pines, 2014). KEN- and D-boxes are the motifs that Cdc20-APC/C recognizes in its substrates to degrade, leading to the hypothesis that BubR1 functions as a pseudo-substrate inhibitor. Evidence for this hypothesis was found in *S. cerevisiae*, where it was demonstrated that BubR1 directly competes with substrates for binding to Cdc20-APC/C (Burton and Solomon, 2007). The structure of the MCC bound to APC/C demonstrated BubR1's ability to simultaneously bind the Cdc20 copy in the MCC, as

well as directly to the substrate-binding pocket of the Cdc20 copy bound as a co-activator of APC/C (Alfieri et al., 2016; Yamaguchi et al., 2016).

The role of Mad2 in the complex is somewhat more nebulous. Mad2 is clearly required for checkpoint activity (Li and Benezra, 1996), and purified Mad2 added to *Xenopus* egg extracts can block APC/C-mediated cyclin B degradation (Li et al., 1997). Mad2 can directly bind and inhibit Cdc20-APC/C, but is a much better inhibitor *in vitro* when combined with BubR1 (Fang, 2002). Mad2 directly promotes BubR1 binding to Cdc20 to form the full MCC complex (Burton and Solomon, 2007; Davenport et al., 2006). However, Mad2 has been shown to be sub-stoichiometric in BubR1-Cdc20 complexes (Nilsson et al., 2008). One hypothesis is that C-Mad2 binding to Cdc20 is just a catalyst for BubR1 incorporation, but is dispensable for direct APC/C inhibition. Indeed, once bound to Cdc20, BubR1 can act as a strong suppressor of APC/C-Cdc20 activity (Han et al., 2013). Additional evidence to prove this model is necessary, as Mad2-containing MCC complexes have been shown to be more stable and efficient inhibitors of APC/C than those lacking Mad2 (Fang, 2002; Tipton et al., 2011; Westhorpe et al., 2011)

More likely, the BBC (BubR1, Bub3, Cdc20) complex is generated from APC/C-bound MCC after it has Mad2, and potentially one copy of Cdc20, ejected from the complex during turnover of APC/C-bound MCC. APC/C-bound MCC has its turnover stimulated by p31comet and APC15, which removes Mad2 and bound Cdc20 from ACP/C (Mansfeld et al., 2011). This disassembly is induced by APC/C-mediated auto-

ubiquitination of Cdc20 in the MCC (Uzunova et al., 2012; Varetti et al., 2011). p31comet has been shown to reduce the levels of Mad2 in BubR1-Cdc20 complexes (Westhorpe et al., 2011) and in combination with another protein, TRIP13, can eject Mad2 from MCC *in vitro,* with the resulting BBC complex only weakly inhibiting APC/C activity (Kaisari et al., 2016). Taken together, Mad2-containing MCC is still probably the primary inhibitor of APC/C-Cdc20 activity.

## 1.4 Inactivating the Checkpoint Signal

Once the checkpoint is satisfied, with all kinetochores properly attached to microtubules, the inhibitory signal needs to be quenched. Essentially all of the processes used to produce the checkpoint signal need to be reversed; Aurora B and Mps1 targets at the kinetochore need to be dephosphorylated, checkpoint proteins need to be removed from kinetochores, MCC formation needs to be halted, and complexes already produced need to be disassembled.

### Reversing kinetochore phosphorylations (Fig 1.2A)

There is a negative feedback loop at actively signaling kinetochores that is required to dephosphorylate kinetochore proteins. BubR1 recruitment to kinetochores is not only important for producing checkpoint complexes, but it also recruits the phosphatase PP2A-B56 to kinetochores, where it antagonizes Aurora B, Plk1, and Mps1 phosphorylations (Espert et al., 2014; Foley et al., 2011; Nijenhuis et al., 2014; Suijkerbuijk et al., 2012). A second phosphatase, PP1, needs to be recruited to fully reverse kinetochore phosphorylations. PP1 is recruited by PP2A-B56 activity, where it

displaces PP2A and completes silencing of checkpoint signaling at the kinetochore, by reversing MELT-repeat phosphorylation and stimulating the removal of outer-kinetochore proteins (Emanuele et al., 2008; London et al., 2012; Nijenhuis et al., 2014; Pinsky et al., 2009; Shepperd et al., 2012; Vanoosthuyse and Hardwick, 2009).

In addition to removing their phosphorylations, Aurora B and Mps1 have to inactivated. As mentioned previously, proper biorientation appears to inactivate Aurora B by pulling its substrates away from its location at the inner centromere (Liu et al., 2009). Mps1 may be directly removed from kinetochores by competing with microtubules for binding Ndc80 of the KMN network (Hiruma et al., 2015; Ji et al., 2015). An alternative hypothesis is that microtubule binding to Ndc80 pulls Mps1 away from its key substrate sites on Knl1 (Aravamudhan et al., 2015).

**Halting checkpoint complex formation (Fig 1.2B,C)**

Mad1:Mad2 complexes also need to be removed from kinetochores to silence the checkpoint. This process is mediated by the RZZ complex, which was initially critical for recruiting Mad1:Mad2 to kinetochores, in conjunction with the protein Spindly (Barisic et al., 2010; Gassmann et al., 2010; Griffis et al., 2007; Howell et al., 2001; Wojcik et al., 2001). Upon microtubule attachment, this complex binds to the microtubule motor protein dynein, which physically removes the checkpoint proteins from the kinetochore.

Another protein critical for blocking further complex formation once the checkpoint is satisfied is p31comet. p31comet, originally CMT2, can directly bind Mad2,

and inhibit checkpoint signaling (Habu et al., 2002; Xia et al., 2004). Mechanistically, p31comet mimics the structure of Mad2, which allows it to bind C-Mad2 at the Mad2-dimerization interface at kinetochores to prevent further conversion of O-Mad2 to C-Mad2 (Fava et al., 2011; Yang et al., 2007).

**Disassembling checkpoint complexes (Fig 1.3A)**

Even with checkpoint complex production halted, MCC already produced needs to be disassembled. As previously mentioned, there is an APC15 and p31comet mediated pathway for disassembling MCC bound to APC/C (Mansfeld et al., 2011). APC15 has been shown to be critical for conformational flexibility of MCC-bound APC/C. This conformational change allows the E2 enzyme, UbcH10, access to Cdc20 in MCC induce its ubiquitination and subsequent release (Alfieri et al., 2016; Yamaguchi et al., 2016). In addition to a role in disassembling MCC bound to APC/C, p31comet can stimulate the disassembly of free MCC in mitotic extracts from HeLa cells (Teichner et al., 2011). This reaction requires ATP, but the protein utilizing ATP was unknown until recently, when it was identified as the AAA+ ATPase TRIP13, which I will discuss in more detail below.

**Figure 1.2. Inactivating Kinetochore Signaling.**

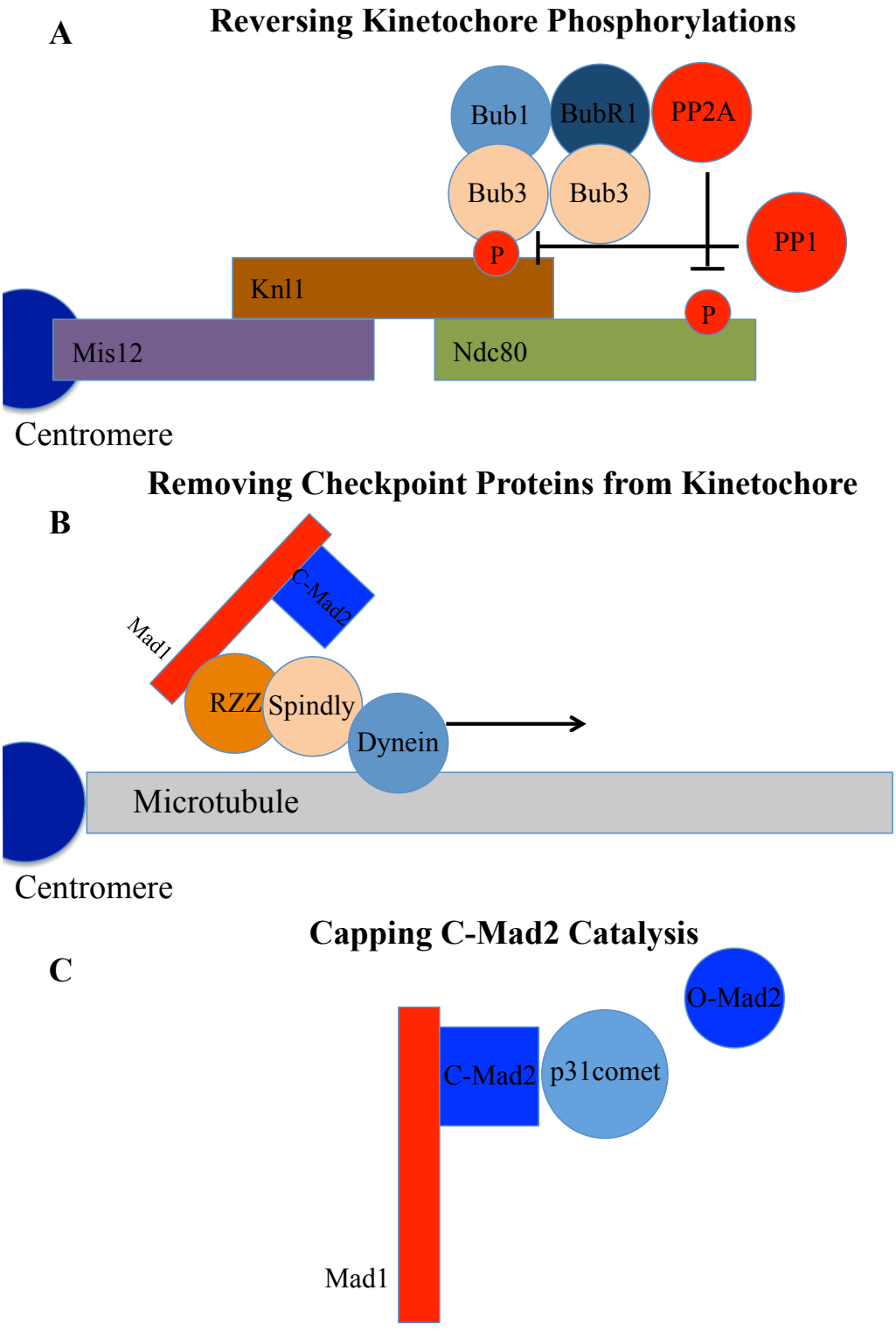

**Figure 1.2. Inactivating kinetochore signaling.**
(**A**) Schematic of recruitment and reversal of kinetochore phosphorylations by PP2A-B56 and PP1. (**B**) Removal of Mad1:Mad2 from kinetochores by RZZ/ Spindly-mediated attachment to microtubule motor Dynein and movement away from kinetochore. (**C**) Capping of C-Mad2 by p31comet prevents further catalysis of O-Mad2 to C-Mad2.

## 1.5 Introduction to TRIP13 (Fig. 1.3B)

TRIP13 (thyroid hormone receptor interacting protein 13) is a member of the AAA+ ATPase family, a class of enzymes that remodel the conformation of their substrates (Hanson and Whiteheart, 2005). TRIP13 was initially identified as a binding partner for rat thyroid hormone receptor beta, but no functional relevance of this interaction has been identified (Lee et al., 1995). The first evidence of the TRIP13's function came from the yeast homolog, PCH2, which is required for the pachytene checkpoint in meiosis; a checkpoint that prevents homologous chromosome segregation if recombination or synapsis are defective (San-Segundo and Roeder, 1999). The mammalian homolog was identified as TRIP13, and mice with homozygous TRIP13 hypomorphic mutations also have defects in meiotic recombination and synapsis (Li et al., 2007; Roig et al., 2010). Interestingly, TRIP13's role in meiosis involves regulating the removal of two HORMA domain-containing proteins, HORMAD1 and HORMAD2, from synapsed chromosomes during meiosis (Wojtasz et al., 2009). The HORMA domain is the major structural element in both Mad2 and p31comet (Rosenberg and Corbett, 2015). Further, TRIP13 can bind to the checkpoint silencing protein, p31comet, in yeast two-hybrid protein-protein interaction screens (Rual et al., 2005; Stelzl et al., 2005). This led to hypothesis that TRIP13 might cooperate with p31comet to help quench the checkpoint and disassemble checkpoint complexes.

**Figure 1.3. Disassembling Checkpoint Complexes.**

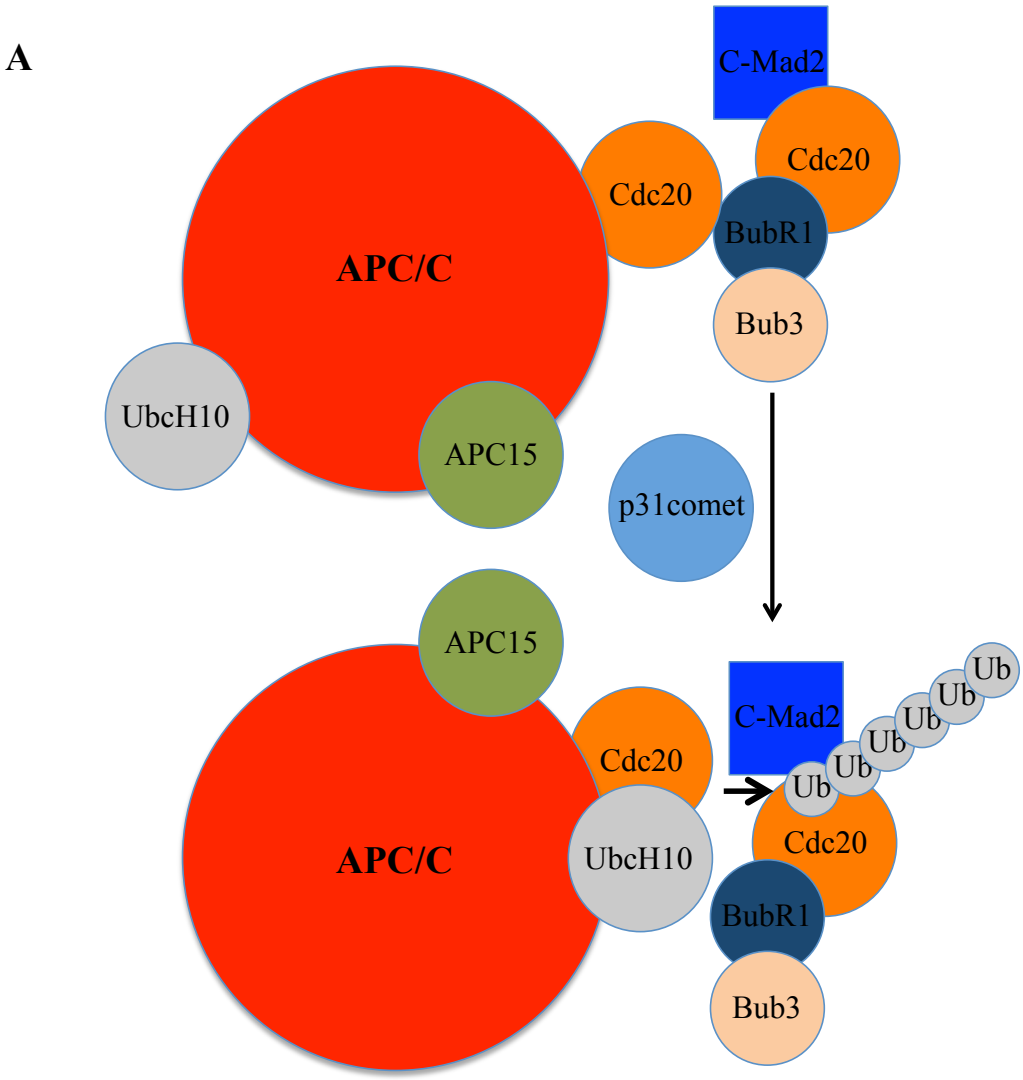

## Disassembling Checkpoint Complexes Cont'd

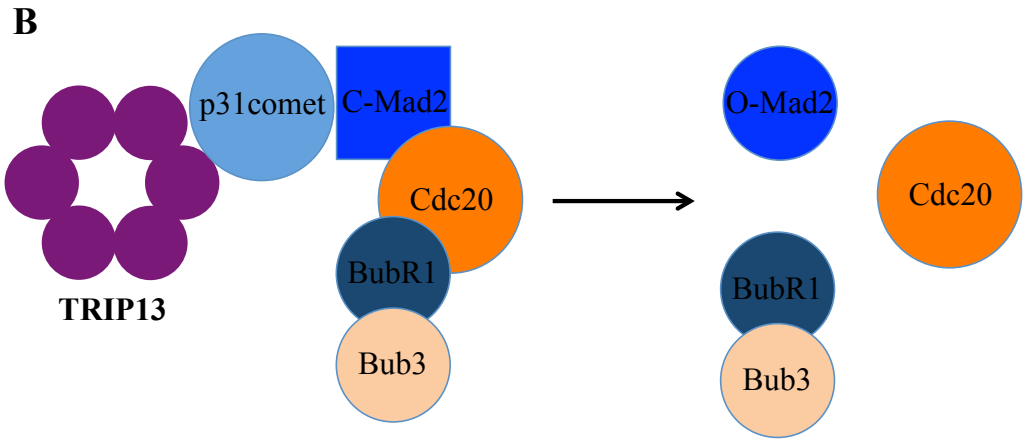


**Figure 1.3. Disassembling checkpoint complexes.**
(**A**) Ubiquitination and disassembly of APC/C-bound mitotic checkpoint complex. BubR1 in MCC binds to APC/C-Cdc20 as a pseudosubstrate. MCC is displaced following auto-ubiquitination by APC/C of Cdc20 on MCC. Ubiquitination activity requires a conformational change in APC/C that gives allows UbcH10 access to MCC. This conformational change require APC15 and is stimulated by p31comet. (**B**) p31comet acts as an adaptor to stimulate TRIP13 binding to MCC, where it catalyzes the conversion of C-Mad2 to O-Mad2 and release from Cdc20.

Evidence for a role for TRIP13 in inactivating the checkpoint has been accumulating after a series of recent experiments. TRIP13 expressed in human cells can interact with p31comet, and localizes to kinetochores in prometaphase (Tipton et al., 2012). Further, TRIP13 knockdown causes a delay in anaphase progression, and depletion of TRIP13 from mitotic cellular extracts slows the disassembly of mitotic checkpoint complexes (Wang et al., 2014). TRIP13's ability to disassemble Mad2-Cdc20 complexes was confirmed by adding only TRIP13, p31comet, and ATP to recombinant Mad2-Cdc20 complexes (Eytan et al., 2014). Mechanistically, p31comet has been shown to act as an adaptor that can simultaneously bind C-Mad2 and TRIP13 (Ye et al., 2015). This allows the recruitment of TRIP13, where its ATPase activity induces the conversion of C-Mad2 back to inactive O-Mad2.

The picture appears more complicated, as p31comet and TRIP13 knockout cells have unexpected phenotypes (Ma and Poon, 2016). p31comet and TRIP13 single and double knockouts in HeLa and HCT116 cells are all viable. This is unexpected if either protein is essential for mitotic exit, at least in an unperturbed mitosis. The basal mitotic timing in knockout cells was not substantially prolonged in either knockout. p31comet knockout cells have a slightly prolonged basal mitotic duration, and have a delayed mitotic exit after release from a mitotic arrest induced by the microtubule-depolymerizing agent, nocodazole. An even greater surprise is that TRIP13 knockout cells, instead of having a prolonged mitosis and an inability to quench the checkpoint, have a relatively unchanged, if not slightly accelerated, basal mitotic duration and an *inability* to arrest in response to nocodazole. p31comet knockout causes an increase in C-Mad2 relative to O-

Mad2, whereas TRIP13 knockout cells contain almost entirely C-Mad2. The authors speculate that the loss of O-Mad2 might underlie the inability to produce checkpoint signal from unoccupied kinetochores in response to nocodazole, even though Mad2 can still localize to kinetochores. Mutation of TRIP13 homolog PCH-2 in *C. elegans* also causes an inability to activate the checkpoint, although in this species there Mad2 recruitment to kinetochores is prevented in the absence of PCH-2, but this is rescued by p31comet mutation (Nelson et al., 2015). Taken together, these results suggest that TRIP13 plays roles both in activating and inactivating checkpoint signaling, but is not essential for mitotic exit in either an unperturbed mitosis or a kinetochore-dependent arrest.

## 1.6 Mitotic Checkpoint Dysfunction and Chromosomal Instability in Cancer (Fig. 1.4)

Genomic instability is a hallmark of cancer (Hanahan and Weinberg, 2011), with gains and losses of chromosomes (aneuploidy) present in 68% of solid tumors (Duijf et al., 2013). Additionally, chromosomal instability is correlated with poor prognosis (Carter et al., 2006). Despite its close association with cancer, the causes and consequences of aneuploidy are still not well understood. Other cell cycle checkpoints are frequently lost in cancer, and it was speculated that a non-functional mitotic checkpoint could lead to premature sister chromatid separation and mis-segregation of chromosomes, leading to aneuploidy. However, mutations in checkpoint genes are extremely rare in cancer (Hernando et al., 2001), and cancer cells typically have a robust checkpoint response when challenged with drugs that activate the checkpoint (Tighe et

al., 2001). Further, complete loss of checkpoint genes, such as Mad2, is embryonic and cell lethal, with loss causing premature cyclin B degradation, and massive chromosome mis-segregation leading to cell death (Dobles et al., 2000; Michel et al., 2004). The only known cancer predisposition syndrome due to checkpoint gene mutation is mosaic variegated aneuploidy, a rare, recessive, disorder that has been linked to mutations in BubR1 (Hanks et al., 2004).

There is significantly more evidence that, instead of having a weakened checkpoint, checkpoint genes are overexpressed in cancer, and their overexpression is correlated with chromosomal instability in human tumors (Carter et al., 2006). In fact, the human homolog of securin, one of the targets of the APC/C that is stabilized by checkpoint signaling, was initially named pituitary tumor-transforming gene (PTTG), and found to be overexpressed in cancer, and capable of transforming cells *in vitro* (Pei and Melmed, 1997; Zou et al., 1999). Mechanistically, the loss of major tumor suppressor pathways, such as the Rb or p53 pathways, leads to transcriptional upregulation of checkpoint genes through E2F and CHR/CDE sites in their promoters (Hernando et al., 2004; Schvartzman et al., 2011). Importantly, overexpression of Mad2 is required for the high levels of chromosomal instability in cells that have lost these tumor suppressors (Schvartzman et al., 2011). Additional pathways commonly dysregulated in cancer may also induce overexpression of checkpoint genes, such as increased Myc pathway signaling (Menssen et al., 2007).

**Figure 1.4. Dysregulation of Mitotic Checkpoint Genes in Cancer.**

**A**

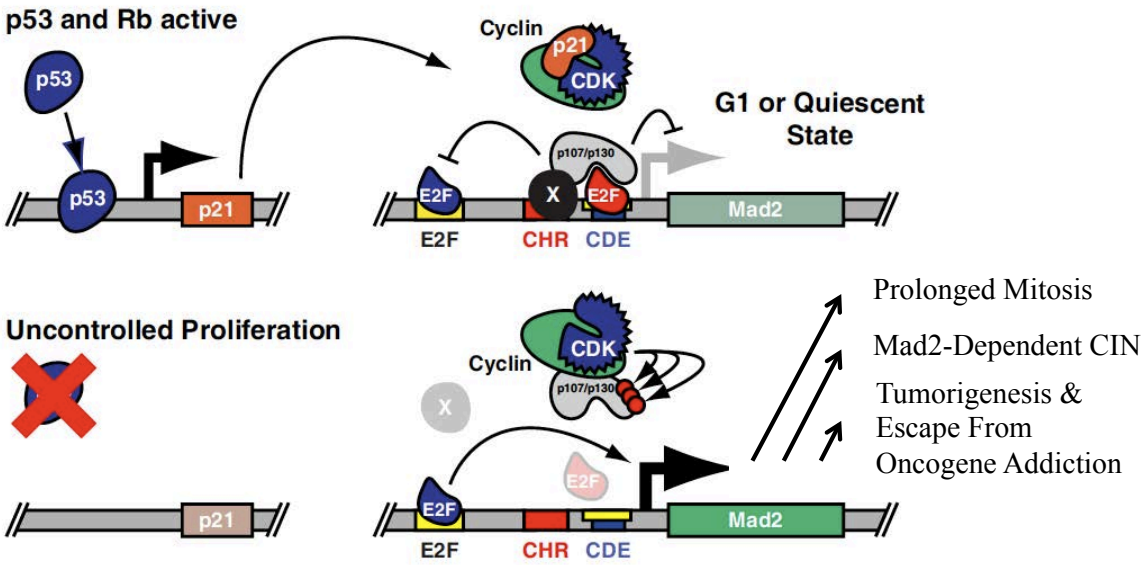


**Figure 1.4. Dysregulation of mitotic checkpoint genes in cancer.**
(**A**) Rb and p53 restrain expression of Mad2, and other checkpoint genes, through E2F and CHR/CDE sites in their promoters. In the absence of these pathways, checkpoint genes become overexpressed, which leads to prolonged mitosis and chromosomal instability (CIN) dependent on high checkpoint gene levels. Adapted from Schvartzman et al., 2010.

In addition to checkpoint genes, the putative checkpoint quenching protein, TRIP13, is also overexpressed in human tumors and similarly correlated with chromosomal instability (Banerjee et al., 2014; Carter et al., 2006). Overexpression of TRIP13 in head and neck cancer cell lines was shown to be oncogenic, and knockdown suppressed growth of cells expressing high levels of TRIP13. At the time, little was known about TRIP13's role in mitosis, and the authors found TRIP13 could interact with DNA repair proteins, and attributed its oncogenic effects to a role in DNA repair.

## 1.7 Modeling Mitotic Checkpoint Dysfunction and Aneuploidy

To model the consequences of aneuploidy *in vivo*, mice have been engineered with either increased or decreased expression of checkpoint genes to induce aneuploidy. Heterozygosity of checkpoint genes, such as Mad1 or Mad2, causes increased aneuploidy and tumorigenesis at long latencies and low penetrance (Iwanaga et al., 2007; Michel et al., 2001). However, as checkpoint gene overexpression is more frequently observed in cancer, overexpression models may be more physiologically relevant.

Overexpression of Hec1 or Mad2 can induce chromosomal instability and tumorigenesis with increased penetrance and shorter latency than models of weakened checkpoint activity (Diaz-Rodríguez et al., 2008; Sotillo et al., 2007). Mechanistically, Mad2 overexpression causes a prolonged mitosis and untimely mitotic exit, leading to aneuploidy (Sotillo et al., 2007). Additionally, Mad2 overexpression can cause hyperstabilization of kinetochore-microtubule attachments, leading to chromosome mis-segregation (Kabeche and Compton, 2012). Importantly, Mad2-overexpressing cells

show not only evidence of whole chromosome instability, but also structural chromosome instability, such as chromosome breaks, deletions and amplifications, and together this may explain the increased tumorigenic phenotype. Additionally, transient Mad2 overexpression can induce sufficient genomic instability in KRAS or HER2-driven models that tumors become no longer addicted to the initiating oncogene (Rowald et al., 2016; Sotillo et al., 2010). These results underscore the potential negative implication of checkpoint gene overexpression in the ability to effectively treat cancer.

Mouse models that generate increased aneuploidy are not pro-tumorigenic in all contexts. For example, cells from CENP-E +/- mice have increased aneuploidy *in vitro* and mice have increased tumorigenesis in a wild-type background. However, CENP-E heterozygosity is tumor suppressive in the tumor-prone background of p19 null mice, extending survival in these animals (Weaver et al., 2007). The authors speculate that too much aneuploidy, which they believe occurs when CENP-E +/- is combined with p19 -/-, is detrimental to tumor growth. Mad2 overexpression in breast cancer mouse models also delays initial tumorigenesis, but increases intratumoral heterogeneity (Rowald et al., 2016).

A caveat of these mouse models that generate aneuploidy through modulating mitotic checkpoint genes is the potential additional roles checkpoint genes may play in other aspects of cell biology, and could contribute to their tumorigenic effect. Thus, groups have tried generating aneuploidy more directly to investigate its effects on cell proliferation and tumorigenesis. Specific trisomies in mouse embryonic fibroblasts

(MEFs) have been generated, with the presence of the extra chromosome found to be growth inhibiting *in vitro*, however, no data has been published on their tumor potential (Williams et al., 2008). However, inducing tetraploidy, a doubling of the normal chromosome numbers, by triggering cytokinesis failure or telomere dysfunction, is tumorigenic (Davoli and de Lange, 2012; Fujiwara et al., 2005). Aneuploidy can theoretically promote tumorigenesis through genetic loss of tumor suppressors or gain of oncogenes. Additionally, recent evidence has shown that chromosome missegregation can lead to potentially tumorigenic structural chromosome instability (S-CIN) through breakage of lagging chromosomes during mitotic exit or chromothripsis of missegregated chromosomes in micronuclei (Janssen et al., 2011; Zhang et al., 2015a). Previous work in the Benezra laboratory has also shown that chromosomal instability can induce escape from oncogene addiction by allowing re-activation of pro-growth signaling pathways (Sotillo et al., 2010).

## 1.8 Thesis Objectives

The aim of this dissertation is to investigate the role of TRIP13 in cells overexpressing Mad2. The role, and importance, of TRIP13 in silencing the checkpoint is still incompletely understood. TRIP13 depletion by siRNA causes only a mildly prolonged mitosis (Wang et al., 2014), and complete knockout of TRIP13 is tolerated, with knockout cells having a relatively normal unperturbed mitosis (Ma and Poon, 2016), inconsistent with a requirement for TRIP13 to quench the checkpoint.

While tumorigenic when expressed systemically in mice, the initial cellular effects of Mad2 overexpression in mouse embryonic fibroblasts are prolonged mitosis

and decreased proliferation (Sotillo et al., 2007). Prolonged mitosis can lead to p53 dependent G1 arrest through stabilization of p53 by 53BP1-USP28 or mitotic cell death, termed mitotic catastrophe (Fong et al., 2016; Gascoigne and Taylor, 2008; Lambrus et al., 2016; Vogel et al., 2004). Thus, it is surprising that Mad2 overexpression is so well tolerated in cancer. Interestingly, TRIP13 is also overexpressed in cancer (Banerjee et al., 2014) and part of the same gene signature as Mad2, for genes correlated with chromosomal instability (Carter et al., 2006). Given that overexpression of TRIP13 may oppose the effects of Mad2 overexpression, I sought to test the hypothesis that TRIP13 may be of increased importance for mitotic exit in Mad2 overexpressing cells.

# CHAPTER 2

# RESULTS

## TRIP13 is overexpressed in Mad2 overexpressing tumors

TRIP13 is overexpressed in a wide range of human tumor types (Fig 2.1A). I investigated the correlation between the expression of TRIP13 and Mad2 in human tumors using the cBioPortal database (cBioPortal.org (Cerami et al., 2012; Gao et al., 2013)). Across numerous datasets from different tumor types, I found that levels of TRIP13 correlated closely with those of Mad2 (Fig. 2.1B). Many mitotic checkpoint genes, including Mad2, have a core E2F/CDE transcription factor binding site in their promoters, and this motif is also found near the transcription start site for TRIP13 (Fig. 2.2A). ChIP-seq data from the Encode database (https://genome.ucsc.edu/ENCODE/), showed that for three different E2F proteins (E2F1/4/6), each could bind near the start site of TRIP13 in HeLa cells (Fig. 2.2B). While E2F1 is considered an activating transcription factor, and E2F4/6 inhibitory, the ability of all three to bind may be due to the HeLa cells being asynchronous, with different E2Fs binding in different phases of the cell cycle. MEFs deficient for the 3 Rb family members (Rb, p107, p130) have elevated levels of Mad2, and I found these cells also have elevated levels of TRIP13 (Fig. 2.2C). TRIP13's expression also is cell cycle regulated, increasing as cells enter into mitosis (Fig. 2.3A) Together, this suggests that expression of TRIP13 is regulated similarly to Mad2 and other checkpoint genes. This is consistent with a recent finding using single-cell transcriptome analysis, identifying correlated Mad2 and TRIP13 expression in mouse 3T3 cells (Macosko et al., 2015). Thus, while TRIP13 is broadly overexpressed in cancer, it is most commonly overexpressed in the context of Mad2 overexpression.

**Figure 2.1. TRIP13 is overexpressed in cancer and correlated with Mad2 expression.**

**A**

| Analysis Type by Cancer | Cancer vs. Normal | |
|---|---|---|
| Bladder Cancer | 3 | |
| Brain and CNS Cancer | | 1 |
| Breast Cancer | 6 | 1 |
| Cervical Cancer | 2 | |
| Colorectal Cancer | 16 | |
| Esophageal Cancer | 2 | |
| Gastric Cancer | 5 | |
| Head and Neck Cancer | 6 | |
| Kidney Cancer | | |
| Leukemia | 1 | 3 |
| Liver Cancer | 4 | |
| Lung Cancer | 9 | |
| Lymphoma | 3 | |
| Melanoma | 1 | |
| Myeloma | | |
| Other Cancer | 2 | 2 |
| Ovarian Cancer | 2 | |
| Pancreatic Cancer | 1 | |
| Prostate Cancer | 1 | |
| Sarcoma | 7 | |
| Significant Unique Analyses | 70 | 7 |
| Total Unique Analyses | 448 | |

**B**

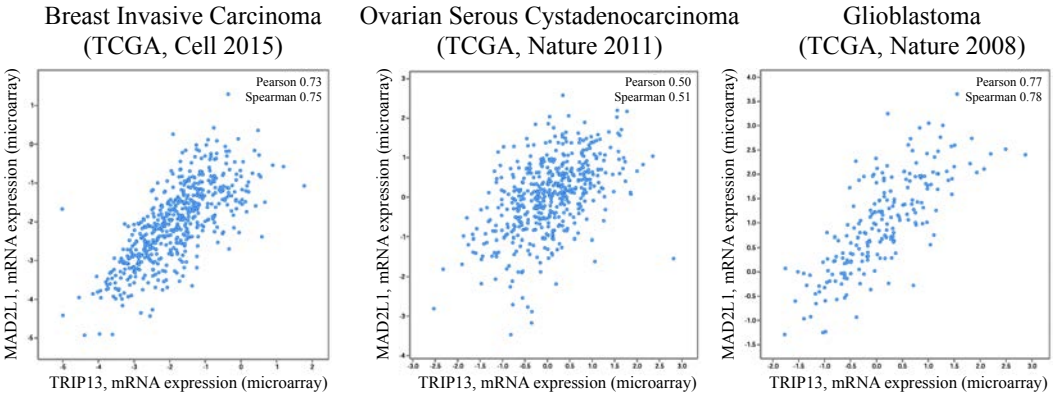


**Figure 2.1. TRIP13 is overexpressed in cancer and correlated with Mad2 expression.**

(**A**) TRIP13 expression in cancer versus normal across multiple tumor types, from oncomine.org. (**B**) Mad2 versus TRIP13 microarray expression data in three representative datasets from cBioPortal.org.

**Figure 2.2. TRIP13 is a potential E2F target.**

**A**

CDE/E2F core

MAD2 +43 GCTT**GGCGG**GGAAG +56

BUBR1 +44 ACTT**GGCGG**CTAGG +57

TRIP13 -200 CCAT**GGCGG**CGCC**GGCGG**CGGGCC -177
-177 CCGA**GGCGG**GGGCT -164
-49 GCGA**GGCGG**GGCCG -36
+41 CTAG**GGCGG**GGCCC +54
+72 CTGT**GGCGG**CGACG +85

**B**

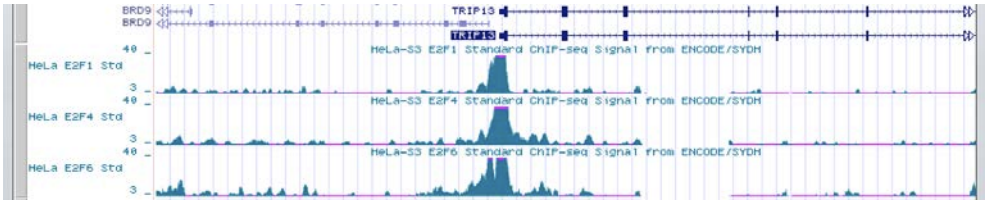


**C**

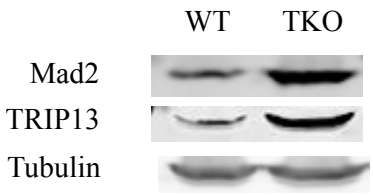


**Figure 2.2. TRIP13 is a potential E2F target.**
(**A**) GGCGG CDE/E2F core sites present between -200 and +100 from the transcription start sites of MAD2, BUBR1, and TRIP13. (**B**) ChIP-Seq data from Encode database (https://genome.ucsc.edu/ENCODE/) for E2F1, E2F4, E2F6 binding near TRIP13 transcription start site in HeLa cells. (**C**) Mad2 and TRIP13 expression are both elevated by Western blot in Wild Type (WT) and Rb-family (Rb, p107, p130) deficient MEFs.

**Figure 2.3. TRIP13 is cell cycle regulated.**

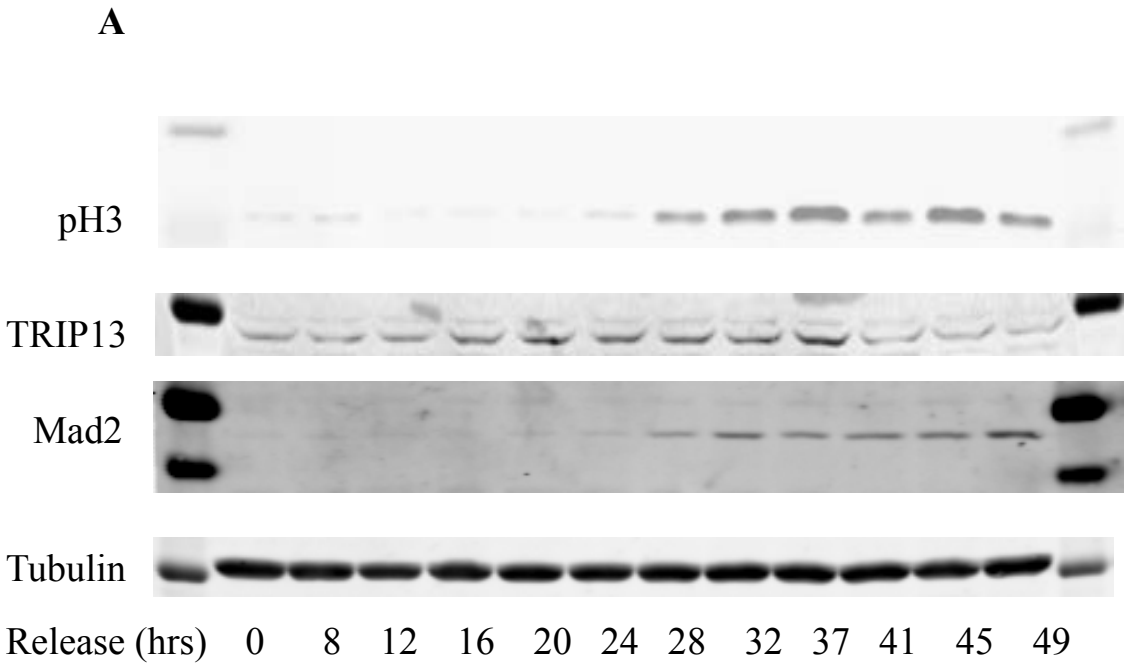


**Figure 2.3. TRIP13 is cell cycle regulated.**
(**A**) Western blot timecourse of IMR90 cells released from serum starvation synchronization.

**TRIP13 overexpression blocks the effects of Mad2 overexpression**

While TRIP13 has been shown to aid in mitotic checkpoint complex disassembly, depletion causes only mild mitotic prolongation (Wang et al., 2014). Dr. Christine Khoo had previously performed an unpublished high-throughput shRNA screen for genes that could modulate the growth of Mad2-overexpressing cells (Fig 2.4A). This screen was performed using human retinal pigment epithelial cells (RPE2) containing a doxycycline inducible HA-Mad2 construct (Sotillo et al., 2007), which will be referred to as RPE-M, and was made by Dr. Christine Khoo. This cell line was transduced with a genome-wide lentiviral library of shRNAs individually in 384 microwell plates and induced to express Mad2 for 2 weeks before cell numbers for each well were measured. shRNAs against TRIP13 reduced the proliferation of Mad2-overexpressing cells, which suggested that TRIP13 may play a more important role in the context of Mad2-overexpression (Fig. 2.4B). Considering TRIP13 is overexpressed in the context of Mad2-overexpression in cancer, and little is known about the effects of TRIP13 overexpression on mitosis, I sought to test the effect of TRIP13 overexpression in normal and Mad2-overexpressing cells. To study the effect of TRIP13 overexpression in the context of Mad2 overexpression, I used the RPE-M cell line. Induction of Mad2 is observed in these cells by 24 hours (Fig. 2.5A). As expected, the overexpression of Mad2 caused an approximately 4-fold increase in mitotic duration from an average of 44 minutes to 217 minutes (Fig. 2.5B). For all experiments, mitotic timing was determined by the duration of cell rounding, however this was confirmed to be correlated with mitotic chromatin dynamics in cells labeled with H2B-mCherry (data not shown). I transduced this RPE-M cell line with a constitutively expressing TRIP13-GFP vector (Fig. 2.5A). Alone, cells

with TRIP13 overexpression had a similar basal mitotic duration compared to parental RPE cells. However, TRIP13 overexpression significantly reduced the prolongation of mitosis induced by Mad2 overexpression from 173 minutes (217-44 minutes) to 10 minutes (48-38 minutes) (Fig. 2.5B).

Prolonged mitosis leads to a p53-dependent G1 arrest (Vogel et al., 2004). Mad2 overexpression in p53 wild type RPE cells led to an accumulation of large, flat, cells of senescent appearance, and caused a dramatic decrease in proliferation (Fig. 2.5C,D). TRIP13 overexpression prevented changes in cell morphology and significantly rescued the ability of Mad2-overexpressing cells to grow (Fig. 2.5C,D). Mad2-overexpresing cells also show evidence of centromere stretching, potentially due to prolonged mitosis even after microtubule attachment, which TRIP13 overexpression also blocked (Fig. 2.6A,B). Mad2 overexpression induced an accumulation of cells with micronuclei, indicative of abnormal chromosome segregation at mitotic exit, and these phenotypes were also blocked by TRIP13 overexpression (Fig. 2.7A,B). Increased chromosomal instability was also observed *in vivo* in xenografts of RPE-M Mad2-overexpressing cells (Fig. 2.8A,B). These cells had p53 knocked down to allow them to continue to grow with a Mad2-induced prolonged mitosis (Fig. 2.9C) TRIP13 overexpression was able to block the increase in aneuploidy in xenografts, but had negligible effect on tumor growth (Fig. 2.8B,C). Thus, while TRIP13 overexpression has little effect on mitotic duration or micronuclei formation in a normal mitosis, it is able to strongly antagonize these effects in Mad2-overexpressing cells. I speculate that tumor-sustaining proliferation rates and chromosome mis-segregation events in Mad2-overexpressing cells requires a finely tuned balance of Mad2 and TRIP13 levels (see below and Discussion).

**Figure 2.4. High-throughput shRNA screen for modifiers of proliferation in Mad2-overexpressing cells.**

**A**

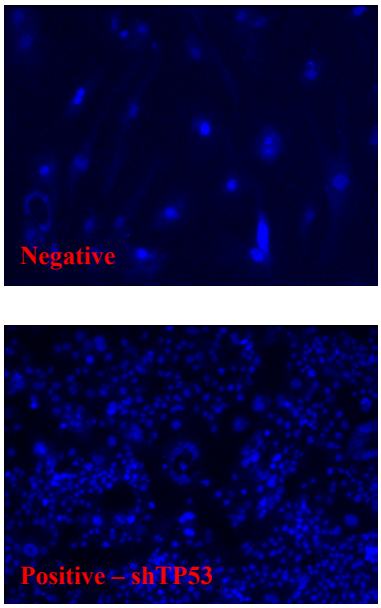


**Sigma shRNA Lentiviral Particle Library**

- 295 384-well microplates
- Covering ~16,000 Genes
- 80,000 shRNAs (Approximately 5 Constructs per Gene)
- Hoechst stain and automated nuclei counting
- ~90 nuclei average across shRNA screen

**B**

| | sh1 | sh2 | sh3 | sh4 | sh5 |
|---|---|---|---|---|---|
| TRIP13 | 3 | 19 | 52 | 62 | 73 |

Nuclei Counts

**Figure 2.4. High-throughput shRNA screen for modifiers of proliferation in Mad2-overexpressing cells.**
(**A**) Images of Hoescht-stained RPE-M cells transduced with control or p53 shRNA after 14 days Mad2 induction. (**B**) Nuclei counts for 5 TRIP13 shRNAs after 14 days Mad2 induction.

**Figure 2.5. TRIP13 overexpression blunts Mad2 overexpression phenotypes.**

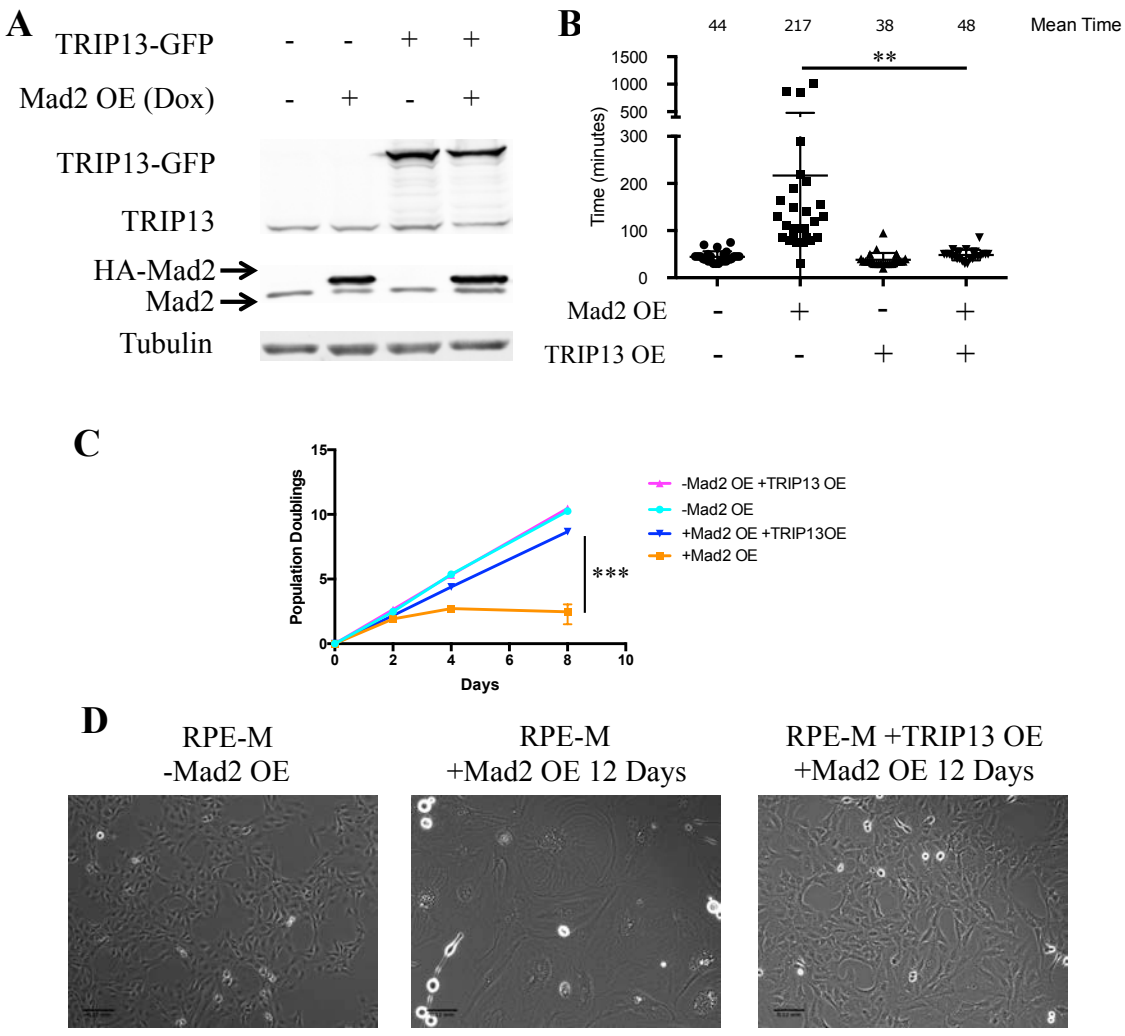


**Figure 2.5. TRIP13 overexpression blunts Mad2 overexpression phenotypes.**
(**A**) Western blot of RPE2 cells transduced with dox-inducible HA-Mad2 construct and/or constitutive TRIP13-GFP construct with or without doxycycline addition for 24 hours. (**B**) Mitotic timing of RPE-M or T13G cells, +/- 24 hours doxycycline, measured by cell rounding in time-lapse images. n ≥20 cells for each condition. (**C**) Equal numbers of RPE-M and T13G cells were plated with or without doxycycline on day 0 and were counted and replated on day 2 and day 4, and counted on day 8. The population doublings of RPE-M and T13G cells is plotted over time. n=3 independent experiments (**D**) Bright field imaging of RPE-M cells without doxycycline treatment and RPE-M and T13G cells with doxycycline treatment for 12 days.

**Figure 2.6. TRIP13 overexpression prevents Mad2-induced centromere separation.**

**A**

RPE-M 5 Days Mad2 OE – Complete Centromere Separation (84% of metaphases)

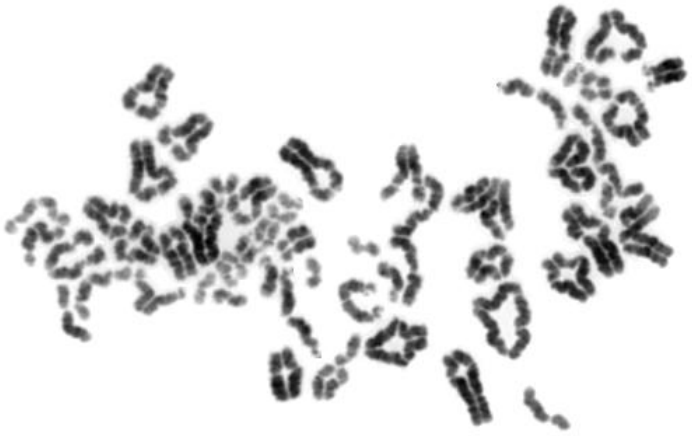

**B**

T13G 5 Days Mad2 OE – Normal Chromosome Alignment (92% of metaphases)

**Figure 2.6. TRIP13 overexpression prevents Mad2-induced centromere separation.**
(**A**) Representative image of metaphase spread for RPE-M cells after 5 days Mad2 overexpression. (**B**) Representative image of metaphase spread for T13G cells after 5 days Mad2 overexpression. 50 metaphases were counted for each condition.

**Figure 2.7. TRIP13 overexpression blocks Mad2-induced micronuclei formation.**

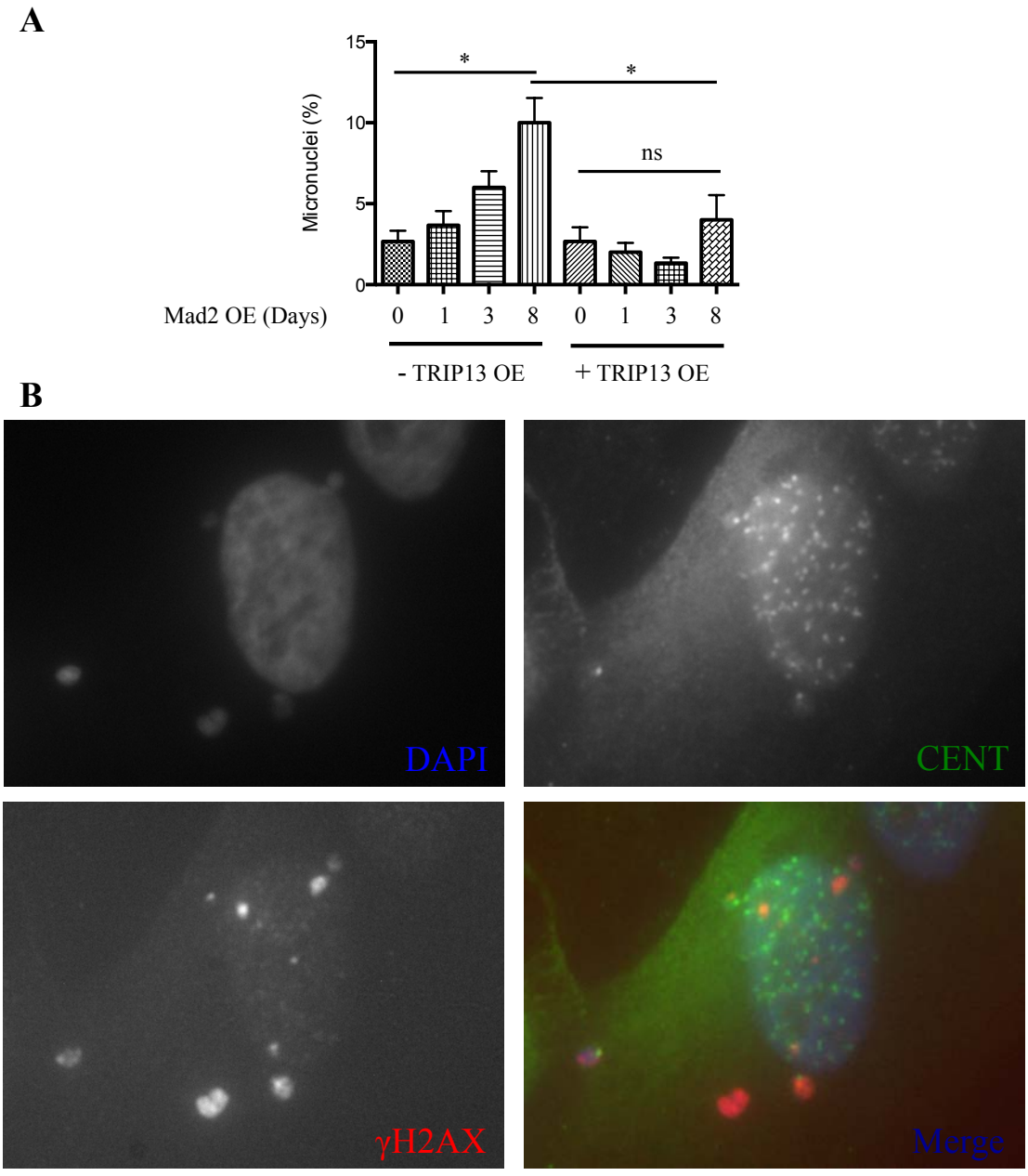


**Figure 2.7. TRIP13 overexpression blocks Mad2-induced micronuclei formation.** (**A**) Quantification of micronuclei in RPE-M or T13G cells with 0, 1, 3, or 8 days Mad2 overexpression. Micronuclei were counted in 100 cells in triplicate by DAPI staining. (**B**) Representative image of micronuclei in RPE-M cell after 3 days Mad2 overexpression. Micronuclei frequently stain positive for centromeres and γH2AX

**Figure 2.8. TRIP13 overexpression blunts Mad2-induced chromosomal instability in xenografts.**

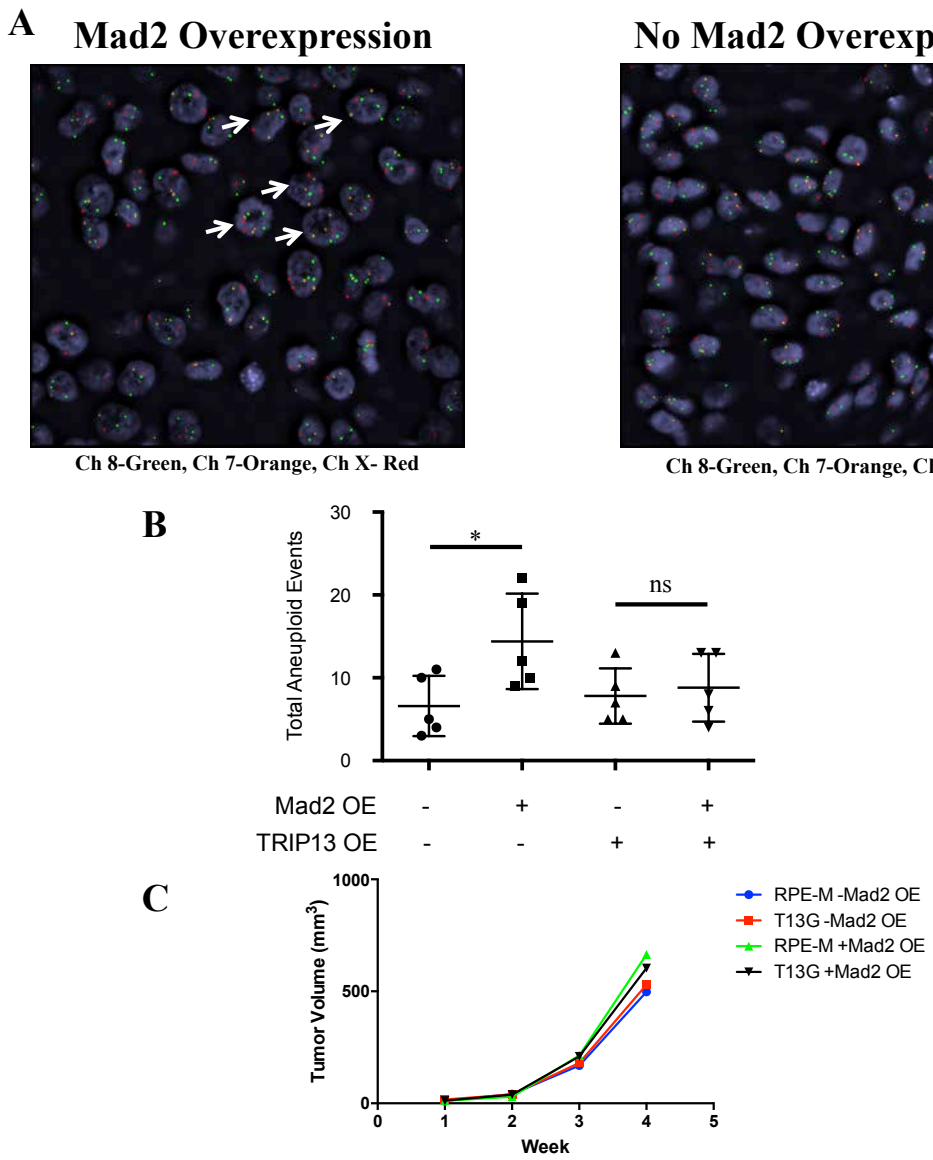


**Figure 2.8. TRIP13 overexpression blunts Mad2-induced chromosomal instability in xenografts.**

(**A**) Representative images of interphase FISH for chromosomes 8, 7, and X on xenografts of RPE-M cells with or without Mad2 induction. Aneuploidy scored as greater than modal number of chromosome (Ch 8:3, Ch 7:2, Ch X:2). White arrows point to aneuploid cells. (**B**) Quantification of total aneuploid chromosomes in RPE-M and T13G cells by interphase FISH in tumor sections after 5 weeks. 100 cells were quantified per mouse, 5 mice per group. (**C**) Quantification of tumor volume over 4 weeks for RPE-M and T13G cells with or without Mad2 overexpression.

**TRIP13 is critical for mitotic exit in Mad2 overexpressing cells**

Given the ability of TRIP13 overexpression to block a Mad2-overexpression induced arrest, I wanted to determine if these cells had an increased dependence on TRIP13 for mitotic exit. To study the ability of Mad2 overexpressing cells to proliferate over time, I knocked down p53 to allow them to continue to divide in the presence of prolonged mitosis (Fig. 2.9C). I tested the effect of TRIP13 knockdown in these cells using two siRNAs previously used to study the effects of TRIP13 loss (Wang et al., 2014). Cells were transfected with either TRIP13 siRNA or control siRNA and were subsequently treated with or without doxycycline to induce Mad2 overexpression. I followed the effect of TRIP13 knockdown on mitotic duration by time-lapse imaging and counted cell numbers to assess the effects on proliferation (Fig. 2.9A).

Both siRNAs were capable of substantially reducing the levels of TRIP13 in inducible Mad2 overexpressing cells (Fig. 2.9B). Consistent with previous studies (Wang et al., 2014), knockdown of TRIP13 with either siRNA caused a mild prolongation of mitosis (1.5-2 fold) in the absence of Mad2 overexpression (Fig. 2.10A). However, while Mad2 overexpression alone caused an average ~3-4 fold increase in mitotic duration, these cells were extremely dependent on TRIP13 for mitotic exit. Knockdown of TRIP13 with either siRNA in Mad2 overexpressing cells caused a severe mitotic arrest, with cells arresting in mitosis on average for more than 20-fold longer than an unperturbed mitosis (Figs. 2.10B, 2.11A). There is some variability in the prolongation of mitosis most likely due to cell-to-cell differences in Mad2 overexpression and TRIP13 knockdown, consistent with TRIP13 knockout cells having less variability (Fig. 2.16C).

**Figure 2.9. Characterization of TRIP13 knockdown in p53 knockdown RPE-M cells.**

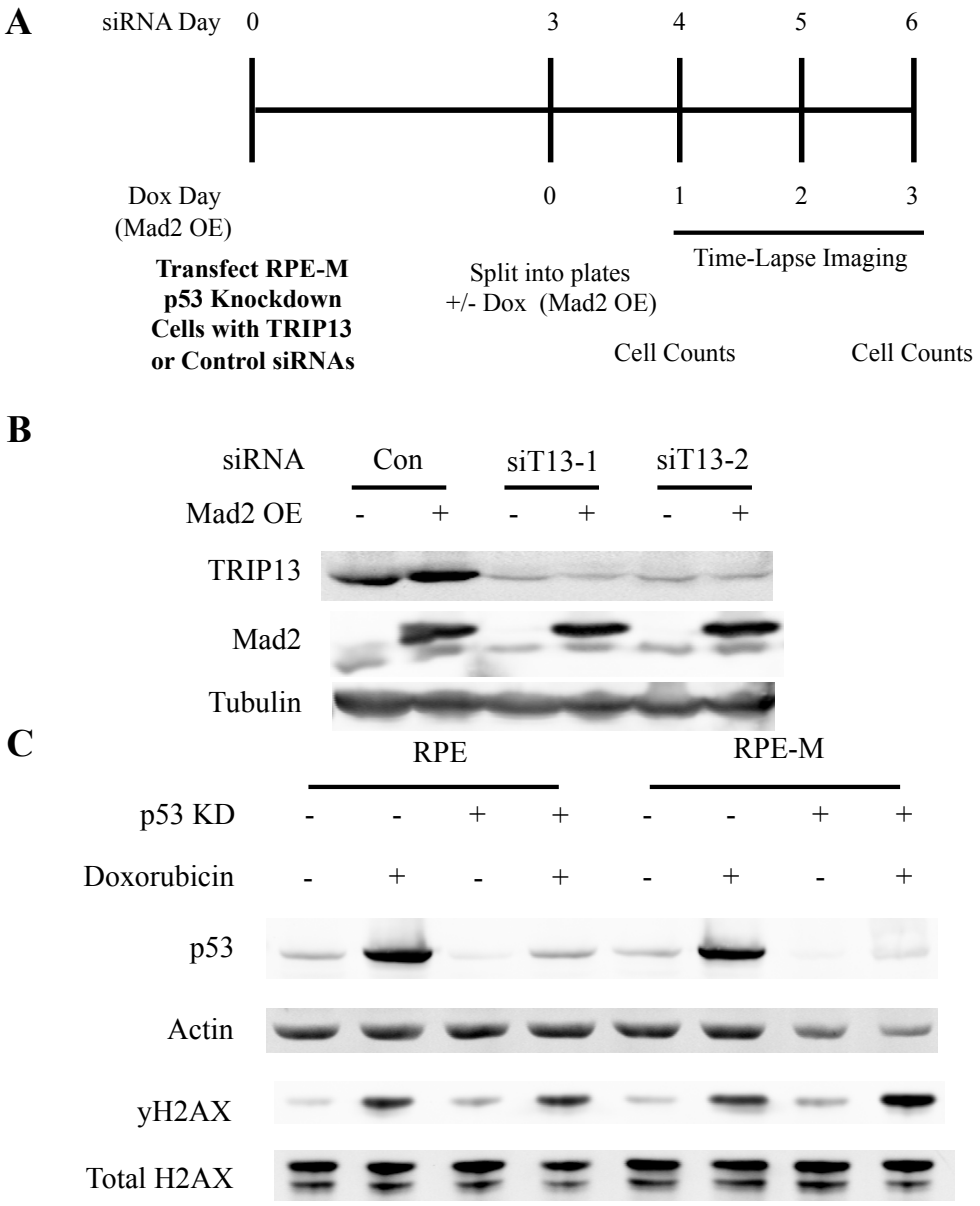


**Figure 2.9. Characterization of TRIP13 knockdown in p53 knockdown RPE-M cells.**
(**A**) Schematic showing transfection of RPE-M p53 knockdown cells with TRIP13 or control siRNAs followed by doxycycline addition after 3 days followed by analysis by cell counting and time-lapse imaging. (**B**) Western blot of TRIP13 knockdown with two independent siRNAs with or without 24 hours of doxycycline treatment. (**C**) Western blot of RPE and RPE-M cells with or without transduction with pLVTH-sip53. Cells were treated +/- 0.2 ug/ml doxorubicin for 11 hours to induce DNA damage.

**Figure 2.10. TRIP13 knockdown causes a severely prolonged mitosis in Mad2-overexpressing cells.**

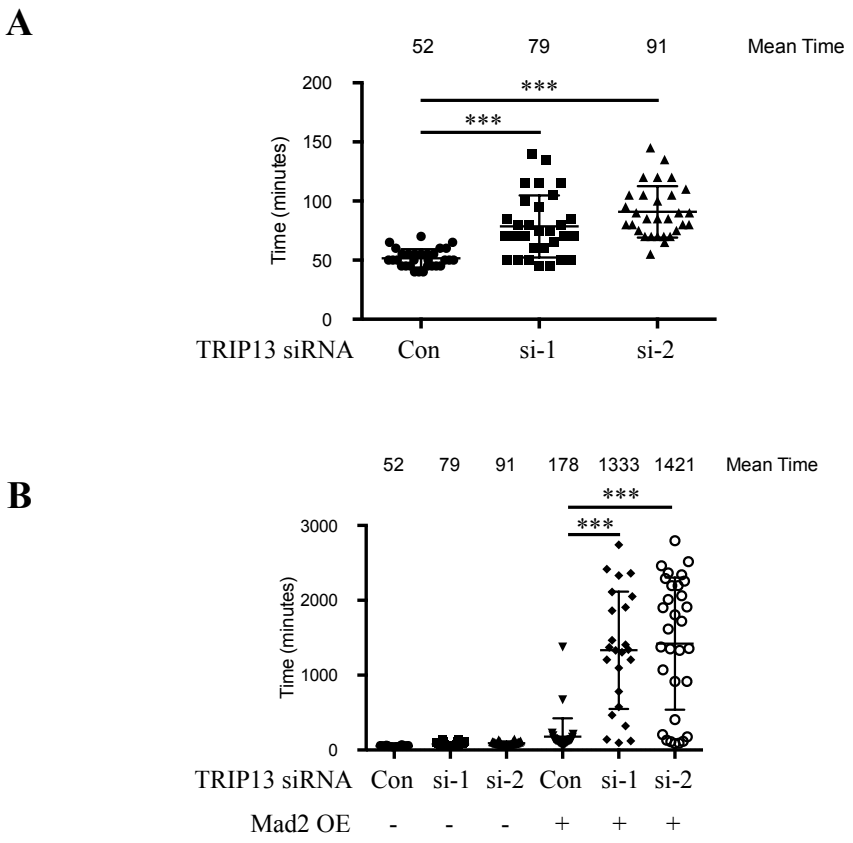


**Figure 2.10. TRIP13 knockdown causes a severely prolonged mitosis in Mad2-overexpressing cells.**

(**A**) Mitotic timing of RPE-M cells transfected with control or TRIP13 siRNA. (**B**) Mitotic timing of RPE-M cells transfected with control or TRIP13 siRNA +/- 24 hours doxycycline. Mitotic timing measured by cell rounding in time-lapse images. n ≥20 cells for each condition.

**Figure 2.11. Time-lapse sequences of RPE cells with or without TRIP13 knockdown and Mad2 overexpression.**

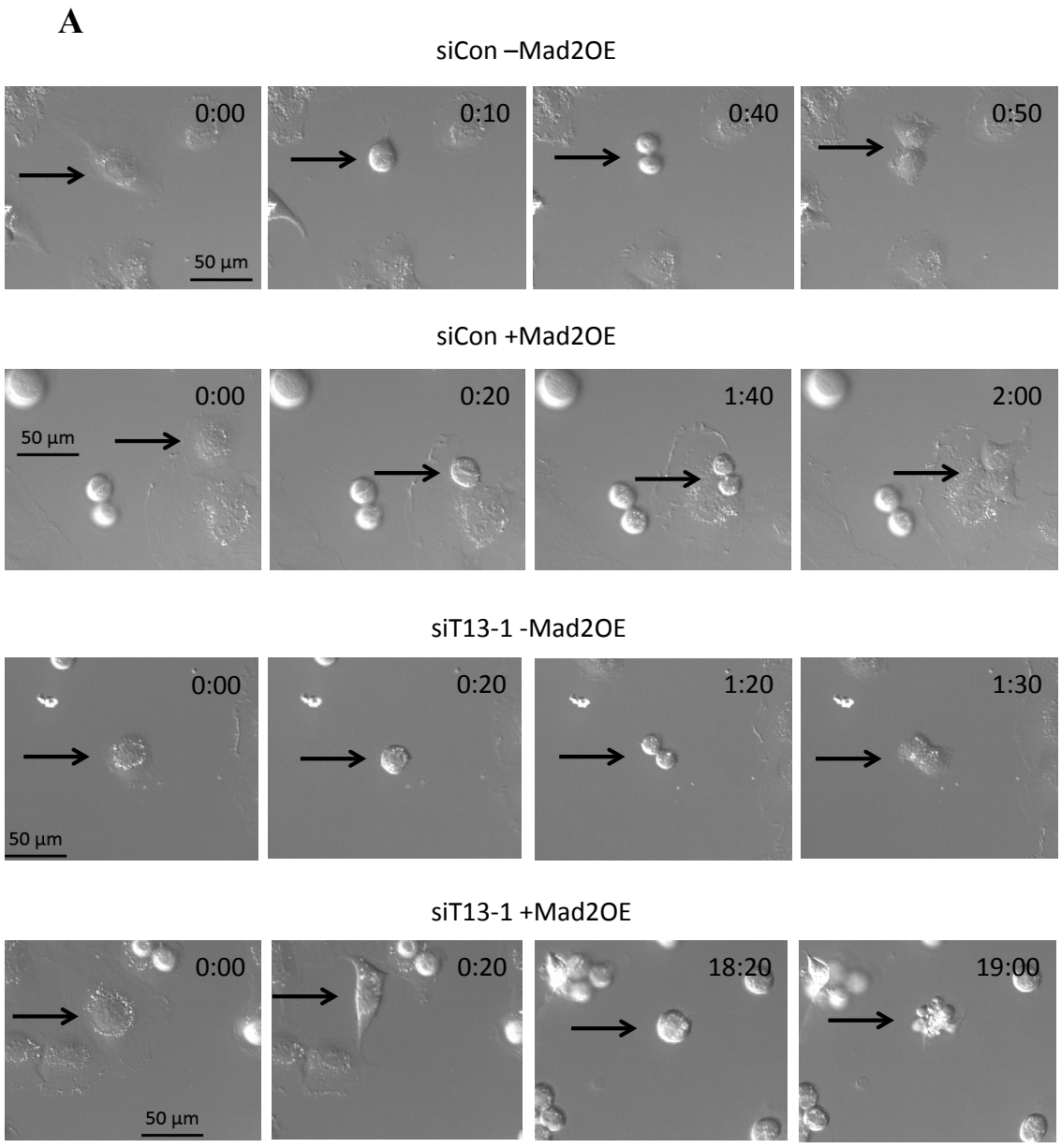


**Figure 2.11. Time-lapse sequences of RPE cells with or without TRIP13 knockdown and Mad2 overexpression.**

(**A**) Representative cells entering mitosis for RPE cells treated with control siRNA or TRIP13 siRNA, with or without Mad2 overexpression. Cells were transfected with control or TRIP13 siRNA 3 days prior to imaging, Mad2 was induced with doxycycline 1 day prior to imaging.. Arrows point to cells that enter and exit mitosis.

To test the effect of TRIP13 knockdown in a system where Mad2 is overexpressed due to loss of the Rb pathway, I used a vector expressing the HPV E6 and E7 proteins, which inhibit p53 and Rb function (Halbert et al., 1992; Yim and Park, 2005). Transduction of parental RPE cells with the vector led to increased Mad2 and TRIP13 expression, as expected for E2F target genes (Fig. 2.12A). Further, expression of the E6/E7 proteins led to an increase in mitotic timing, from an average of 39 minutes to 53 minutes (Fig. 2.12B). TRIP13 knockdown further prolonged mitosis in E6/E7 transduced cells to an average of 118 minutes. These results demonstrate the ability of TRIP13 loss to exacerbate mitotic arrest in a model of oncogene-induced Mad2 overexpression.

**TRIP13 knockdown is synthetic lethal with Mad2 overexpression**

I tested the growth of cells with TRIP13 knockdown with or without Mad2 overexpression to confirm that this increased mitotic arrest was associated with a decrease in proliferation. While either TRIP13 knockdown or Mad2 overexpression alone caused only a mild decrease in proliferation, both TRIP13 siRNAs induced an almost complete block of cell proliferation upon Mad2 induction (Fig, 2.13A). Time-lapse imaging showed evidence of cells undergoing a mitotic cell death (Fig 2.11A), and I observed an increase in γH2AX and cleaved caspase 3 by Western blot only in cells with the combination of TRIP13 siRNA and Mad2 overexpression (Fig. 2.13B).

**Figure 2.12. TRIP13 knockdown in E6/E7 cells causes mitotic delay.**

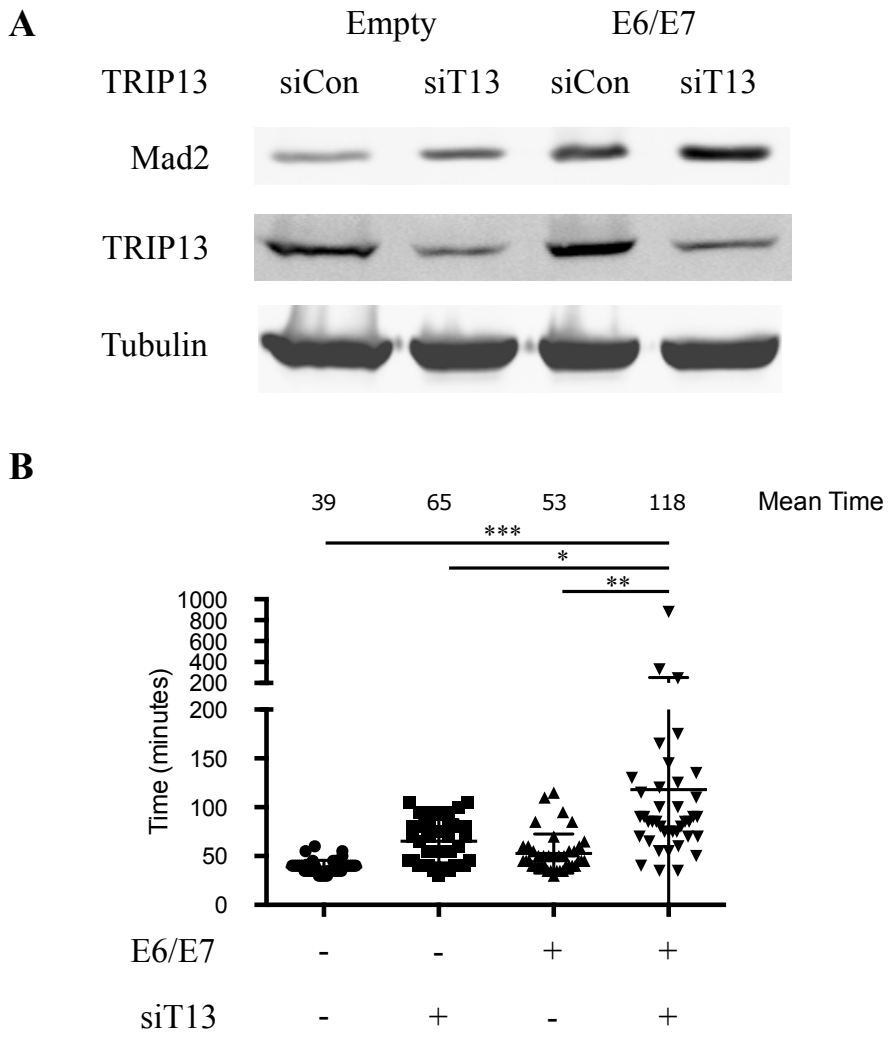


**Figure 2.12. TRIP13 knockdown in E6/E7 cells causes mitotic delay.**
(**A**) Western blot of cells transduced with empty or E6/E7 expressing pLXSN vectors and transfected with control or TRIP13 siRNA #1. (**B**) Quantification of mitotic duration of pLXSN-Empty and E6/E7 transfected with control or TRIP13 siRNA #1.

**Figure 2.13. TRIP13 knockdown and Mad2 overexpression combine to reduce cell growth in culture.**

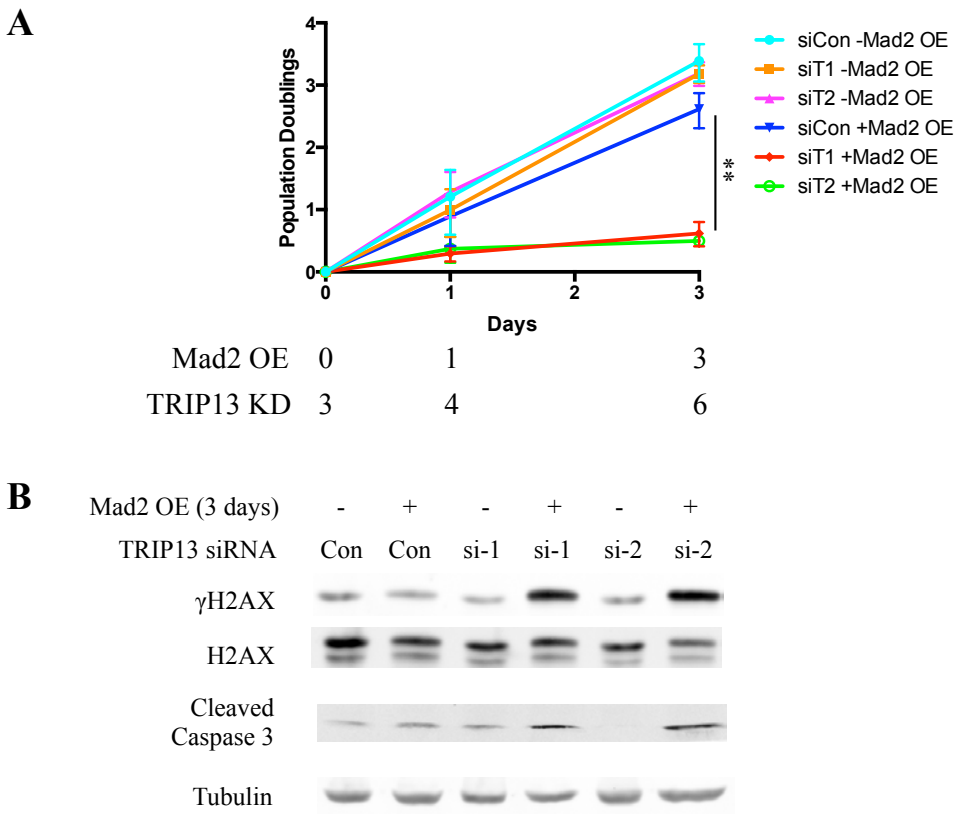


**Figure 2.13. TRIP13 knockdown and Mad2 overexpression combine to reduce cell growth in culture.**
(**A**) Equal numbers of RPE-M cells transfected with TRIP13 or control siRNAs were plated with or without doxycycline on day 0 and were counted and replated on day 1 and counted on day 3. The number of population doublings is plotted over time. n=3 independent experiments. (**B**) Western blot of γH2AX and cleaved caspase 3 on RPE-M cells transfected with siRNAs for 6 days +/- Mad2 overexpression for 3 days.

To investigate the long-term effects of TRIP13 knockdown in the presence or absence of Mad2 overexpression, I inserted a dox-inducible TRIP13 shRNA-expressing construct into the parental RPE si-p53 cells or the dox-inducible, Mad2-overexpressing, RPE-M si-p53 cells. Cells expressing this hairpin had substantial knockdown of TRIP13 after doxycycline treatment (Fig, 2.14A). Nude mice were injected by Rozario Thomas with either RPE with control or TRIP13 shRNA, or RPE-M cells with control or TRIP13 shRNA. All mice were maintained on doxycycline for 5 weeks. At 5 weeks, the majority of mice injected with control cells, or cells with only Mad2 overexpression or TRIP13 knockdown alone, grew large tumors (Fig, 2.14B). However, tumor formation was almost completely blocked for cells that had combined overexpression of Mad2 and TRIP13 knockdown, with small or undetectable tumors present after 5 weeks (Fig. 2.14B). Similar results were seen with a 2$^{nd}$ shRNA against TRIP13 (Fig 2.14C). I observed occasional escape of clones of cells in culture over long duration induction of Mad2 and TRIP13 shRNA. These clones frequently showed loss of expression from the TRIP13 shRNA construct, suggesting growth escape was dependent on restoring TRIP13 levels (Fig. 2.15A,B).

**Figure 2.14. TRIP13 knockdown and Mad2 overexpression combine to reduce cell growth in xenografts.**

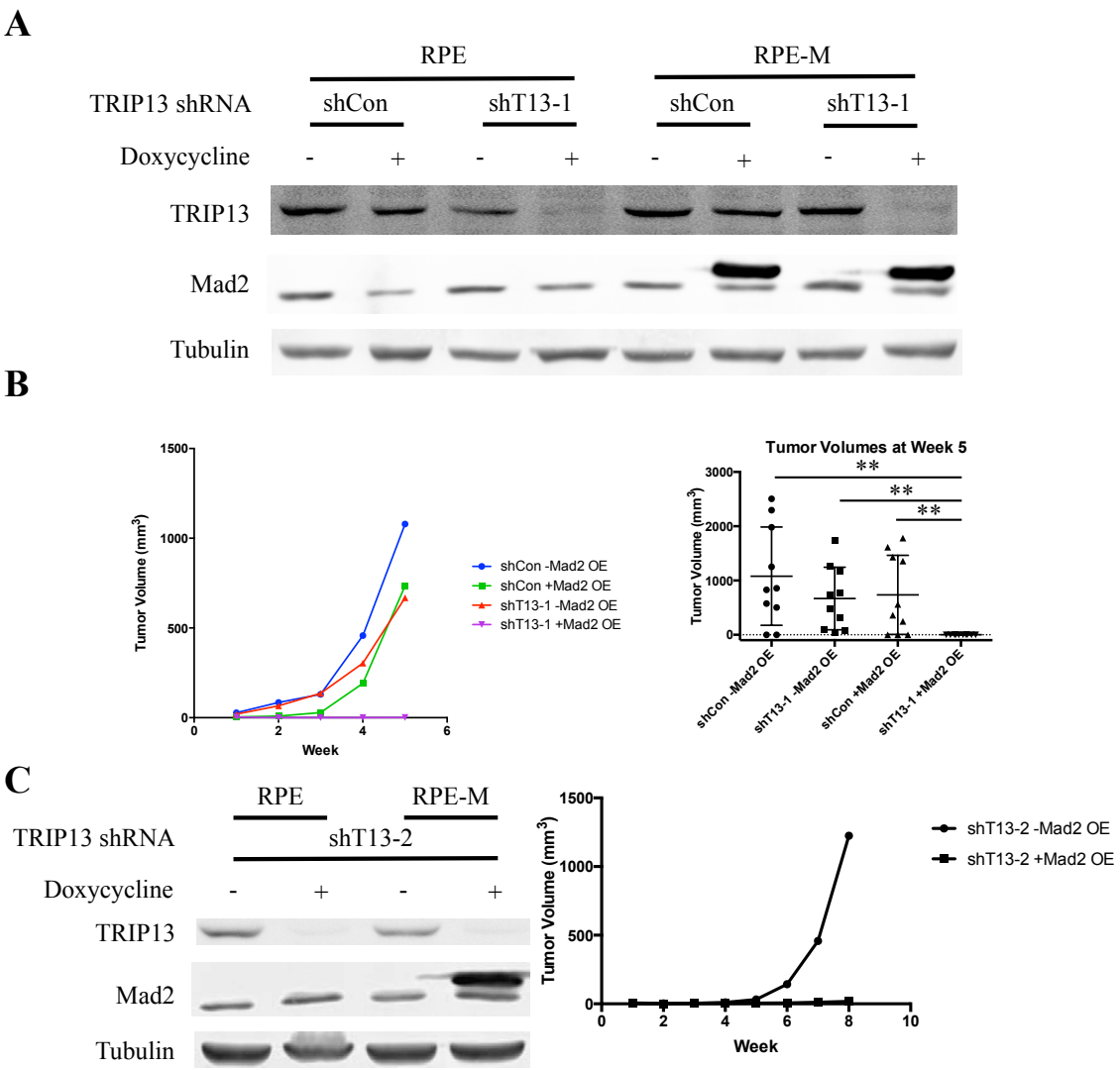


**Figure 2.14. TRIP13 knockdown and Mad2 overexpression combine to reduce cell growth in xenografts.**

(**A**)Western blot of Mad2 and TRIP13 on parental RPE and Mad2-inducible RPE-M cells transduced with a doxycycline-inducible TRIP13 or control shRNA construct. (**B**) Tumor volumes over time of RPE and RPE-M cells transduced with TRIP13 or control shRNA injected subcutaneously into nude mice (n=10). Mice were continuously fed with doxycycline-containing feed. Tumor volumes at week 5 are shown on the right. (**C**) Western blot of RPE and RPE-M transduced with TRIP13 shRNA #2 (Left). Tumor volumes over time of RPE and RPE-M cells transduced with a second TRIP13 shRNA injected subcutaneously into nude mice (n=10). Mice were continuously fed with doxycycline-containing feed (Right).

**Figure 2.15. Loss of shRNA expression in escape colonies.**

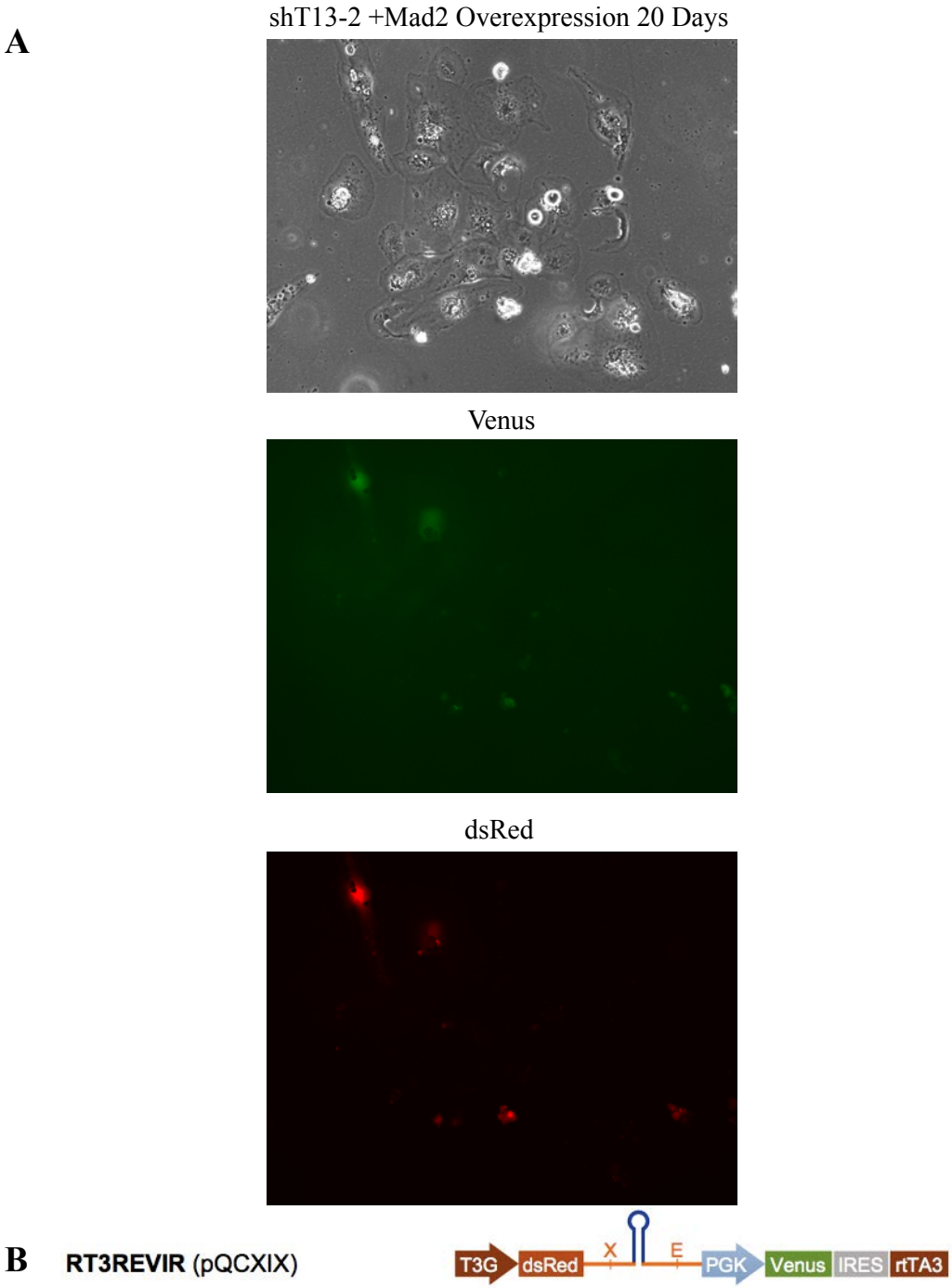


**Figure 2.15. Loss of shRNA expression in escape colonies.**
(**A**) Brightfield (Top), Venus (Middle), dsRed (Bottom) images of a colony of RPE-M sh2 cells 20 days after doxycycline. (**B**) Schematic of RT3REVIR shRNA Construct

**Generation and Mitotic Phenotypes of TRIP13 Knockout Cells**

Prior studies have shown that complete knockout of TRIP13 is not lethal to cells, but, surprisingly, leads to a defect in the ability to arrest in nocodazole (Ma and Poon, 2016). TRIP13 knockout cells still had the ability to recruit Mad2 to kinetochores in the presence of nocodazole but were significantly reduced in their ability to form Mad2-Cdc20 complexes. Notably, the vast majority of the Mad2 found in these TRIP13 knockout cells was in the closed conformer, suggesting that open Mad2 may be necessary for a robust nocodazole arrest.

I generated TRIP13 knockout RPE-M si-p53 cells with CRISPR-Cas9 by inducing frameshift mutations in the first exon (Fig. 2.16A). Similar to results seen in HeLa or HCT116 cells (Ma and Poon, 2016), the unperturbed mitotic timing of these cells was similar to those of parental cells, and also had a decreased ability to arrest in nocodazole (Fig. 2.16B). However, these cells did not completely lack the ability to inhibit anaphase progression, as overexpression of Mad2 was able to induce mitotic arrests of over 20 hours (Fig. 2.16C). TRIP13 knockout cells also showed significantly reduced ability proliferate *in vivo* in xenografts when Mad2 was induced (Fig. 2.17A). I also generated TRIP13 knockout cells in parental RPE cells that contained frameshift mutations in the first exon (Fig. 2.18A). I occasionally saw colonies of TRIP13 knockout RPE-M cells growing after prolonged Mad2 overexpression. Interestingly, these cells lost induction of Mad2, again underlining the strength of the synthetic lethal relationship (Fig. 2.19A). I also reconstituted TRIP13 knockout cells with TRIP13-GFP (Fig. 2.19A), and this largely rescued mitotic arrest induced by Mad2 (data not shown).

**Figure 2.16. TRIP13 knockout cells fail to arrest in nocodazole but have severe arrests after Mad2-overexpression.**

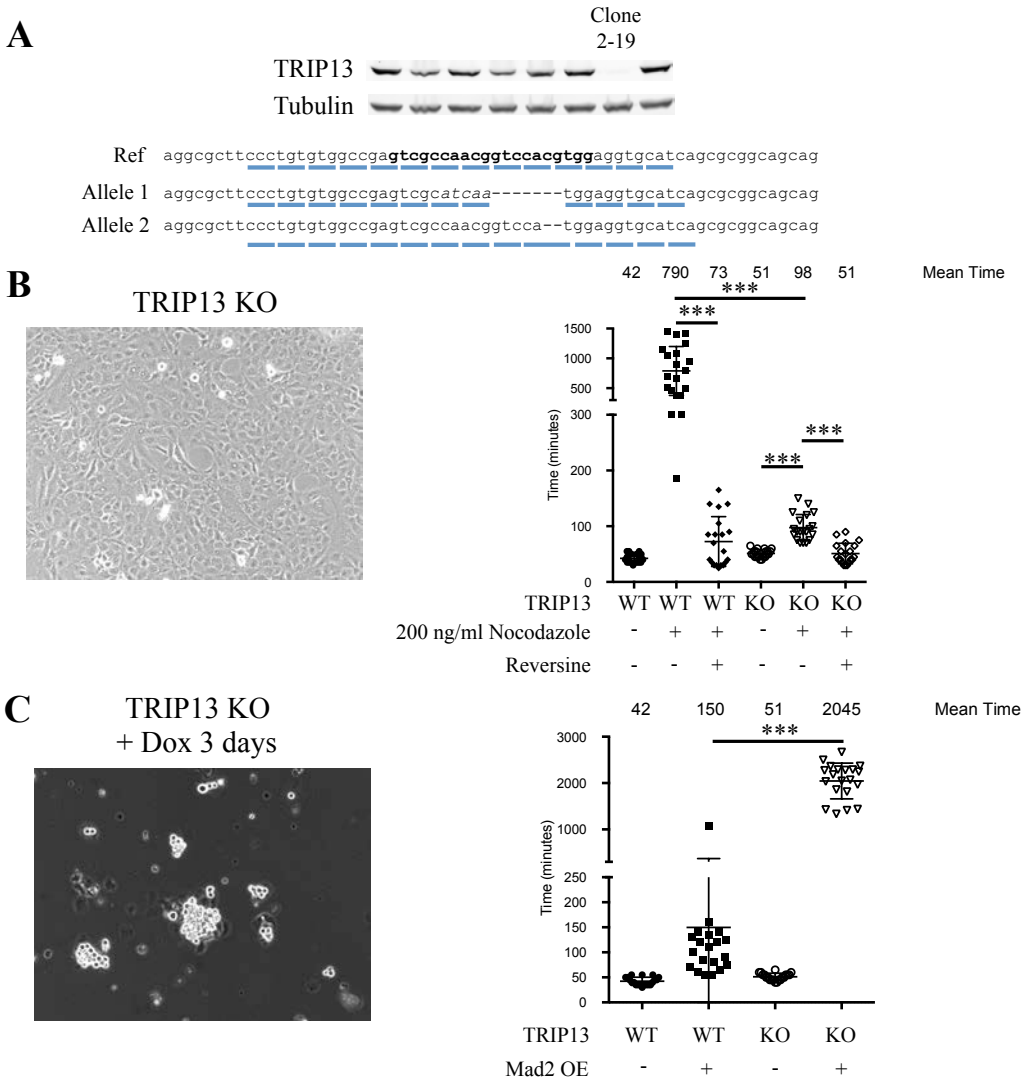


**Figure 2.16. TRIP13 knockout cells fail to arrest in nocodazole but have severe arrests after Mad2-overexpression.**

(**A**) Validation of CRISPR-Cas9 knockout of TRIP13. Cell clones were screened for TRIP13 loss by Western blot. DNA from clone 2-19 was cloned and sequenced, with one allele having net deletion of seven base pairs and the second allele having a deletion of two base pairs, both leading to loss of reading frame. (**B**) Morphology of TRIP13 knockout cells by bright field microscopy (Left). Quantification of mitotic timing in RPE-M and TRIP13 knockout cells treated with +/- 200 ng/ml nocodazole 4 hours prior to imaging +/- 0.5 uM reversine 1 hour prior to imaging (Right). n ≥20 cells for each condition. (**C**) Morphology of TRIP13 knockout cells after 3 days Mad2 overexpression by bright field microscopy (Left). Quantification of mitotic timing in RPE-M and TRIP13 knockout cells treated with +/- doxycycline 16 hours prior to imaging (Right). n ≥20 cells for each condition.

**Figure 2.17 Mad2 overexpression in TRIP13 knockout cell xenografts delays tumor growth.**

**A**

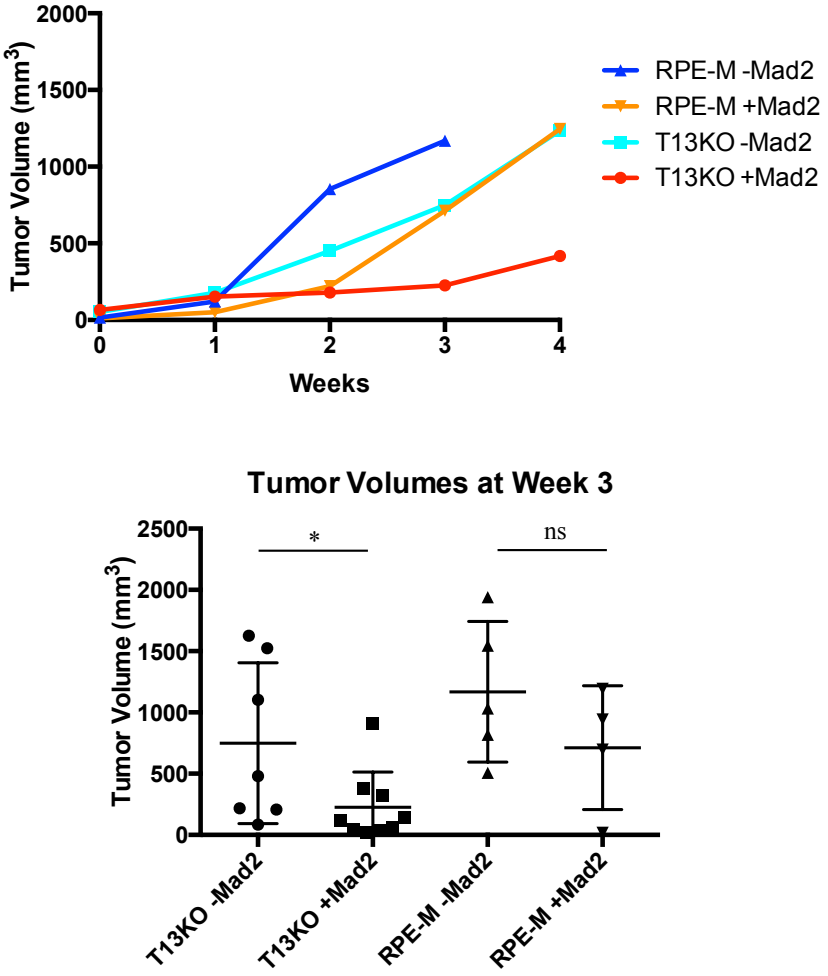


**Figure 2.17. Mad2 overexpression in TRIP13 knockout cell xenografts delays tumor growth.**

(**A**) Tumor volumes over time of RPE-M and T13KO cells injected subcutaneously into nude mice. 1 million cells of either cell line were injected into nude mice and switched to either on or off doxycycline-containing feed once tumors became palpable. (n = 7 T13KO –Mad2; n = 9 T13KO +Mad2; n = 5 RPE-M –Mad2; n = 4 RPE-M +Mad2 ). Tumor volumes at week 3 are shown below.

**Figure 2.18. Validation of TRIP13 knockout parental RPE cells.**

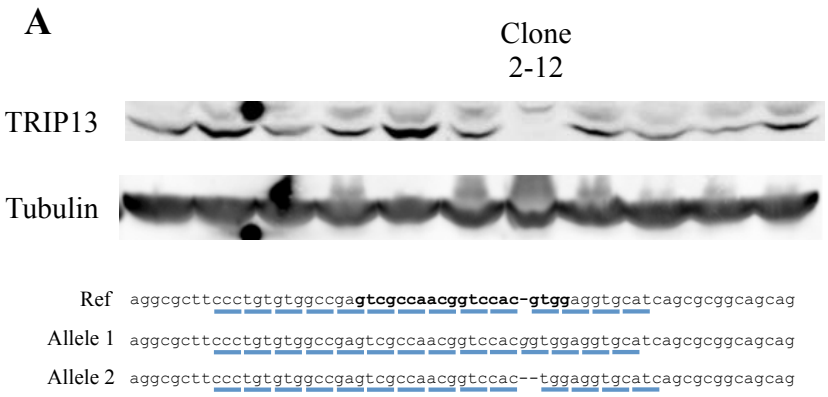


**Figure 2.18. Validation of TRIP13 knockout parental RPE cells.**
(**A**) Validation of CRISPR-Cas9 knockout of TRIP13. Cell clones were screened for TRIP13 loss by Western blot. DNA from clone 2-12 was cloned and sequenced, with one allele having a 1 base pair deletion and the second allele having a 1 base pair insertion, both leading to loss of reading frame

**Figure 2.19. Reconstitution of T13KO RPE-M cells with TRIP13-GFP. Loss of Mad2 expression after 30 days Mad2 induction in T13KO cells.**

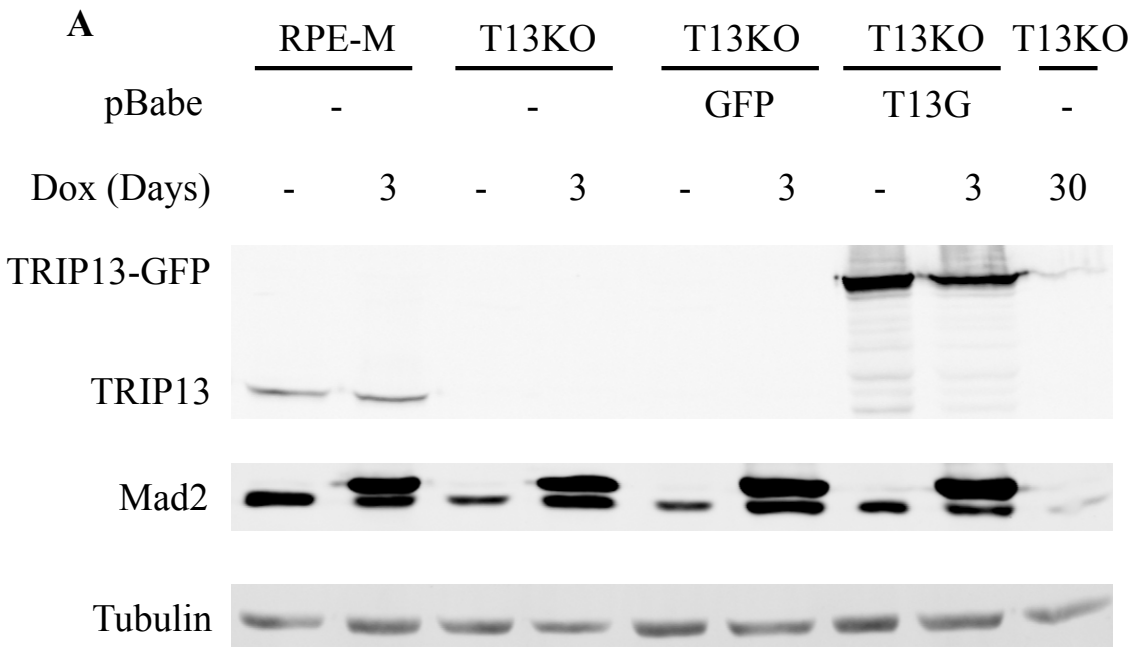


**Figure 2.19. Reconstitution of T13KO RPE-M cells with TRIP13-GFP and loss of Mad2 expression after 30 days Mad2 induction in T13KO cells.**
(**A**) Western blot of RPE-M, T13KO and T13KO cells reconstituted with pBabe-GFP or pBabe-T13G treated with or without doxycycline for 3 days, or T13KO cells treated with doxycycline for 30 days.

**Divergent roles of TRIP13 in Mad2-overexpression arrest versus nocodazole arrest**

I sought to determine how TRIP13 knockdown and overexpression affected the timing of low dose nocodazole arrests of a duration similar to Mad2 overexpression. RPE cells treated with 15 ng/ml nocodazole had a 191 minute average mitotic duration and 155 minute median mitotic duration, compared to 245 minute and 93 minute respective mean and median mitotic durations for Mad2 overexpressing cells (Fig. 2.20A). While TRIP13 knockdown induced severely prolonged mitosis when Mad2 was overexpressed (1447 and 1568 mean and median mitotic durations) it did not cause similarly severely prolonged mitoses in low-dose nocodazole cells (102 and 80 minute mean and median mitotic durations) (Fig. 2.20B). Additionally, I found TRIP13 overexpression, while able to blunt a Mad2-overexpression induced arrest, had no effect on a low dose nocodazole arrest (Fig. 2.20A). This demonstrates there is a difference in the ability of TRIP13 to quench a kinetochore-produced nocodazole arrest versus a Mad2-overexpression arrest.

Given the ability of TRIP13 to disassemble mitotic checkpoint complexes *in vitro*, I tested the consequences of TRIP13 knockout in Mad2-overexpressing cells on induced-checkpoint silencing. I used the Mps1 inhibitor, reversine, to induce silencing. Continued Mps1 activity is necessary for the formation of MCC and maintenance of arrest in nocodazole (Hewitt et al., 2010; Maciejowski et al., 2010; Santaguida et al., 2010). I found that the arrest caused by Mad2 overexpression in TRIP13 knockout or knockdown cells was largely resistant to reversine (Fig. 2.21A,B). This demonstrates that TRIP13 is necessary for reversine-induced exit in Mad2-overexpressing cells.

**Figure 2.20. Divergent roles of TRIP13 in Mad2-overexpression arrest versus nocodazole arrest.**

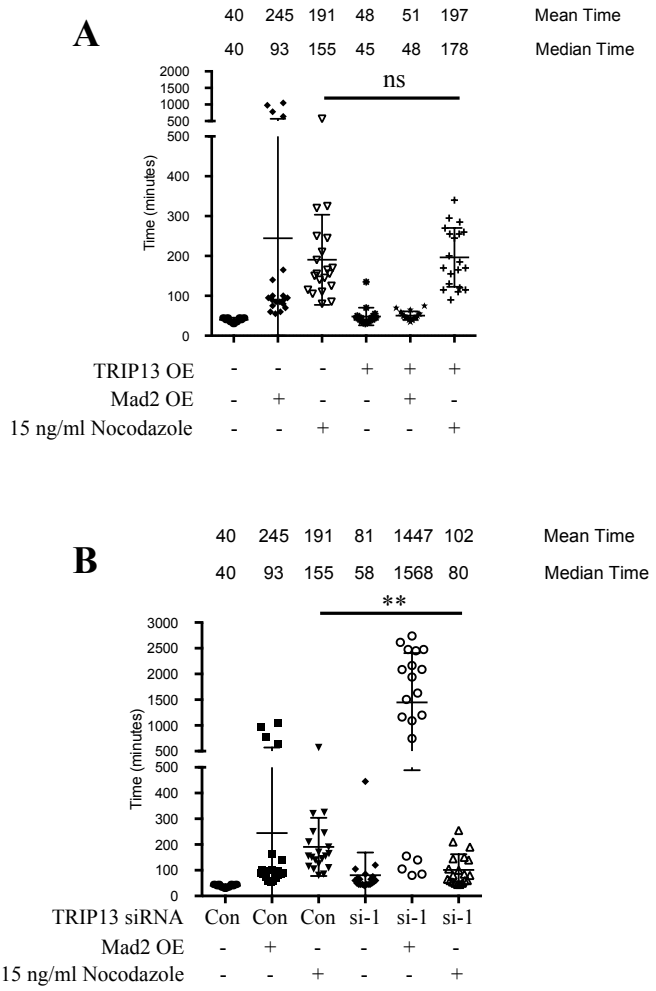


**Figure 2.20. Divergent roles of TRIP13 in Mad2-overexpression arrest versus nocodazole arrest.**

(**A**) Mitotic timing of RPE-M or T13G cells treated with doxycycline for 24 hours or a low dose of nocodazole (15 ng/ml) 4 hours prior to imaging. n ≥20 cells for each condition. (**B**) Mitotic timing of RPE-M cells transfected with control siRNA or TRIP13 siRNA #1 4 days prior to imaging and treated with either doxycycline (24 hours) or low-dose (15 ng/ml) nocodazole (4 hours) prior to imaging. n ≥20 cells for each condition.

**Figure 2.21. TRIP13 is necessary for reversine-induced mitotic exit from a Mad2-overexpression arrest.**

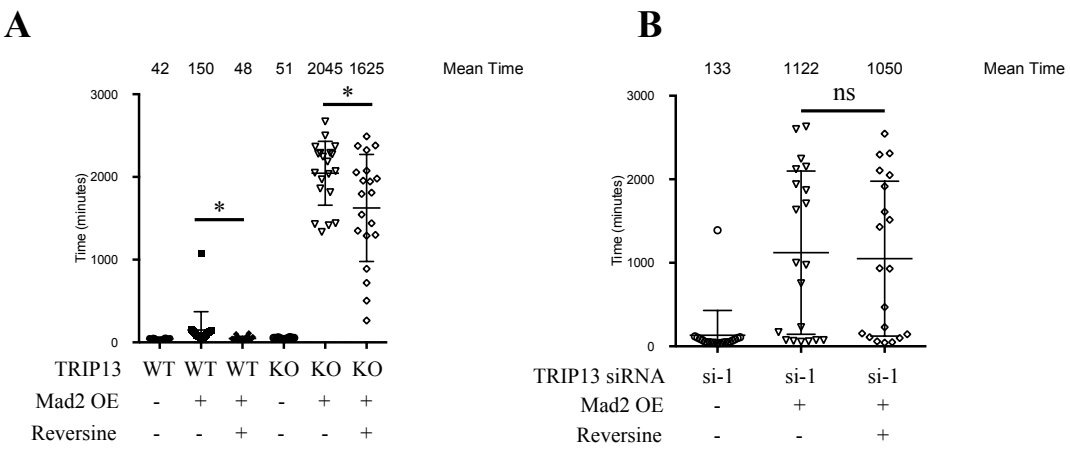


**Figure 2.21. TRIP13 is necessary for reversine-induced mitotic exit from a Mad2-overexpression arrest.**

(**A**) Mitotic timing of TRIP13 wild-type or knockout cells with or without Mad2-overexpression or reversine (0.5 μM) treatment. (**B**) Mitotic timing of TRIP13 knockdown cells with or without Mad2-overexpression or reversine (0.5 μM) treatment. Mad2 induced 24 hours prior to imaging with doxycycline, reversine added 1 hour prior to imaging. n ≥20 cells for each condition.

To directly investigate the effect of reversine on the disassembly of Mad2-Cdc20 complexes in mitotically arrested cells, I immunoprecipitated Cdc20 in cells arrested with nocodazole and the proteasome inhibitor MG132. As previously seen in TRIP13 knockout cells (Ma and Poon, 2016) there was a significant reduction in the amount of Mad2-Cdc20 complex formed in nocodazole in the absence of TRIP13 (lane 5 vs. lane 1 of Cdc20 IP, Fig. 2.22A). However, when Mad2 was overexpressed, this rescued the ability of Mad2 and BubR1 to bind Cdc20 in TRIP13 knockout cells (lane 7 vs. lane 5 of Cdc20 IP, Fig. 2.22A). Further, the ability of reversine to induce disassembly of complexes was reduced in Mad2-overexpressing TRIP13 knockout cells compared to wild-type and Mad2-overexpressing cells (lane 8 vs. lane 7 and lane 6 vs. lane 5 of Cdc20 IP, Fig. 2.22A,B). These results suggest that when Mad2 is overexpressed in TRIP13 knockout cells, Mad2-Cdc20 complexes can form, but are unable to be readily disassembled, causing a buildup of inhibitory complexes, quantified in Fig. 2.22B, which leads to an extremely severe mitotic arrest.

**Figure 2.22. TRIP13 knockout cells have reduced ability to disassemble MCC in the presence of reversine.**

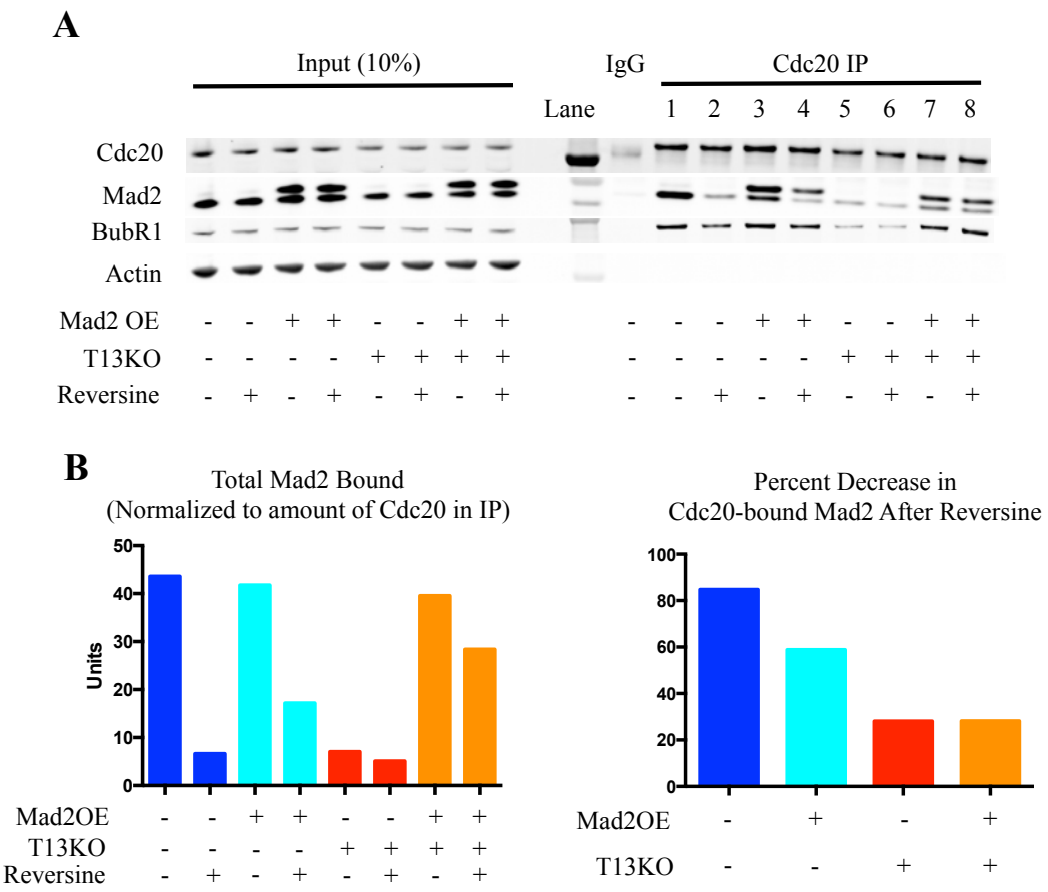


**Figure 2.22. TRIP13 knockout cells have reduced ability to disassemble MCC in the presence of reversine.**

(**A**) Western blot of Cdc20 IPs from mitotic RPE-M and TRIP13 knockout cells +/- Mad2 overexpression +/- reversine. RPE-M and TRIP13 knockout cells were synchronized with 20 hours treatment of Cdk1 inhibitor RO-3306 +/- doxycycline 8 hours after 10 μM RO-3306 addition. Cells were released into fresh media for 30 minutes followed by treatment with 50 ng/ml nocodazole and 10 μM MG132 for 3 hours +/- 1 μM reversine for the last 1.5 hours. Mitotic cells were harvested by mitotic shakeoff. (**B**) Quantification of Mad2 in Cdc20 IPs in (A) normalized to Cdc20 for each condition (Left). Quantification of the reduction in normalized Mad2 levels in Cdc20 IP after reversine addition for each condition (Right).

# CHAPTER 3

# DISCUSSION

TRIP13 has been identified as a putative mitotic checkpoint quenching protein, working in concert with $p31^{comet}$ to inactivate C-Mad2-containing mitotic checkpoint complexes. However, the effects others have observed upon TRIP13 depletion have been mild on an unperturbed mitosis, and the effects of overexpression on mitosis have not been adequately investigated. While TRIP13 is overexpressed in cancer and correlated with chromosomal instability, it is frequently co-overexpressed with Mad2 (Fig. 2.1A,B). Further, TRIP13's expression appears cell cycle regulated with expression controlled by the Rb/E2F, similarly to checkpoint genes (Figs. 2.2, 2.3). Thus, I do not believe that TRIP13 overexpression causes chromosomal instability by inducing a weakened checkpoint. Instead, as TRIP13 expression is co-regulated with other checkpoint genes, its overexpression potentially buffers the effects of checkpoint gene overexpression. $p31^{comet}$ has also been shown to be regulated similarly to Mad2 and buffer Mad2 overexpression effects on proliferation (Date et al., 2013).

I investigated the effects of TRIP13 overexpression on the phenotypes associated with Mad2 overexpression. Previous work from the Benezra laboratory demonstrated that Mad2 overexpression causes prolonged mitosis and aneuploidy in MEFs (Sotillo et al., 2007). Further, overexpression of Mad2 in RPE cells caused a p53-dependent inhibition of proliferation, but this was significantly ameliorated by co-overexpression of TRIP13 (Fig, 2.5C). It is possible that loss of p53/Rb pathways simultaneously lead to transcriptional upregulation of checkpoint genes as well as the ability to tolerate a

prolonged mitosis. I did not see evidence of a dramatically weakened checkpoint with TRIP13 overexpression, either on basal mitotic timing (Fig. 2.5B) or in response to a low dose of nocodazole (Fig. 2.20A). Conversely, overexpression of TRIP13 was sufficient to prevent a Mad2 overexpression-induced arrest of similar duration to low dose of nocodazole (Fig. 2.20A). TRIP13 overexpression blunted many Mad2-induced phenotypes, such as centromere stretching (Fig. 2.6), and chromosomal instability both in culture and in xenografts (Figs. 2.7, 2.8). This suggests that TRIP13 overexpression in cancer cells may not be causing a weakened checkpoint, but may be buffering the effects of elevated checkpoint gene expression. I speculate that such buffering facilitates a state whereby Mad2 overexpression is not dramatically impairing proliferation but at the same time can still induce chromosome instability. While I have not identified that precise balance in RPE cells, I believe that cancer cells undergo strong selective pressure to achieve such a state of sustained growth and extensive tumor heterogeneity.

Previously, there has been limited investigation into the effects of TRIP13 overexpression on mitosis. Wang et al. showed that TRIP13 overexpression potentially causes a decrease in Mad1-Mad2 interaction in interphase cells (Wang et al., 2014), but so far the consequences on mitotic timing in different conditions has not been studied. My results show that TRIP13 overexpression can have a significant impact on mitotic timing specifically in the context of a Mad2 overexpression-induced arrest (Fig 2.5B).

Banerjee et al. also investigated the effects of TRIP13 overexpression in cancer, but focused on a potential DNA repair role for TRIP13 in promoting non-homologous

end joining (NHEJ) (Banerjee et al., 2014). They found TRIP13 overexpression could accelerate head and neck squamous cell carcinoma (HNSCC) cell line growth but with increased dependency on NHEJ. They also found that the growth of HNSCC cell lines that overexpressed TRIP13 was impaired if TRIP13 was inhibited, and attributed this to effects on DNA repair. It would be interesting to test if some of the growth inhibitory effects of TRIP13 reduction in these cells are also attributable to its roles in mitosis.

Mad2 is frequently overexpressed in tumors and is correlated with chromosomal instability, which is associated with poor prognosis (Carter et al., 2006; Schvartzman et al., 2010). I was intrigued by the possibility that Mad2 overexpressing cells would be at increased dependency on TRIP13, due to its putative role in quenching checkpoint signaling and the ability of TRIP13 overexpression to antagonize the effects of Mad2 overexpression. While in an unperturbed mitosis TRIP13 knockdown caused only a mild mitotic delay, as has been observed previously (Wang et al., 2014), in the presence of Mad2 overexpression TRIP13 knockdown caused a synergistically prolonged mitotic arrest frequently of >20 hours (Fig. 2.10B). I also knocked down TRIP13 in RPE cells transduced to express the HPV E6/E7 proteins, which led to Mad2 overexpression through inhibition of Rb and p53 pathways. My results are consistent with elevated Mad2 creating an increased dependency on TRIP13 for mitotic exit. However, the mitotic prolongation in these cells, both with and without TRIP13 knockdown, was less than what I observed in Mad2 inducible overexpressing cells (Figs. 2.12B, 2.10B). This is probably explained by the lower amount of Mad2 overexpression in these cells compared to the inducible overexpressing cells (Figs 2.12A, 2.9B). There are also additional

pathways dysregulated in cancer, such as the Myc pathway, may play a role in causing the very high levels of Mad2 seen in cancer (Menssen et al., 2007).

A recent paper demonstrated that loss of cohesion of sister chromatids may lead to further reactivation of the checkpoint and prolonged mitotic arrest (de Lange et al., 2015). I see evidence of a threshold effect of some Mad2 overexpressing cells have severely prolonged mitosis whereas others have a much more mild prolongation (Figs. 2.5B, 2.10B). Further, I see centromere stretching in metaphase spreads (Fig. 2.6A) and have seen what appears to be cohesion fatigue and chromatid scattering in H2B-GFP time-lapse imaging of Mad2-overexpressing cells (data not shown). Thus, this mechanism of reactivation of checkpoint signaling after cohesion fatigue due to an initially prolonged mitosis may also partially explain the severity of the mitotic arrests I observe when combining Mad2 overexpression with TRIP13 loss.

There are potentially multiple pathways for quenching mitotic checkpoint complexes in addition to TRIP13 and/or p31comet dependent pathways. For instance, APC15 has been shown to be critical for removing MCC that is already bound to APC/C (Mansfeld et al., 2011). TRIP13 does not appear required for quenching of the checkpoint in an unperturbed mitosis, as knockdown causes only mild mitotic delays. Thus, it is possible that the APC15 pathway is largely sufficient for dealing with checkpoint complexes formed during a normal mitosis. However, when Mad2 is overexpressed, it appears that these pathways are no longer adequate to cope with this excessive inhibitory signal, and TRIP13 becomes necessary in this situation.

The differential requirement for TRIP13 in an unperturbed mitosis versus a Mad2-prolonged mitosis raised the question if TRIP13 would be similarly important in the context of other mitotic arrests. I tested the effect of TRIP13 knockdown or overexpression on a low-dose nocodazole arrest that approximated the length of a Mad2-induced arrest. I found that TRIP13 knockdown did not synergize with, and TRIP13 overexpression did not block, this low-dose nocodazole arrest (Fig. 2.20A,B). This suggests that there is a qualitative difference in the role of TRIP13 in a nocodazole-dependent kinetochore produced arrest versus a Mad2-overexpression induced arrest. Others have shown that there can be different requirements for disassembly of different pools of MCC (Ma and Poon, 2011).

A potential source for non-kinetochore generated MCC is from cytosolic conversion of O-Mad2 to C-Mad2. Mad2 has previously been shown to spontaneously convert from O-Mad2 to C-Mad2 (Luo et al., 2004), although at slow rates that would not be sufficient for responsiveness to kinetochore attachment status. However, over time, this spontaneous conversion could produce a sufficient amount of kinetochore-independent inhibitory complexes and the cell may need a mechanism to disrupt them. Mad2 can directly inhibit APC/C-Cdc20, but requires a 50x higher concentration than BubR1, and this is ~15x more than its estimated concentration in mitotic HeLa cells (Tang et al., 2001). Mad2 overexpression may, by mass action, cause an increase in the amount of direct inhibition of APC/C-Cdc20 or spontaneous MCC formation. There is some evidence for these multiple pools in yeast, where Mad2-overexpression can cause a

kinetochore-independent arrest (Mariani et al., 2012). If TRIP13 were more critical for reversing the formation of this type of complex, it would explain my results showing a clear differential importance for TRIP13 in a nocodazole versus Mad2-induced arrest (Fig. 2.20A,B). Another potential non-kinetochore source of MCC is production from the nuclear pore in interphase (Rodriguez-Bravo et al., 2014). Given TRIP13 overexpression's potential ability to affect Mad1:Mad2 complex formation in interphase (Wang et al., 2014), the effect of TRIP13 on this pool of MCC deserves further study as well. This new model of TRIP13's role in the checkpoint is summarized in Fig. 3.1.

A surprising and interesting phenotype that has been reported in TRIP13 knockout cells is their deficiency in producing a robust checkpoint response to nocodazole (Ma and Poon, 2016). I corroborated those results in my TRIP13 knockout cells (Fig. 2.16B), but found that when Mad2 was overexpressed, TRIP13 knockout cells strongly arrested and regained the ability to form checkpoint complexes (Figs. 2.16C and 2.21A). The previously studied TRIP13 knockout cells showed the vast majority of Mad2 was present in the closed conformer (Ma and Poon, 2016), and the authors speculated that recycling of C-Mad2 to O-Mad2 by TRIP13 may be necessary for checkpoint complex formation in the presence of nocodazole. It is possible that Mad2 overexpression is providing a greater source of newly produced O-Mad2, even in the absence of TRIP13, to allow complex formation to still take place.

**Figure 3.1. Multiple pathways for mitotic checkpoint complex assembly and disassembly.**

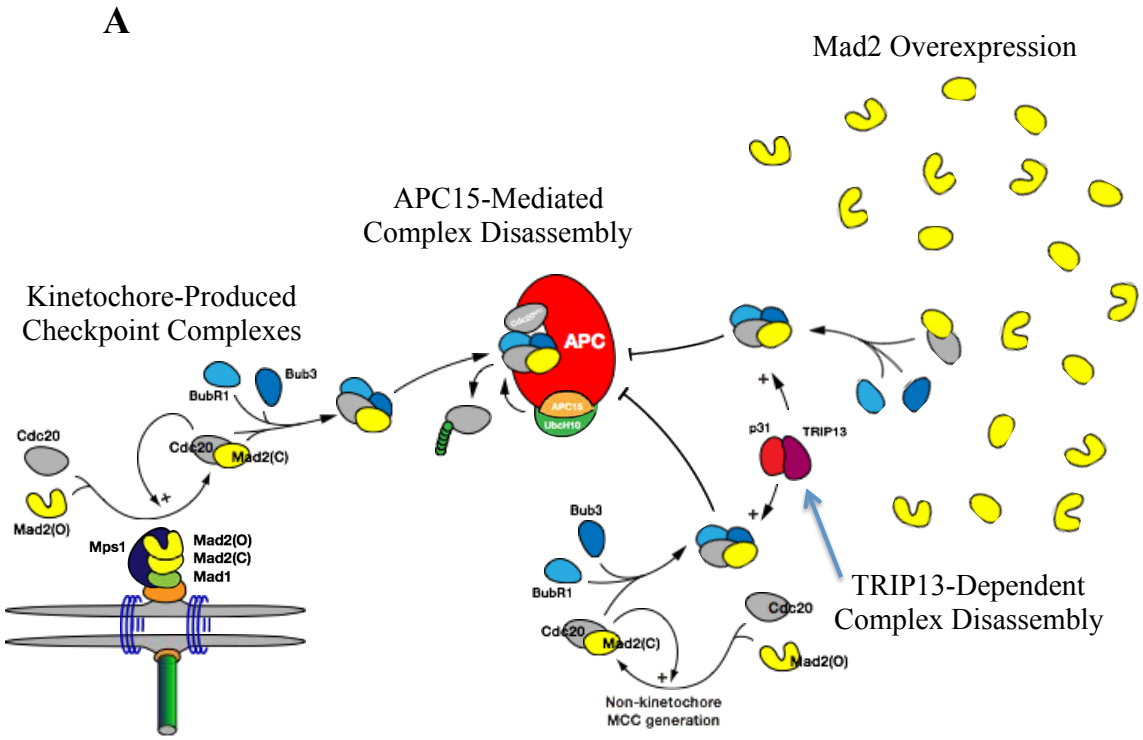


**Figure 3.1. Multiple pathways for mitotic checkpoint complex assembly and disassembly.**
(**A**) Model of multiple pathways for checkpoint complex assembly and disassembly. Kinetochore-produced complexes are largely independent of TRIP13-mediated disassembly, and can be disassembled through APC15-mediated ubiquitination of MCC bound to APC/C. Mad2 overexpression-produced complexes and non-kinetochore generated MCC are dependent on TRIP13 for disassembly. Figure made by Dr. Juan Manuel Schvartzman.

TRIP13's putative role is in disassembling mitotic checkpoint complexes, however, due to the deficiency in checkpoint signaling in TRIP13 knockout cells, it is difficult to assess if these cells have a reduced ability to disassemble complexes. Since mitotic arrest can be induced in TRIP13 knockout cells with Mad2 overexpression, I tested if the Mps1 inhibitor, reversine, could induce these cells to disassemble checkpoint complexes and exit mitosis. I found that cells arrested with Mad2 overexpression and TRIP13 knockout, or knockdown, were resistant to reversine-induced exit (Fig. 2.21). Further, these cells had a deficiency in their ability to disassemble complexes (Fig. 2.22). These results suggest the arrest I see when overexpressing Mad2 in TRIP13 deficient cells is due to a critical role for TRIP13 in disassembling Mad2-produced complexes.

While further work needs to be done to fully understand the mechanism of the relatively mild effects of TRIP13 loss on an unperturbed mitosis versus its necessity in Mad2-overexpressing cells, we can take advantage of this relationship as a potential way to target Mad2-overexpressing cells. In normal cells, reduction of TRIP13 caused only a mild effect on proliferation *in vitro* (Fig. 2.13A). Additionally, genetically engineered TRIP13 hypomorph mice with severe reductions in TRIP13 protein levels are viable and grossly normal, although born at non-mendelian ratios and sometimes presenting with smaller body size (Li et al., 2007; Roig et al., 2010). However, in Mad2-overexpressing cells, TRIP13 knockdown caused severe reductions in proliferative capacity *in vitro* (Fig. 2.13A) and in tumor formation (Fig. 2.14B,C). Further strengthening the evidence for the synthetic lethality between Mad2 overexpression and TRIP13 loss, I also observe that cells that eventually escape growth inhibition either regain TRIP13 expression or lose

Mad2 induction (Figs. 2.15, 2.18). Previous work has shown inhibiting APC/C activity by depleting Cdc20 can be an effective way to reduce cancer cell proliferation (Manchado et al., 2010), however, this approach will probably have significant toxicity to any dividing cell, similar to antimitotic chemotherapeutics. The approach of targeting TRIP13 may potentially have a better toxicity profile than these other approaches, as it should only cause severe mitotic arrest in Mad2-overexpressing tumor cells.

In a previous effort to target Mad2 overexpressing cells, Bian et al. performed a synthetic genetic array screen in yeast for genes whose deletion specifically reduces the viability of Mad2 overexpressing cells, and identified PPP2R1A, a subunit of the phosphatase PP2A, as a potential target (Bian et al., 2014). As an AAA-ATPase, TRIP13 is potentially a more readily druggable target. Other AAA-ATPases, particularly p97, have been targeted with small molecules that show promise as cancer therapeutics (Anderson et al., 2015; Zhou et al., 2015). The strength of the synthetic lethality of TRIP13 loss with Mad2 overexpression makes targeting TRIP13 a new therapeutic opportunity in the management of aneuploid tumors.

# CHAPTER 4

# PERSPECTIVES AND FUTURE DIRECTIONS

## 4.1 Role of TRIP13 in the Mitotic Checkpoint

In this study, I identified Mad2-overexpression as a condition where TRIP13 becomes critical for mitotic exit. This is in contrast to an unperturbed mitosis, or a nocodazole-induced arrest, where modulation of TRIP13 has only mild effects. This potentially resolves some questions, as well as poses new ones, for how TRIP13 works in mitosis. While having the *in vitro* ability to disassemble Mad2-Cdc20 complexes, it was unclear when and where TRIP13 was using this activity in cells, considering the mild phenotypes observed. Mad2 overexpression is an interesting condition to study, as it is frequently overexpressed in cancer, which may have inadvertently led to the identification of the actual substrate for TRIP13 in the cell. Understanding the differences between the condition TRIP13 appears critical (Mad2 overexpression), and the conditions where it appears not essential for silencing (unperturbed mitosis, and nocodazole arrest), will be crucial for further understanding TRIP13's function.

One explanation that may fit my data is that TRIP13 works primarily on a kinetochore-independent pool of mitotic checkpoint complex or Mad2-Cdc20 complex. This could distinguish Mad2-induced complex formation versus that formed during a nocodazole arrest, as Mad2 overexpression has been shown in yeast to be able to activate the checkpoint independent of kinetochores (Mariani et al., 2012). In a normal cell, when Mad2 is not overexpressed, Mad2 may accumulate in its closed conformation over time, and may need TRIP13 to recycle it back to the open conformer to allow kinetochore-

dependent MCC formation. This could explain the presence of almost exclusively the closed conformer in TRIP13 knockout cells, and their inability to robustly activate the checkpoint in nocodazole (Ma and Poon, 2016) and Figs. 2.16B, 2.21A. While our results showing TRIP13 overexpression and knockdown did not significantly shorten or lengthen, respectively, the timing of a nocodazole arrest, the Mad2-recycling role may obscure the importance of TRIP13 in these circumstances. To disentangle the potential contributions of TRIP13 in checkpoint complex disassembly from those in recycling C-Mad2 to O-Mad2, an interesting experiment would be to complement TRIP13 knockout cells with an auxin-inducible degron tagged version of TRIP13. After arresting cells in mitosis with nocodazole, one could test the necessity of TRIP13 for exit from a nocodazole arrest by depleting TRIP13 and then releasing cells from the arrest. If after allowing complexes to form normally in nocodazole, this acute depletion of TRIP13 causes prolongation of mitosis in nocodazole treated cells, it would suggest TRIP13 does, in fact, also play a role in this type of arrest, but is counterbalanced by loss of checkpoint complex production.

There are a number of potential experiments that may advance our understanding of TRIP13. To further investigate the role of TRIP13 in a kinetochore-independent arrest, one could test the effect of overexpressing different Mad2 mutants, in comparison to wild-type, in TRIP13 knockout cells. There are Mad2 dimerization mutants that would prevent kinetochore production of C-Mad2, but should still allow it to bind to Cdc20 and BubR1. One mutant in particular, tested in yeast, with the residue and interface conserved in mammalian Mad2, is the R126A mutant, which was able to still induce a kinetochore-

independent arrest when overexpressed (Mariani et al., 2012). They also used a Bub1-GFP construct to show that a Mad2-overexpression arrest occurs even when kinetochores are no longer producing checkpoint signal. Additionally, one could test the expected lack of an effect of TRIP13 depletion on disassembly of MCC bound to APC/C by comparing siRNA against TRIP13, p31comet and APC15. One could arrest cells in mitosis to generate APC/C-bound MCC and then induce disassembly with reversine in the various conditions followed by immunoprecipitation of APC3 and blotting for the effect on MCC component binding, as in (Mansfeld et al., 2011).

It may also be interesting to test the effect of modulating TRIP13 with or without Mad2 overexpression on the production of interphase MCC. Preliminary evidence from (Wang et al., 2014) showed that TRIP13 overexpression may disrupt Mad1:Mad2 complexes at nuclear pores in interphase. It may be worth better resolving the localization of TRIP13 in interphase, and specifically test if it localizes to nuclear pores, similar to p31comet (Fava et al., 2011). Further, in the high-throughput shRNA screen for modulators of Mad2 proliferation (Fig. 2.4), shRNA against numerous nuclear pore genes rescued the viability of Mad2-overexpresing cells (data not shown), which may suggest nuclear pores are necessary for the Mad2 overexpression phenotype.

## 4.2 Roles of TRIP13 Outside of the Mitotic Checkpoint

The ability of TRIP13 in meiosis to regulate additional HORMA-domain containing proteins (Wojtasz et al., 2009), suggests that TRIP13 may have roles in other pathways that rely on HORMA proteins. A previous study found a potential role for

TRIP13 in DNA repair, with TRIP13 binding to Ku70/Ku80 and knockdown causing reduced non-homologous end joining (NHEJ) activity in repair assays (Banerjee et al., 2014). It's unclear if this effect is mediated by TRIP13 interactions with HORMA-domain containing proteins, but Rev7 (Mad2L2 in humans) contains the HORMA domain and has been shown to play a role in DNA repair and repair pathway choice (Boersma et al., 2015; Xu et al., 2015). Additionally, the autophagy proteins, Atg13 and Atg101, contain HORMA domains (Suzuki et al., 2015). It would be interesting to test TRIP13 knockout cells for effects on DNA repair and autophagy phenotypes. Lastly, p31comet has recently been found to play an important role in inhibiting Mad2-induced blockade of insulin signaling (Choi et al., 2016). Whether or not TRIP13 plays a role in helping p31comet perform this function is unknown and should be tested.

### 4.3 TRIP13 as a Target in Cancer

I also identified TRIP13 as a potential novel target for tumors that overexpress Mad2. There are many steps in between the initial findings here, and actually bringing the approach to the clinic. First, a small molecule would be the easiest way to target TRIP13, which, as an AAA+ ATPase, should be relatively easy to screen for. Another ATPase in the same family, p97/VCP, has had small molecules identified from screens against its ATPase activity (Anderson et al., 2015; Zhou et al., 2015). Studies by (Eytan et al., 2014) and (Ye et al., 2015) have identified *in vitro* conditions where TRIP13's activity can be measured, and may be starting points for designing a chemical library screen. An initial experiment should be to test if an ATPase-dead mutant of TRIP13 fails to rescue the mitotic exit and proliferation defects in TRIP13 knockout cells with Mad2

overexpression. This will be important to confirm that targeting the ATPase activity of TRIP13 will be sufficient to induce the desired effects. TRIP13 ATPase activity has previously been shown to be required for its effects on MCC disassembly and mitotic exit (Wang et al., 2014; Ye et al., 2015).

Secondly, the findings presented here should be validated in other systems where Mad2 and/or TRIP13 are overexpressed, such as cancer cell lines, or cell lines where the Rb and/or p53 pathways are dysregulated. I attempted to perform this experiment using the HPV E6/E7 proteins to inhibit p53 and Rb pathways, but the only modest increase in Mad2 and TRIP13 in these cells may suggest I did not adequately inhibit these pathways (Fig. 2.12). Repeating these experiments, or testing the effects of TRIP13 loss in other systems of Rb/p53 pathway dysregulation will be useful for being able to generalize these findings to other systems. Additionally, TRIP13 knockdown in head and neck cancer cell lines has previously been shown to slow their proliferation
(Banerjee et al., 2014). It would be worthwhile testing in these cells, and across a panel of cancer cell lines, the effect of TRIP13 knockdown on mitotic duration, and if the severity of the phenotypes correlate with the levels of Mad2 expression in these cell lines.

One last consideration is the possibility of resistance to TRIP13 targeted therapy, which I have already observed in my system, due to either loss of TRIP13 knockdown or loss of induced Mad2 overexpression (Figs. 2.15, 2.18). This is a concern, as continued Mad2 overexpression may not be required for tumor maintenance (Sotillo et al., 2010). However, the cause of Mad2 overexpression in cancer cells is likely due to loss of tumor

suppressor pathways that *are* drivers of tumor growth, so it may not be as easy to lose Mad2 overexpression in human tumors. Further, while resistance may eventually arise, the evidence of growth inhibition shown here in xenografts, as well as in *in vivo* experiments performed by others (Banerjee et al., 2014), demonstrate that TRIP13 inhibition may still be sufficient to delay tumor growth.

## 4.3 Mad2-Induced DNA Damage and Chromothripsis

Prior to focusing on TRIP13, I had started a project to understand the mechanisms of accumulating DNA damage in Mad2-overexpressing cells. Below are my initial findings, and suggestions for potential future directions. Mad2 overexpression in MEFs causes both numerical and structural instability (Sotillo et al., 2007). Additionally, Mad2 overexpression in RPE-M cells slowly causes accumulation of γH2AX over time (Fig. 4.1A). I sought to determine the mechanisms of this DNA damage. A number of recent papers have suggested mechanisms by which chromosomal mis-segregation can lead not only to aneuploidy, but also to DNA damage in mis-segregated chromosomes. One mechanism occurs when mis-segregated chromosomes form micronuclei, which are later damaged in future cell cycles due to defective recruitment of DNA replication and repair factors to the micronucleus (Crasta et al., 2012). When chromosomes are not properly attached to spindle poles, they can remain as lagging chromosomes or anaphase bridges, and not move with the remaining chromosomes toward the poles. I observe this in Mad2 overexpressing RPE-M cells in time-lapse imaging, where lagging chromosomes or anaphase bridges resolve into micronuclei in the daughter cells after cytokinesis (Fig. 4.2A). I also observe an accumulation of micronuclei over time in RPE-M during

continued Mad2 overexpression (Fig. 2.7). Notably, the majority of these micronuclei are γH2AX positive, and may contribute to the γH2AX signal accumulating in these cells.

An additional mechanism of chromosome mis-segregation leading to DNA damage is where a mis-segregated chromosome caught in the cleavage furrow is directly damaged during an attempted cytokinesis (Janssen et al., 2011). I may see some evidence of a similar phenotype in Mad2-overexpressing RPE-M cells. Specifically, I see numerous cells that failed cytokinesis and are multinucleated, however, I see occasional cells with abnormal centromere signals at the interface between two lobes of a nucleus, potentially indicative of the point of cytokinesis failure (Fig. 4.3A). Notably, the site of the abnormal centromere signal is also γH2AX positive. Thus, this mechanism of trapped chromatin in the cleavage furrow may be another source of DNA damage in Mad2-overexpressing cells. In the majority of multinucleated Mad2-overexpressing cells produced after cytokinesis failure multiple γH2AX foci are scattered throughout the nuclei, but do not consistently overlap with centromere signals (Fig. 4.4A). A quantification of the accumulation of micronuclei and multinucleated cells during Mad2 overexpression is shown in Fig. 4.5A.

**Figure 4.0.1. DNA Damage in Mad2 Overexpressing Cells.**

**A**

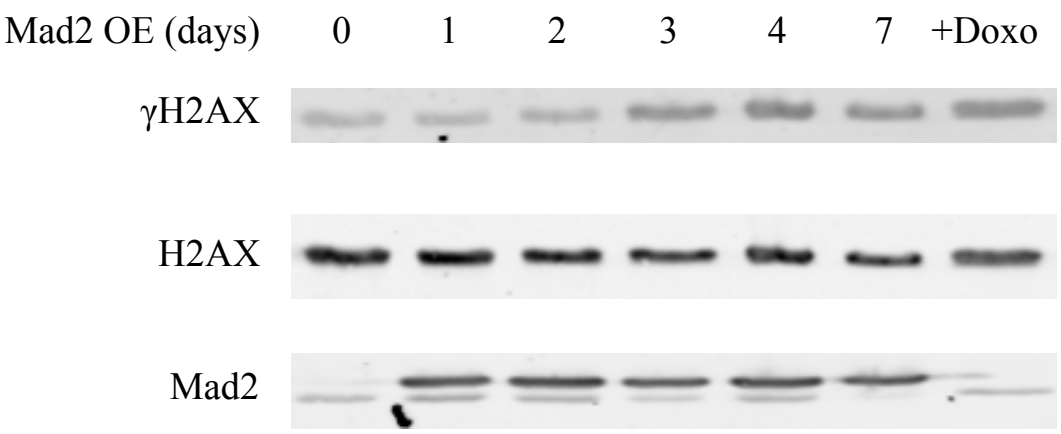


**Figure 4.1. DNA Damage in Mad2 Overexpressing Cells.**
(**A**) Western blot timecourse of DNA damage after Mad2 overexpression in RPE-M cells compared to 12 hours doxorubicin (+Doxo).

**Figure 4.2. Time-Lapse Imaging Stills of Chromosome Mis-segregation in RPE-M Cells.**

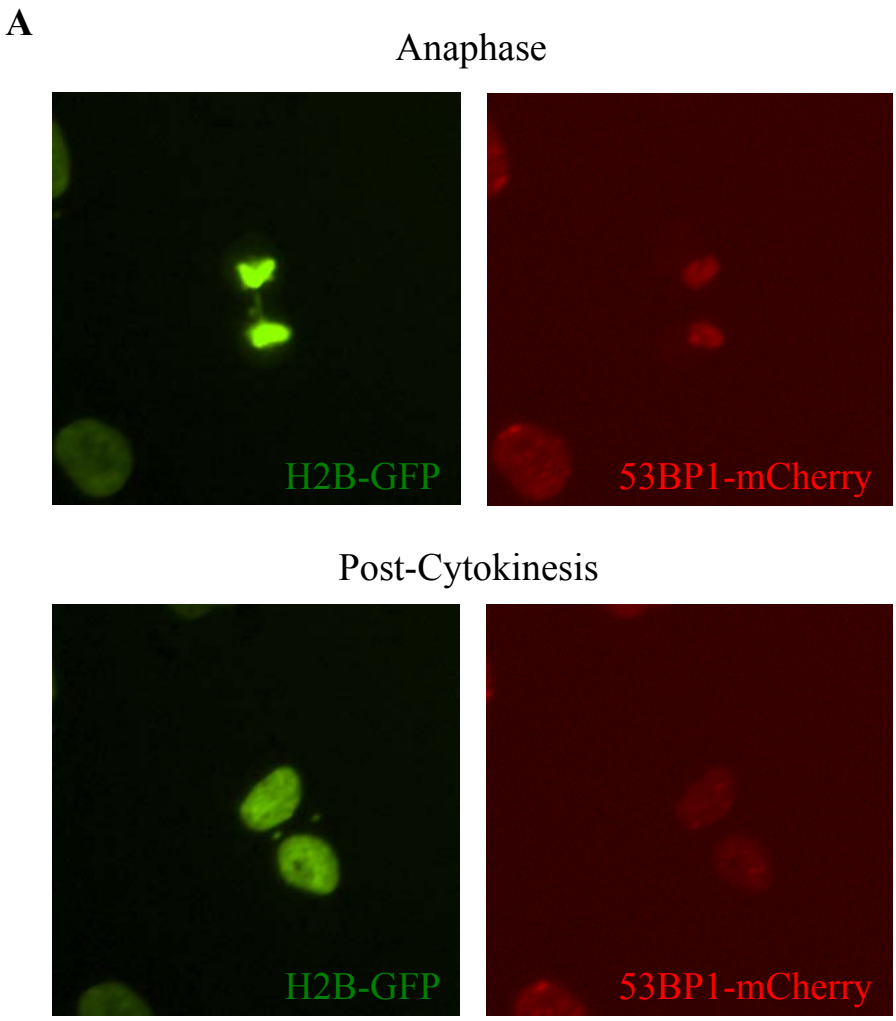


**Figure 4.2. Time-Lapse Imaging Stills of Chromosome Missegregation in RPE-M Cells.**
(**A**) Stills from time-lapse imaging of H2B-GFP and 53BP1-mCherry RPE-M cells. Lagging chromosome and anaphase bridge (top) resolve to micronuclei after mitotic exit (bottom).

**Figure 4.3. DNA Damage in Mad2-Overexpressing Cell After Failed Cytokinesis.**

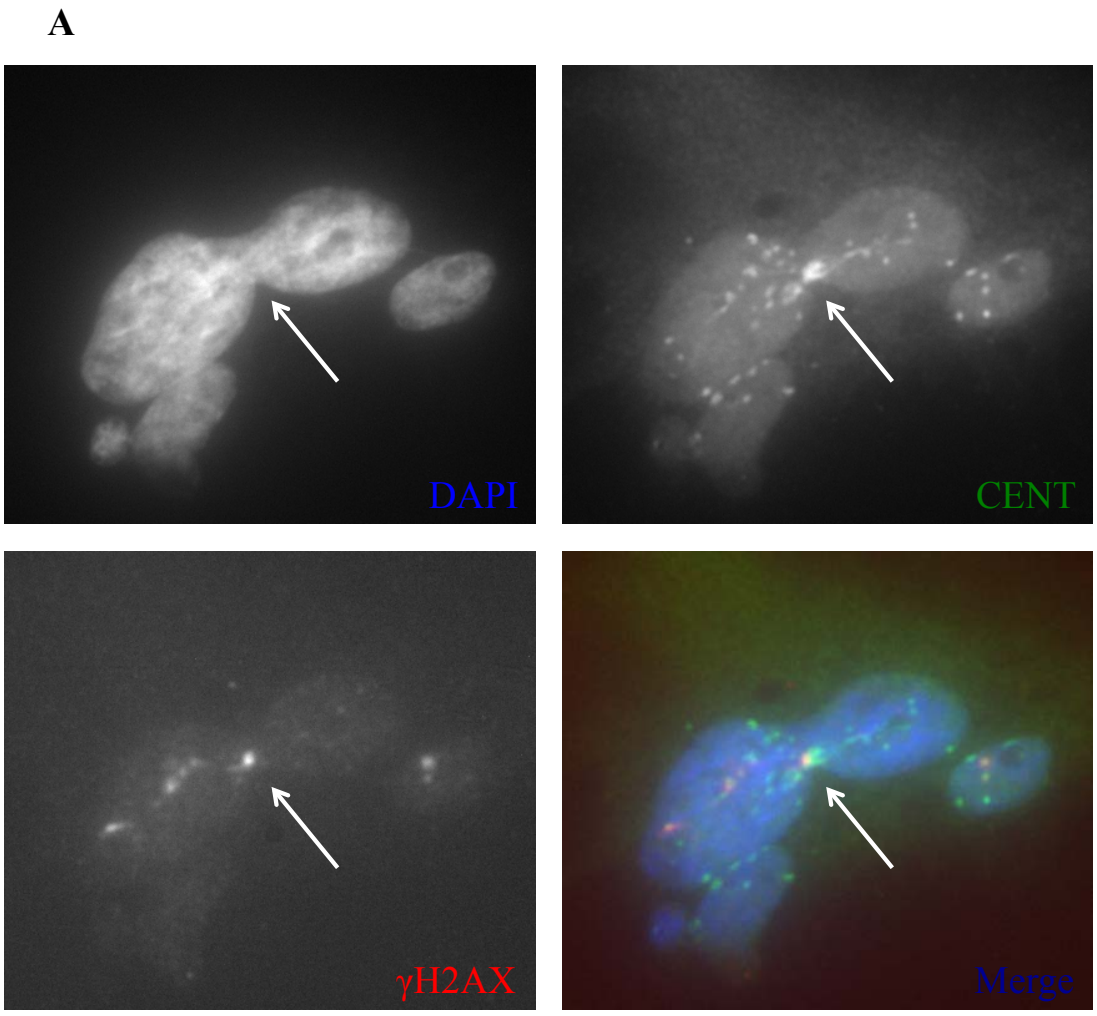


**Figure 4.3. DNA Damage in Mad2-Overexpressing Cell After Failed Cytokinesis.**
(**A**) Immunofluorescence imaging of RPE-M cell after 9 days Mad2 overexpression. Arrow points to the interface in a multi-lobed nucleus with γH2AX positive distorted centromere signal.

**Figure 4.4. DNA Damage in Multinucleated Cell.**

**A**

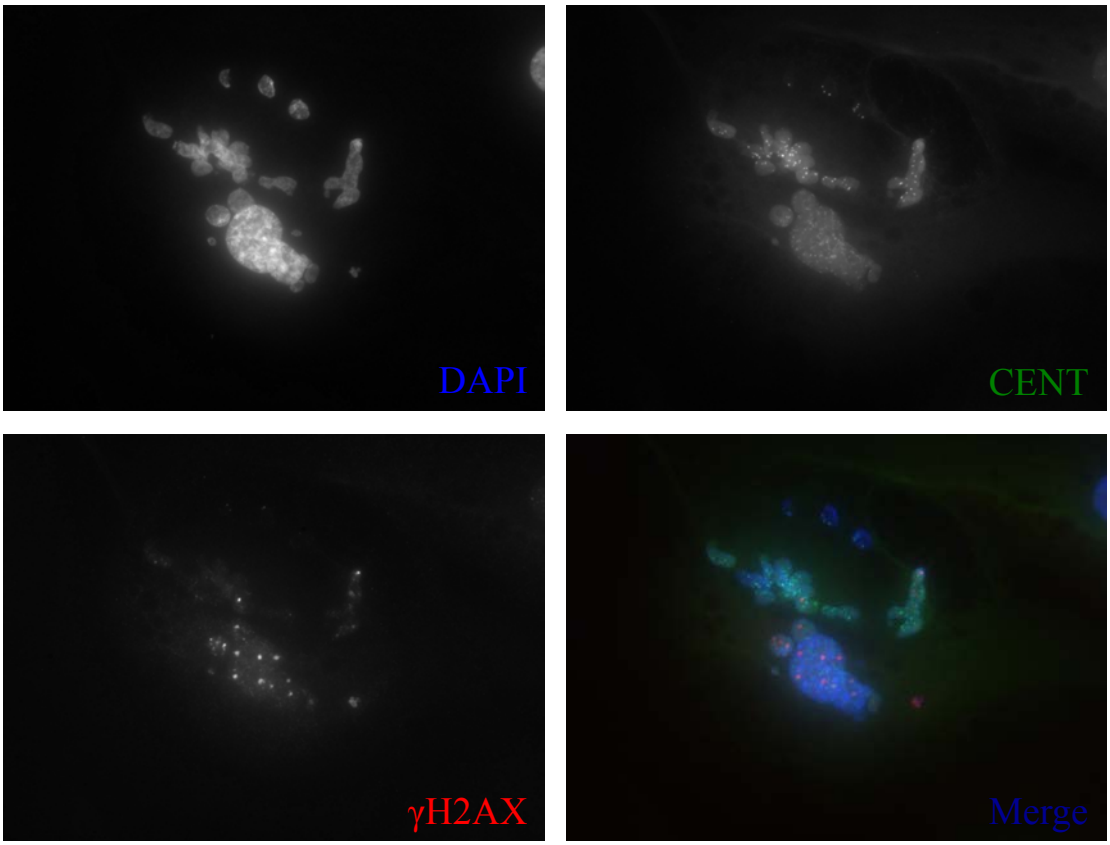


**Figure 4.4. DNA Damage in Multinucleated Cell**
(**A**) Immunofluorescence imaging of RPE-M cell after 9 days Mad2 overexpression. Multiple γH2AX foci are visible throughout the nucleus.

**Figure 4.5. Quantification of Micronuclei and Multinuclei after Mad2 Overexpression.**

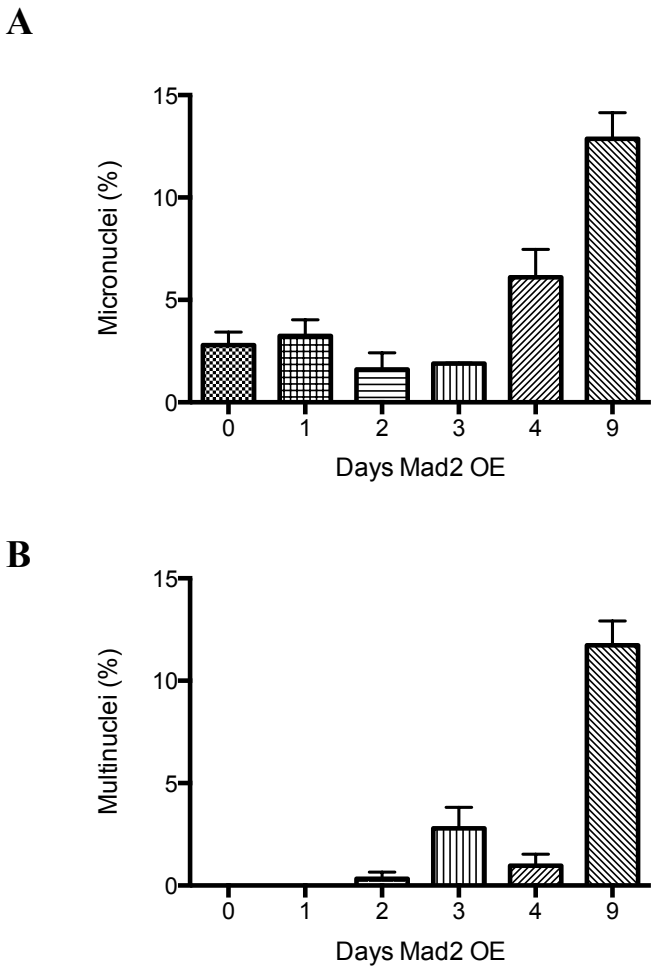


**Figure 4.5. Quantification of Micronuclei and Multinuclei after Mad2 Overexpression.**

(**A**) Quantification of micronuclei in RPE-M cells with 0, 1, 2, 3, 4 or 9 days Mad2 overexpression. Micronuclei were counted in 100 cells in triplicate by DAPI staining for small extra-nuclear DAPI signal. (**B**) Quanitifcation of multinucleated RPE-M cells with 0, 1, 2, 3, 4 or 9 days Mad2 overexpression. Multinuclei were counted in 100 cells in triplicate by DAPI staining for small multiple large nuclei in a single cell.

Lastly, prolonged mitosis frequently leads to a p53-dependent cell cycle arrest, and a recent study found that p53 may be activated due to telomere uncapping leading to ends recognized as DNA damage during a prolonged mitosis (Hayashi et al., 2012). Additionally, the cell can sense a prolonged mitosis through a 53BP1-USP28 pathway, independent of their role in DNA repair, which causes stabilization of p53 and induces cell cycle arrest (Fong et al., 2016; Lambrus et al., 2016). Chromosome missegregation itself may also be sensed by p53 through an H3.3 Ser31 phosphorylation that occurs on missegregating chromosomes (Hinchcliffe et al., 2016). I attempted to look at DNA damage in metaphase spreads of RPE-M cells after Mad2 overexpression by using cytospin to visualize mitotic chromosomes. I did notice some localization of γH2AX signal near ends of chromosomes, although telomere fluorescence *in situ* hybridization would be necessary to confirm that these signals are actually at telomeres (Fig 4.6A).

Taken together, this data suggests all three of these mechanisms may be playing a role in the accumulation in γH2AX signal in Mad2-overexpressing cells. It may be worthwhile to further investigate the timing and mechanism of DNA damage by using a live-cell fluorescent sensor of DNA damage. I had attempted to use 53BP1, but it does not localize to micronuclei or damage in mitosis efficiently (Fig 4.7A), whereas MDC1 appears able to localize to DNA damage in micronuclei (Fig. 4.7B). Thus, fluorescently labeled MDC1 may be useful in time-lapse imaging experiments for determining the timing and location of DNA damage in Mad2-overexpressing cells.

**Figure 4.6. DNA Damage Near Chromosome Ends in Cytospun Mad2-Overexpressing Mitotic Cells.**

**A**

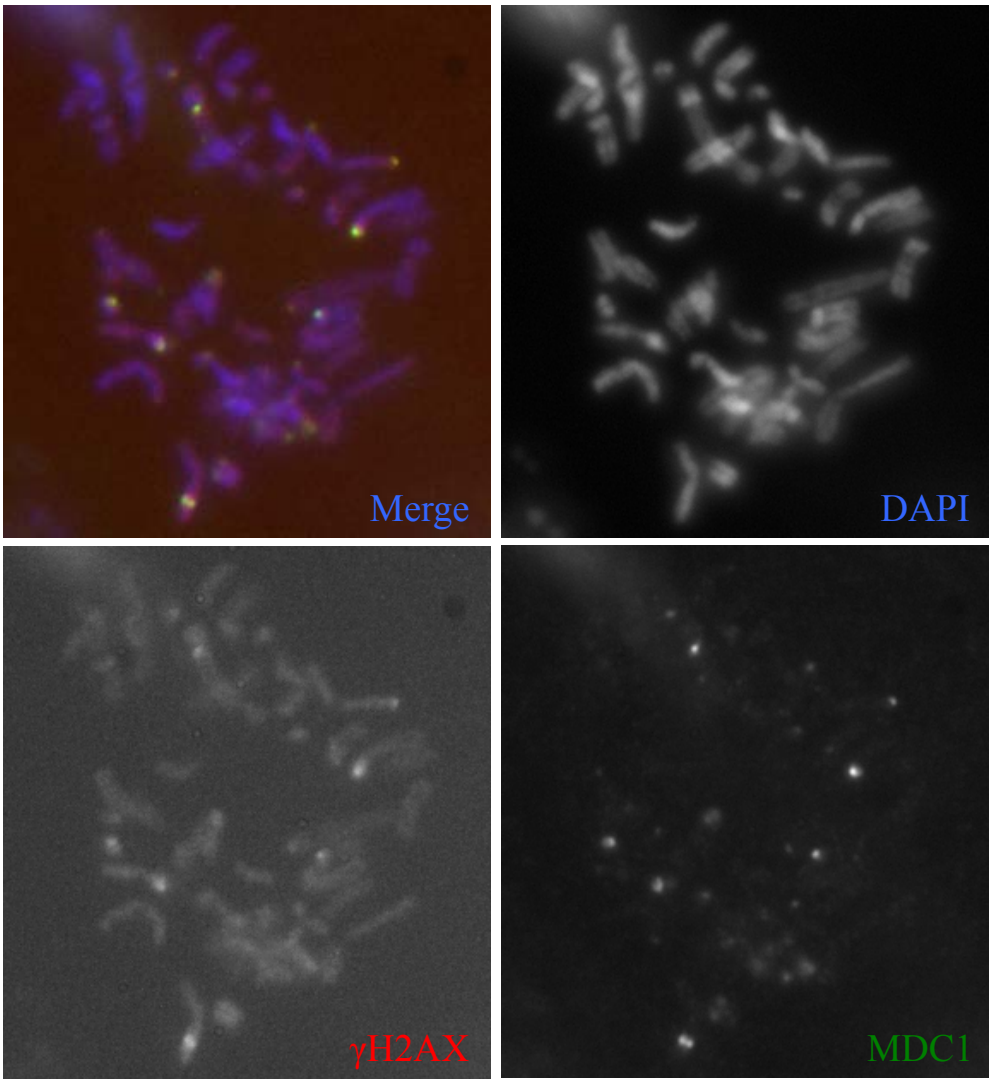


**Figure 4.6. DNA Damage Near Chromosome Ends in Cytospun Mad2-Overexpressing Mitotic Cells.**
(**A**) Immunofluorescence imaging of cytospun RPE-M cell after 2 days Mad2 overexpression.

**Figure 4.7. MDC1, but not 53BP1, Localizes to DNA Damage in Micronuclei.**

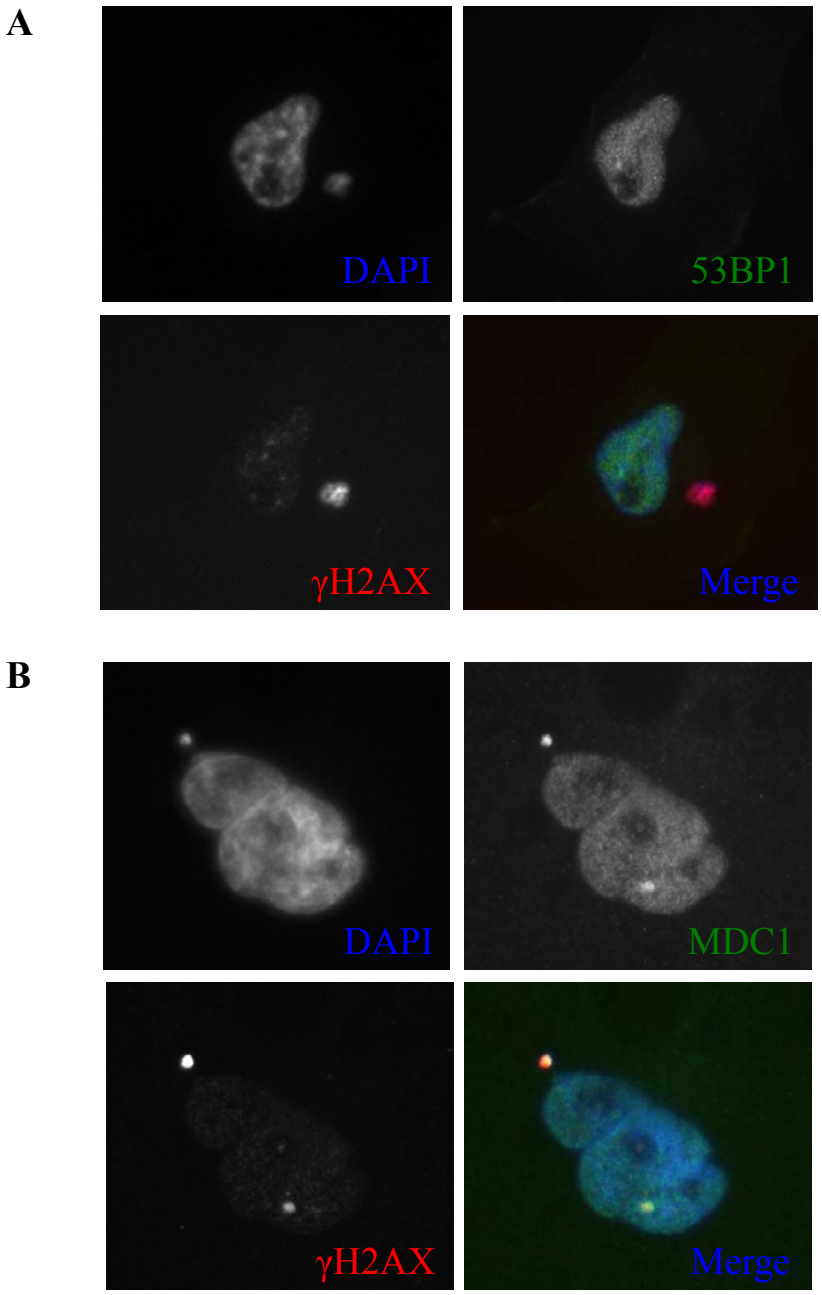


**Figure 4.7. MDC1 but not 53BP1 Localizes to DNA Damage in Micronuclei**
(**A**) 53BP1 and γH2AX immunofluorescence imaging of RPE-M cell with micronucleus after Mad2 overexpression. (**B**) MDC1 and γH2AX immunofluorescence imaging of RPE-M cell with micronucleus after Mad2 overexpression.

Chromothripsis, the pulverization of a single chromosome that is then stitched back together with extreme numbers of intrachromosomal rearrangements, has recently been identified as a mutational type in human cancers (Stephens et al., 2011). This accumulation of many mutations simultaneously is redefining the view of how some tumors evolve, where single events can lead to punctuated evolution of the tumor, instead of the slow, stepwise, fashion tumor development was previously expected to follow (Notta et al., 2016). Mechanistically, how chromothripsis occurs is still being understood, but recent papers have suggested that micronuclei and telomere crisis can induce chromothripsis-like phenotypes in cells (Maciejowski et al., 2015; Zhang et al., 2015a). Due to the ability of Mad2 overexpression to generate γH2AX positive micronuclei, Mad2 overexpression may also induce chromothripsis. It may be interesting to confirm if Mad2 overexpression can induce these phenotypes both *in vitro* as well as in spontaneous tumors in mice overexpressing Mad2. To my knowledge, chromothripsis has not been observed or modeled in mice, so if transient Mad2-overexpression can induce tumors with chromothripsis, this may be a useful model system to study the evolutionary dynamics in tumors with this form of DNA damage.

## 4.4 Myc-Induced Checkpoint Hyperactivation and SUMOylation Dependency

One last project that I had initiated, but did not generate any preliminary data on, was testing if checkpoint gene overexpression could be driven by Myc, and if checkpoint gene overexpressing cells are more dependent on SUMOylation pathways. This project comes from the finding that Myc overexpression is synthetic lethal with inhibition of SUMOylation machinery (Kessler et al., 2012). Specifically, the authors found that a set

of Myc-activated genes became instead repressed by Myc when SUMOylation machinery was inhibited. Interestingly, a large number of the genes that were differentially regulated by Myc and SUMOylation were mitotic genes correlated with Mad2 overexpression and genes in the CIN70 chromosomal instability signature (Fig. 4.8A,B and (Carter et al., 2006)). Further, Myc has been previously shown to be able to induce overexpression of checkpoint genes, including Mad2, leading to a prolongation of mitosis (Menssen et al., 2007). These findings suggest a number of potentially interesting future directions. First, does Myc overexpression drive checkpoint gene overexpression similar to loss of Rb/p53 pathways, and is the chromosomal instability dependent on high Mad2 levels? Second, are Myc-driven tumors thus more dependent on TRIP13, making TRIP13 a therapeutic target in these tumors? Lastly, is inhibition of SUMOylation machinery similarly synthetic lethal with other mechanisms of checkpoint gene overexpression, such as loss of Rb/p53 pathways or direct Mad2-overexpression?

**Figure 4.8. SUMOylation-Dependent Myc Gene Signature Similar to Mitotic Checkpoint Gene Signature Overexpressed in Cancer.**

**A**

Genes Correlated with Mad2

| | | | |
|---|---|---|---|
| 1.000 | MAD2L1 | 1.000 | MAD2L1 |
| 0.965 | CCNA2 | 0.948 | CCNB2 |
| 0.965 | TTK | 0.948 | BUB1B |
| 0.955 | CCNB1 | 0.948 | UBE2C |
| 0.955 | CCNB1 | 0.948 | TOP2A |
| 0.950 | UHRF1 | 0.948 | DTL |
| 0.948 | MELK | 0.947 | CENPK |
| 0.948 | CASC5 | 0.944 | NEK2 |
| 0.948 | KIF11 | 0.944 | KIF18B |
| 0.948 | CDC20 | 0.944 | GTSE1 |
| 0.948 | KIF2C | 0.940 | SPAG5 |
| 0.948 | HMMR | 0.939 | RACGAP1 |
| 0.948 | KIF14 | 0.939 | TYMS |
| 0.948 | - | 0.939 | TYMS |
| 0.948 | PBK | 0.939 | CDK1 |
| 0.948 | TPX2 | 0.939 | CDK1 |
| 0.948 | KIF20A | 0.932 | FBXO5 |
| 0.948 | NUF2 | 0.932 | MLF1IP |
| 0.948 | - | 0.931 | GINS1 |
| 0.948 | BIRC5 | 0.931 | ZWINT |
| 0.948 | NUSAP1 | 0.931 | CDK1 |

Oncomine, Janoueix-Lerosey Brain

Genes in CIN70 Signature (Carter et al., 2006)

CIN70 Carter et al., 2006

1. TPX2
2. PRC1
3. FOXM1
4. CDC2
5. C20orf24/TGIF2
6. MCM2
7. H2AFZ
8. TOP2A
9. PCNA
10. UBE2C
11. MELK
12. TRIP13
13. CNAP1
14. MCM7
15. RNASEH2A
16. RAD51AP1
17. KIF20A
18. CDC45L
19. MAD2L1
20. ESPL1
21. CCNB2
22. FEN1
23. TTK
24. CCT5
25. RFC4
26. ATAD2
27. ch-TOG
28. NUP205
29. CDC20
30. CKS2
31. RRM2
32. ELAVL1
33. CCNB1
34. RRM1
35. AURKB
36. MSH6
37. EZH2
38. CTPS
39. DKC1
40. OIP5
41. CDCA8
42. PTTG1
43. CEP55
44. H2AFX
45. CMAS
46. BRRN1
47. MCM10
48. LSM4
49. MTB
50. ASF1B
51. ZWINT
52. TOPK
53. FLJ10036
54. CDCA3
55. ECT2
56. CDC6
57. UNG
58. MTCH2
59. RAD21
60. ACTL6A
61. GPIandMGC13096
62. SFRS2
63. HDGF
64. NXT1
65. NEK2
66. DHCR7
67. STK6
68. NDUFAB1
69. KIAA0286
70. KIF4A

**Figure 4.8. SUMOylation-Dependent Myc Gene Signature Similar to Mitotic Checkpoint Gene Signature Overexpressed in Cancer.**
(**A**) Genes whose expression is correlated with Mad2 in human cancer (oncomine.org Janoueix-Lerosey Brain data set) (Left). CIN70 gene signature from Carter et al., 2006 (Right). Circled in red are the top 17 ranked genes with SUMOylation dependent Myc expression

# CHAPTER 5

# METHODS

## Cell culture and chemicals

RPE2 cells were cultured in a 1:1 mixture of DME and Ham's F12 and supplemented with 15 mM HEPES, 10% fetal bovine serum, L-glutamine, and 100U/ml penicillin/streptomycin. MEFs were cultured in DME supplemented with 10% fetal bovine serum, L-glutamine, 0.001% B-Mercaptoethanol, and 100U/ml penicillin/streptomycin. IMR90 cells in MEM media supplemented with 10% fetal bovine serum, L-glutamine, and 100U/ml penicillin/streptomycin. Multiple nocodazole (15-200 ng/ml) (Sigma) and reversine (0.5-1 uM) (Sigma) concentrations were used, as indicated in figure legends. Other chemicals were used at the following concentrations: 10 uM MG132 (Enzo Life Sciences), 10 uM RO-3306 (Calbiochem), 5 μg/ml doxycycline (BD Biosciences), 0.2 μg/ml doxorubicin (Sigma).

For cell synchronization for Cdc20 immunoprecipitation, cells were synchronized with 20 hours treatment of Cdk1 inhibitor RO-3306 +/- doxycycline 8 hours after 10 uM RO-3306 addition. Cells were released into fresh media for 30 minutes followed by treatment with 50 ng/ml nocodazole and 10 uM MG132 for 3 hours +/- 1 uM reversine for the last 1.5 hours. Mitotic cells were harvested by mitotic shakeoff.

For IMR90 cell synchronization, cells were cultured in serum-free media for 3 days followed by release into serum containing media and harvest at the indicated timepoints.

## Description of constructs

Retroviral constructs were produced by transfecting 293GP2 cells and Lentiviral constructs were produced by transfecting 293T cells using standard Lipofectamine 2000 (Thermo Fisher) protocol. Target cells were transduced with 1:1 viral media to fresh media in 8 μg/ml polybrene.

All PCR amplifications was performed with Phusion Hot Start II polymerase (New England BioLabs)

Mad2-overexpressing RPE-M cells were made by co-transfecting RPE2 cells with pTRE-HA-Mad2 (mouse) and pCAGGS-rtTA (puromycin) and subsequent single cell clones were tested for Mad2 induction by Western blot. The TRIP13 overexpression construct was made by cloning TRIP13 cDNA (Open Biosystems) into pBabe-GFP. TRIP13 cDNA was amplified and cloned into a pBabe-GFP (blasticidin) construct with XhoI and MfeI/EcoRI downstream of the GFP tag. The p53 siRNA construct was cloned from pLVTH-sip53 (Addgene #12239). GFP was removed, and neomycin resistance cloned in using MluI and XmaI.

The siRNAs were obtained from Dhamacon siGenome; siT13-1: TRIP13 ORF (D-016262-01); siT13-2: TRIP13 3' UTR (D-016262-21); siCon: siGENOME non-targeting siRNA #2 (D-001210-02). Cells were transfected with 25 nM siRNAs with Lipofectamine 2000 (Thermo Fisher). Inducible shRNA constructs were cloned into the RT3REVIR shRNA backbone (derived from pQCXIX) (Fellmann et al., 2013). The antisense guide sequence for TRIP13 shRNA #1 was: ATCACCAAACACAATATTATGT, and for TRIP13 shRNA #2 was: TTTGACTTCCACATCGTATACC, and the antisense guide sequence for the Control

shRNA was: TAGATAAGCATTATAATTCCTA. Cells were selected by growing single cell clones from Venus positive cells and testing for dsRed induction and knockdown upon doxycycline addition for 3 days.

TRIP13 knockout cells were made by cloning TRIP13 gRNA (target sequence gtcgccaacggtccacgtgg) into pX330 expressing Cas9 (Addgene), by digesting the vector with BbsI and ligated to annealed and phosphorylated sgRNA oligonucleotides. RPE-M sip53-neo cells, or parental RPE cells, were nucleofected with the 5 μg px330-gRNA and 1 μg GFP in Amaxa buffer V using A-023 program on an Amaxa nucleofector as per manufacturer's protocol. Single cells were FACS sorted and clones were grown and tested for loss of TRIP13 expression by Western blot. DNA was extracted from clone 2-19 with DNeasy Blood & Tissue kit (Qiagen). DNA was amplified and sequenced for mutations at the predicted cut site by Topo cloning with the Zero Blunt TOPO PCR cloning kit (Thermo Fisher).

pLXSN-E6/E7 (Halbert et al., 1992) was a gift from the Prasad Jallepalli lab. Parental RPE cells were transduced with the vector and selected with G418 (500 μg/ml) for 10 days.

H2B-GFP (Michael Overholtzer laboratory) and 53BP1-mCherry (Addgene, #19835) constructs were transduced into RPE-M cells followed by sorting for fluorescent cells.

Time-lapse imaging and Immunofluorescence

Micronuclei were scored by counting the number of cells with DAPI signals

outside of the main nucleus. Multinucleated cells were scored by counting the number of cells with multiple large DAPI signals in a single cell. 100 cells were counted per condition, in triplicate. Cells were fixed with 4% PFA for 20 minutes at room temperature, followed by blocking with 10% normal goat serum, incubation with primary antibody (CREST 1:100, γH2AX 1:1000) at 4 degrees overnight, incubation with secondary (1:1000 goat anti-human Alexa Fluor 568 & goat anti-mouse Alexa Fluor 488) for 1 hour room temperature, DAPI 1 μg/ml 5 minutes room temperature, mounted on coverslips with Aqua-Mount (Fisher).

Immunofluorescence of MDC1 and 53BP1 were performed with Abcam ab11171 (Rabbit), and Santa Cruz sc-22760 (Rabbit), and corresponding secondary antibodies, respectively.

For time-lapse imaging, cells were plated onto 6 or 12 well glass bottom plates (MatTek) and imaged with DIC imaging using a Zeiss Axis Observer Microscope with a Plan-apochromat 20x/0.8 M27 objective and Zen Acquisition 2.0 software. Images were taken every 5 minutes, with 7 z-stacks 3 microns apart taken for each point. Mitotic duration was measured by timing from when the cells rounded to when they flattened back on the plate.

For cytospin, cells were incubated with 74 μL/10 mL colcemid in media for 2 hours. Cells were harvested by mitotic shakeoff and resuspended in 0.2% KCl and 0.2% trisodium citrate hypotonic buffer (1 mL buffer per 10 cm plate of cells) at room temperature for 5-10 minutes. Cells were cytocentrifuged onto SuperFrost Plus glass slides (Menzel-Glaser) at 1200g for 10 min in a Shandon Cytospin 4. Slides were

immediately fixed in 1% TCA for 15 minutes at 4 degrees, immunofluorescence was with proceeded as above.

Proliferation assays and Xenografts

For cell culture proliferation assays, cells were counted and plated in equal numbers, and subsequently counted and replated in equal numbers on each day of the analysis as indicated. Experiments were performed in three biological replicates. Cumulative fold was measured by multiplying the fold changes in cell number at each time point.

Xenografts were performed by injecting 1 million cells per condition subcutaneously into nude mice aged 5-6 weeks. Mice were maintained with or without doxycycline containing feed, as indicated, for the entirety of the shRNA xenograft experiment. For the TRIP13 knockout xenograft, cells were injected and mice were switched to food either with or without doxycycline when tumors became palpable ~10-50 $mm^3$. Tumor sizes were measured with calipers every week. Volume was calculated by tumor volume = $0.5*length*width^2$.

Interphase FISH for Aneuploidy

Interphase FISH staining was performed by the Molecular Cytogenetics core facility. FISH markers for chromosomes X, 7 and 8 were used. 100 cells per tumor section were counted, and aneuploidy was counted for cells containing signals that were greater than the modal number for that chromosome. Five mice per condition were scored for aneuploidy.

Metaphase Spreads

Metaphase spreads were performed by the Molecular Cytogenetics core facility. 50 metaphases were counted per condition.

High-Throughput shRNA Screen

RPE-M cells were transduced with Sigma's shRNA Lentiviral Particle library in 384-well microplates. Cells were induced to express Mad2 with doxycycline for 2 weeks and cells were counted by automated nuclei counting of Hoechst stained nuclei.

Antibody Techniques

Antibodies used were: Mad2 (Clone 48): Mouse, BD Biosciences. BubR1 (A300-995A): Rabbit, Bethyl Laboratories. Actin (A2066): Rabbit, Sigma. Beta-Tubulin (T4026): Mouse, Sigma. TRIP13: Rabbit, Song-Tao Liu lab. p53 (DO-1): Mouse, Santa Cruz Biotechnology. Cleaved Caspase-3 (Asp175) (9661): Rabbit, Cell Signaling Technology. Total H2AX (07-627): Rabbit, EMD Millipore. pSer139 H2AX (JBW301): Mouse, EMD Millipore. Cdc20 (E-7): Mouse, Santa-Cruz. Normal Mouse IgG (sc-2025): Mouse, Santa Cruz Biotechnology. CREST anti-centromere HCT-0100: Human, Immunovision. Alexa Fluor 568 anti-human secondary: Goat, Life Technologies. Alexa Fluor 488 anti-mouse secondary: Goat, Life Technologies.

Immunoprecipitation was performed as described previously(Rodriguez-Bravo et al., 2014). In brief, whole cell extracts were lysed by nitrogen cavitation (2000 psi, 5 min; Parr Instruments) in buffer B (140 mM NaCl, 30 mM HEPES, pH 7.8, 10 mM sodium pyrophosphate, 10 mM NaF, 10 mM PMSF, 0.3 mM sodium orthovanadate, 20 mM b-

glycerophosphate, 1 mM DTT, 1x protease inhibitor cocktail) 300 μg total protein was loaded onto 30 μL Protein G Dynabeads (Fisher) conjugated to 2.5 μg Cdc20 or normal mouse IgG and incubated 2 hours at 4C. Beads were washed 3x with buffer B and eluted in 2x sample buffer at 70C for 10 minutes.

Lysates for Western blot were prepared by resuspending whole cell extracts in lysis buffer (0.5% NP40, 50 mM TRIS HCl pH 7.5, 150 mM NaCl, 1 mM EDTA, 1x complete mini protease inhibitor cocktail (Roche)) for 30 minutes on ice. Histones were extracted from remaining pellet by resuspending in 0.1 M HCl for 30 minutes at room temperature. Proteins were resolved by SDS-PAGE, and then transferred to a PVDF membrane, blocked in Odyssey blocking buffer, and incubated with primary antibodies in Odyssey blocking buffer + 0.05% Tween 20 overnight at 4C. After washing and incubation with IRDye secondary antibodies (in Odyssey blocking buffer), membranes were imaged and quantified on a Li-Cor Odyssey scanner.

Statistical Methods

All statistical analyses were performed using an unpaired two-tailed t test. * denotes $p < 0.05$, ** denotes $p < 0.01$, *** denotes $p < 0.001$, ns denotes not significant.

## BIBLIOGRAPHY


Alfieri, C., Chang, L., Zhang, Z., Yang, J., Maslen, S., Skehel, M., and Barford, D. (2016). Molecular basis of APC/C regulation by the spindle assembly checkpoint. In Nature, pp. 431-436.

Anderson, D.J., Le Moigne, R., Djakovic, S., Kumar, B., Rice, J., Wong, S., Wang, J., Yao, B., Valle, E., Kiss von Soly, S*., et al.* (2015). Targeting the AAA ATPase p97 as an Approach to Treat Cancer through Disruption of Protein Homeostasis. In Cancer Cell, pp. 653-665.

Aravamudhan, P., Goldfarb, A.A., and Joglekar, A.P. (2015). The kinetochore encodes a mechanical switch to disrupt spindle assembly checkpoint signalling. Nat Cell Biol *17*, 868-879.

Banerjee, R., Russo, N., Liu, M., Basrur, V., Bellile, E., Palanisamy, N., Scanlon, C.S., van Tubergen, E., Inglehart, R.C., Metwally, T*., et al.* (2014). TRIP13 promotes error-prone nonhomologous end joining and induces chemoresistance in head and neck cancer. In Nat Commun, pp. 4527.

Barisic, M., Sohm, B., Mikolcevic, P., Wandke, C., Rauch, V., Ringer, T., Hess, M., Bonn, G., and Geley, S. (2010). Spindly/CCDC99 is required for efficient chromosome congression and mitotic checkpoint regulation. In Mol Biol Cell, pp. 1968-1981.

Bian, Y., Kitagawa, R., Bansal, P.K., Fujii, Y., Stepanov, A., and Kitagawa, K. (2014). Synthetic genetic array screen identifies PP2A as a therapeutic target in Mad2-overexpressing tumors. In Proc Natl Acad Sci USA, pp. 1628-1633.

Boersma, V., Moatti, N., Segura-Bayona, S., Peuscher, M.H., van der Torre, J., Wevers, B.A., Orthwein, A., Durocher, D., and Jacobs, J.J.L. (2015). MAD2L2 controls DNA repair at telomeres and DNA breaks by inhibiting 5' end resection. In Nature, pp. 537-540.

Burton, J.L., and Solomon, M.J. (2007). Mad3p, a pseudosubstrate inhibitor of APCCdc20 in the spindle assembly checkpoint. Genes Dev *21*, 655-667.

Campbell, M.S., Chan, G.K., and Yen, T.J. (2001). Mitotic checkpoint proteins HsMAD1 and HsMAD2 are associated with nuclear pore complexes in interphase. J Cell Sci *114*, 953-963.

Carter, S.L., Eklund, A.C., Kohane, I.S., Harris, L.N., and Szallasi, Z. (2006). A signature of chromosomal instability inferred from gene expression profiles predicts clinical outcome in multiple human cancers. In Nat Genet, pp. 1043-1048.

Cerami, E., Gao, J., Dogrusoz, U., Gross, B.E., Sumer, S.O., Aksoy, B.A., Jacobsen, A., Byrne, C.J., Heuer, M.L., Larsson, E.*, et al.* (2012). The cBio cancer genomics portal: an open platform for exploring multidimensional cancer genomics data. In Cancer Discov, pp. 401-404.

Cheeseman, I.M., Chappie, J.S., Wilson-Kubalek, E.M., and Desai, A. (2006). The conserved KMN network constitutes the core microtubule-binding site of the kinetochore. Cell *127*, 983-997.

Choi, E., Zhang, X., Xing, C., and Yu, H. (2016). Mitotic Checkpoint Regulators Control Insulin Signaling and Metabolic Homeostasis. Cell *166*, 567-581.

Ciferri, C., Pasqualato, S., Screpanti, E., Varetti, G., Santaguida, S., Dos Reis, G., Maiolica, A., Polka, J., De Luca, J.G., De Wulf, P.*, et al.* (2008). Implications for kinetochore-microtubule attachment from the structure of an engineered Ndc80 complex. Cell *133*, 427-439.

Crasta, K., Ganem, N.J., Dagher, R., Lantermann, A.B., Ivanova, E.V., Pan, Y., Nezi, L., Protopopov, A., Chowdhury, D., and Pellman, D. (2012). DNA breaks and chromosome pulverization from errors in mitosis. In Nature.

Date, D.A., Burrows, A.C., Venere, M., Jackson, M.W., and Summers, M.K. (2013). Coordinated regulation of p31(Comet) and Mad2 expression is required for cellular proliferation. In Cell Cycle.

Davenport, J., Harris, L.D., and Goorha, R. (2006). Spindle checkpoint function requires Mad2-dependent Cdc20 binding to the Mad3 homology domain of BubR1. Exp Cell Res *312*, 1831-1842.

Davoli, T., and de Lange, T. (2012). Telomere-driven tetraploidization occurs in human cells undergoing crisis and promotes transformation of mouse cells. Cancer Cell *21*, 765-776.

Dawson, I.A., Roth, S., and Artavanis-Tsakonas, S. (1995). The Drosophila cell cycle gene fizzy is required for normal degradation of cyclins A and B during mitosis and has homology to the CDC20 gene of Saccharomyces cerevisiae. J Cell Biol *129*, 725-737.

De Antoni, A., Pearson, C.G., Cimini, D., Canman, J.C., Sala, V., Nezi, L., Mapelli, M., Sironi, L., Faretta, M., Salmon, E.D.*, et al.* (2005). The Mad1/Mad2 complex as a template for Mad2 activation in the spindle assembly checkpoint. In Curr Biol, pp. 214-225.

de Lange, J., Faramarz, A., Oostra, A.B., de Menezes, R.X., van der Meulen, I.H., Rooimans, M.A., Rockx, D.A., Brakenhoff, R.H., van Beusechem, V.W., King, R.W.*, et al.*

(2015). Defective sister chromatid cohesion is synthetically lethal with impaired APC/C function. In Nat Commun, pp. 8399.

DeLuca, J.G., Gall, W.E., Ciferri, C., Cimini, D., Musacchio, A., and Salmon, E.D. (2006). Kinetochore microtubule dynamics and attachment stability are regulated by Hec1. Cell *127*, 969-982.

Diaz-Rodríguez, E., Sotillo, R., Schvartzman, J.-M., and Benezra, R. (2008). Hec1 overexpression hyperactivates the mitotic checkpoint and induces tumor formation in vivo. In Proc Natl Acad Sci USA, pp. 16719-16724.

Ditchfield, C., Johnson, V.L., Tighe, A., Ellston, R., Haworth, C., Johnson, T., Mortlock, A., Keen, N., and Taylor, S.S. (2003). Aurora B couples chromosome alignment with anaphase by targeting BubR1, Mad2, and Cenp-E to kinetochores. J Cell Biol *161*, 267-280.

Dobles, M., Liberal, V., Scott, M.L., Benezra, R., and Sorger, P.K. (2000). Chromosome missegregation and apoptosis in mice lacking the mitotic checkpoint protein Mad2. In Cell, pp. 635-645.

Duijf, P.H., Schultz, N., and Benezra, R. (2013). Cancer cells preferentially lose small chromosomes. Int J Cancer *132*, 2316-2326.

Emanuele, M.J., Lan, W., Jwa, M., Miller, S.A., Chan, C.S., and Stukenberg, P.T. (2008). Aurora B kinase and protein phosphatase 1 have opposing roles in modulating kinetochore assembly. J Cell Biol *181*, 241-254.

Espert, A., Uluocak, P., Bastos, R.N., Mangat, D., Graab, P., and Gruneberg, U. (2014). PP2A-B56 opposes Mps1 phosphorylation of Knl1 and thereby promotes spindle assembly checkpoint silencing. J Cell Biol *206*, 833-842.

Eytan, E., Wang, K., Miniowitz-Shemtov, S., Sitry-Shevah, D., Kaisari, S., Yen, T.J., Liu, S.-T., and Hershko, A. (2014). Disassembly of mitotic checkpoint complexes by the joint action of the AAA-ATPase TRIP13 and p31comet. In Proc Natl Acad Sci USA.

Fang, G. (2002). Checkpoint protein BubR1 acts synergistically with Mad2 to inhibit anaphase-promoting complex. Mol Biol Cell *13*, 755-766.

Fava, L.L., Kaulich, M., Nigg, E.A., and Santamaria, A. (2011). Probing the in vivo function of Mad1:C-Mad2 in the spindle assembly checkpoint. In EMBO J.

Foley, E.A., Maldonado, M., and Kapoor, T.M. (2011). Formation of stable attachments between kinetochores and microtubules depends on the B56-PP2A phosphatase. In Nat Cell Biol, pp. 1265-1271.

Fong, C.S., Mazo, G., Das, T., Goodman, J., Kim, M., O'Rourke, B.P., Izquierdo, D., and Tsou, M.-F.B. (2016). 53BP1 and USP28 mediate p53-dependent cell cycle arrest in response to centrosome loss and prolonged mitosis. In Elife.

Fraschini, R., Beretta, A., Sironi, L., Musacchio, A., Lucchini, G., and Piatti, S. (2001). Bub3 interaction with Mad2, Mad3 and Cdc20 is mediated by WD40 repeats and does not require intact kinetochores. EMBO J *20*, 6648-6659.

Fujiwara, T., Bandi, M., Nitta, M., Ivanova, E.V., Bronson, R.T., and Pellman, D. (2005). Cytokinesis failure generating tetraploids promotes tumorigenesis in p53-null cells. Nature *437*, 1043-1047.

Gao, J., Aksoy, B.A., Dogrusoz, U., Dresdner, G., Gross, B., Sumer, S.O., Sun, Y., Jacobsen, A., Sinha, R., Larsson, E.*, et al.* (2013). Integrative analysis of complex cancer genomics and clinical profiles using the cBioPortal. In Sci Signal, pp. pl1.

Gascoigne, K.E., and Taylor, S.S. (2008). Cancer cells display profound intra- and interline variation following prolonged exposure to antimitotic drugs. In Cancer Cell, pp. 111-122.

Gassmann, R., Holland, A.J., Varma, D., Wan, X., Civril, F., Cleveland, D.W., Oegema, K., Salmon, E.D., and Desai, A. (2010). Removal of Spindly from microtubule-attached kinetochores controls spindle checkpoint silencing in human cells. In Genes Dev, pp. 957-971.

Glotzer, M., Murray, A.W., and Kirschner, M.W. (1991). Cyclin is degraded by the ubiquitin pathway. Nature *349*, 132-138.

Griffis, E.R., Stuurman, N., and Vale, R.D. (2007). Spindly, a novel protein essential for silencing the spindle assembly checkpoint, recruits dynein to the kinetochore. In J Cell Biol, pp. 1005-1015.

Habu, T., Kim, S.H., Weinstein, J., and Matsumoto, T. (2002). Identification of a MAD2-binding protein, CMT2, and its role in mitosis. In EMBO J, pp. 6419-6428.

Haering, C.H., Farcas, A.M., Arumugam, P., Metson, J., and Nasmyth, K. (2008). The cohesin ring concatenates sister DNA molecules. Nature *454*, 297-301.

Halbert, C.L., Demers, G.W., and Galloway, D.A. (1992). The E6 and E7 genes of human papillomavirus type 6 have weak immortalizing activity in human epithelial cells. In J Virol, pp. 2125-2134.

Han, J.S., Holland, A.J., Fachinetti, D., Kulukian, A., Cetin, B., and Cleveland, D.W. (2013). Catalytic Assembly of the Mitotic Checkpoint Inhibitor BubR1-Cdc20 by a Mad2-Induced Functional Switch in Cdc20. In Mol Cell.

Han, J.S., Vitre, B., Fachinetti, D., and Cleveland, D.W. (2014). Bimodal activation of BubR1 by Bub3 sustains mitotic checkpoint signaling. Proc Natl Acad Sci U S A *111*, E4185-4193.

Hanahan, D., and Weinberg, R.A. (2011). Hallmarks of cancer: the next generation. In Cell, pp. 646-674.

Hanks, S., Coleman, K., Reid, S., Plaja, A., Firth, H., Fitzpatrick, D., Kidd, A., Mehes, K., Nash, R., Robin, N.*, et al.* (2004). Constitutional aneuploidy and cancer predisposition caused by biallelic mutations in BUB1B. Nat Genet *36*, 1159-1161.

Hanson, P.I., and Whiteheart, S.W. (2005). AAA+ proteins: have engine, will work. In Nat Rev Mol Cell Biol, pp. 519-529.

Hauf, S., Cole, R.W., LaTerra, S., Zimmer, C., Schnapp, G., Walter, R., Heckel, A., van Meel, J., Rieder, C.L., and Peters, J.M. (2003). The small molecule Hesperadin reveals a role for Aurora B in correcting kinetochore-microtubule attachment and in maintaining the spindle assembly checkpoint. J Cell Biol *161*, 281-294.

Hayashi, M.T., Cesare, A.J., Fitzpatrick, J.A.J., Lazzerini-Denchi, E., and Karlseder, J. (2012). A telomere-dependent DNA damage checkpoint induced by prolonged mitotic arrest. In Nat Struct Mol Biol.

Hernando, E., Nahlé, Z., Juan, G., Diaz-Rodriguez, E., Alaminos, M., Hemann, M., Michel, L., Mittal, V., Gerald, W., Benezra, R.*, et al.* (2004). Rb inactivation promotes genomic instability by uncoupling cell cycle progression from mitotic control. In Nature, pp. 797-802.

Hernando, E., Orlow, I., Liberal, V., Nohales, G., Benezra, R., and Cordon-Cardo, C. (2001). Molecular analyses of the mitotic checkpoint components hsMAD2, hBUB1 and hBUB3 in human cancer. In Int J Cancer, pp. 223-227.

Hewitt, L., Tighe, A., Santaguida, S., White, A.M., Jones, C.D., Musacchio, A., Green, S., and Taylor, S.S. (2010). Sustained Mps1 activity is required in mitosis to recruit O-Mad2 to the Mad1-C-Mad2 core complex. In J Cell Biol, pp. 25-34.

Hinchcliffe, E.H., Day, C.A., Karanjeet, K.B., Fadness, S., Langfald, A., Vaughan, K.T., and Dong, Z. (2016). Chromosome missegregation during anaphase triggers p53 cell cycle arrest through histone H3.3 Ser31 phosphorylation. In Nat Cell Biol, pp. 668-675.

Hiruma, Y., Sacristan, C., Pachis, S.T., Adamopoulos, A., Kuijt, T., Ubbink, M., von Castelmur, E., Perrakis, A., and Kops, G.J. (2015). CELL DIVISION CYCLE. Competition between MPS1 and microtubules at kinetochores regulates spindle checkpoint signaling. Science *348*, 1264-1267.

Hornig, N.C., Knowles, P.P., McDonald, N.Q., and Uhlmann, F. (2002). The dual mechanism of separase regulation by securin. Curr Biol *12*, 973-982.

Howell, B.J., McEwen, B.F., Canman, J.C., Hoffman, D.B., Farrar, E.M., Rieder, C.L., and Salmon, E.D. (2001). Cytoplasmic dynein/dynactin drives kinetochore protein transport to the spindle poles and has a role in mitotic spindle checkpoint inactivation. In J Cell Biol, pp. 1159-1172.

Howell, B.J., Moree, B., Farrar, E.M., Stewart, S., Fang, G., and Salmon, E.D. (2004). Spindle checkpoint protein dynamics at kinetochores in living cells. In Curr Biol, pp. 953-964.

Hoyt, M.A., Totis, L., and Roberts, B.T. (1991). S. cerevisiae genes required for cell cycle arrest in response to loss of microtubule function. Cell *66*, 507-517.

Iwanaga, Y., Chi, Y.-H., Miyazato, A., Sheleg, S., Haller, K., Peloponese, J.-M., Li, Y., Ward, J.M., Benezra, R., and Jeang, K.-T. (2007). Heterozygous deletion of mitotic arrest-deficient protein 1 (MAD1) increases the incidence of tumors in mice. In Cancer Res, pp. 160-166.

Izawa, D., and Pines, J. (2014). The mitotic checkpoint complex binds a second CDC20 to inhibit active APC/C. In Nature.

Janssen, A., van der Burg, M., Szuhai, K., Kops, G.J.P.L., and Medema, R.H. (2011). Chromosome segregation errors as a cause of DNA damage and structural chromosome aberrations. In Science, pp. 1895-1898.

Ji, Z., Gao, H., and Yu, H. (2015). CELL DIVISION CYCLE. Kinetochore attachment sensed by competitive Mps1 and microtubule binding to Ndc80C. Science *348*, 1260-1264.

Kabeche, L., and Compton, D.A. (2012). Checkpoint-Independent Stabilization of Kinetochore-Microtubule Attachments by Mad2 in Human Cells. In Curr Biol.

Kaisari, S., Sitry-Shevah, D., Miniowitz-Shemtov, S., and Hershko, A. (2016). Intermediates in the assembly of mitotic checkpoint complexes and their role in the regulation of the anaphase-promoting complex. In Proc Natl Acad Sci USA.

Kessler, J.D., Kahle, K.T., Sun, T., Meerbrey, K.L., Schlabach, M.R., Schmitt, E.M., Skinner, S.O., Xu, Q., Li, M.Z., Hartman, Z.C.*, et al.* (2012). A SUMOylation-dependent transcriptional subprogram is required for Myc-driven tumorigenesis. In Science, pp. 348-353.

Knowlton, A.L., Lan, W., and Stukenberg, P.T. (2006). Aurora B is enriched at merotelic attachment sites, where it regulates MCAK. In Curr Biol, pp. 1705-1710.

Kops, G.J., Kim, Y., Weaver, B.A., Mao, Y., McLeod, I., Yates, J.R., 3rd, Tagaya, M., and Cleveland, D.W. (2005). ZW10 links mitotic checkpoint signaling to the structural kinetochore. J Cell Biol *169*, 49-60.

Lambrus, B.G., Daggubati, V., Uetake, Y., Scott, P.M., Clutario, K.M., Sluder, G., and Holland, A.J. (2016). A USP28-53BP1-p53-p21 signaling axis arrests growth after centrosome loss or prolonged mitosis. J Cell Biol *214*, 143-153.

Lampson, M.A., Renduchitala, K., Khodjakov, A., and Kapoor, T.M. (2004). Correcting improper chromosome-spindle attachments during cell division. Nat Cell Biol *6*, 232-237.

Lee, J.W., Choi, H.S., Gyuris, J., Brent, R., and Moore, D.D. (1995). Two classes of proteins dependent on either the presence or absence of thyroid hormone for interaction with the thyroid hormone receptor. In Mol Endocrinol, pp. 243-254.

Li, R., and Murray, A.W. (1991). Feedback control of mitosis in budding yeast. Cell *66*, 519-531.

Li, X.C., Li, X., and Schimenti, J.C. (2007). Mouse pachytene checkpoint 2 (trip13) is required for completing meiotic recombination but not synapsis. In PLoS Genet, pp. e130.

Li, Y., and Benezra, R. (1996). Identification of a human mitotic checkpoint gene: hsMAD2. In Science, pp. 246-248.

Li, Y., Gorbea, C., Mahaffey, D., Rechsteiner, M., and Benezra, R. (1997). MAD2 associates with the cyclosome/anaphase-promoting complex and inhibits its activity. In Proc Natl Acad Sci USA, pp. 12431-12436.

Liu, D., Vader, G., Vromans, M.J., Lampson, M.A., and Lens, S.M. (2009). Sensing chromosome bi-orientation by spatial separation of aurora B kinase from kinetochore substrates. Science *323*, 1350-1353.

London, N., and Biggins, S. (2014). Mad1 kinetochore recruitment by Mps1-mediated phosphorylation of Bub1 signals the spindle checkpoint. Genes Dev *28*, 140-152.

London, N., Ceto, S., Ranish, J.A., and Biggins, S. (2012). Phosphoregulation of Spc105 by Mps1 and PP1 regulates Bub1 localization to kinetochores. Curr Biol *22*, 900-906.

Luo, X., Tang, Z., Rizo, J., and Yu, H. (2002). The Mad2 spindle checkpoint protein undergoes similar major conformational changes upon binding to either Mad1 or Cdc20. In Mol Cell, pp. 59-71.

Luo, X., Tang, Z., Xia, G., Wassmann, K., Matsumoto, T., Rizo, J., and Yu, H. (2004). The Mad2 spindle checkpoint protein has two distinct natively folded states. Nat Struct Mol Biol *11*, 338-345.

Ma, H.T., and Poon, R.Y.C. (2011). Orderly Inactivation of the Key Checkpoint Protein Mitotic Arrest Deficient 2 (MAD2) during Mitotic Progression. In J Biol Chem, pp. 13052-13059.

Ma, H.T., and Poon, R.Y.C. (2016). TRIP13 Regulates Both the Activation and Inactivation of the Spindle-Assembly Checkpoint. In Cell Rep, pp. 1086-1099.

Maciejowski, J., George, K.A., Terret, M.-E., Zhang, C., Shokat, K.M., and Jallepalli, P.V. (2010). Mps1 directs the assembly of Cdc20 inhibitory complexes during interphase and mitosis to control M phase timing and spindle checkpoint signaling. In J Cell Biol, pp. 89-100.

Maciejowski, J., Li, Y., Bosco, N., Campbell, P.J., and de Lange, T. (2015). Chromothripsis and Kataegis Induced by Telomere Crisis. Cell *163*, 1641-1654.

Macosko, E.Z., Basu, A., Satija, R., Nemesh, J., Shekhar, K., Goldman, M., Tirosh, I., Bialas, A.R., Kamitaki, N., Martersteck, E.M.*, et al.* (2015). Highly Parallel Genome-wide Expression Profiling of Individual Cells Using Nanoliter Droplets. In Cell, pp. 1202-1214.

Malureanu, L.A., Jeganathan, K.B., Hamada, M., Wasilewski, L., Davenport, J., and van Deursen, J.M. (2009). BubR1 N terminus acts as a soluble inhibitor of cyclin B degradation by APC/C(Cdc20) in interphase. Dev Cell *16*, 118-131.

Manchado, E., Guillamot, M., de Cárcer, G., Eguren, M., Trickey, M., García-Higuera, I., Moreno, S., Yamano, H., Cañamero, M., and Malumbres, M. (2010). Targeting Mitotic Exit Leads to Tumor Regression In Vivo: Modulation by Cdk1, Mastl, and the PP2A/B55α,δ Phosphatase. In Cancer Cell, pp. 641-654.

Mansfeld, J., Collin, P., Collins, M.O., Choudhary, J.S., and Pines, J. (2011). APC15 drives the turnover of MCC-CDC20 to make the spindle assembly checkpoint responsive to kinetochore attachment. In Nat Cell Biol.

Mapelli, M., Massimiliano, L., Santaguida, S., and Musacchio, A. (2007). The Mad2 conformational dimer: structure and implications for the spindle assembly checkpoint. In Cell, pp. 730-743.

Mariani, L., Chiroli, E., Nezi, L., Muller, H., Piatti, S., Musacchio, A., and Ciliberto, A. (2012). Role of the Mad2 Dimerization Interface in the Spindle Assembly Checkpoint Independent of Kinetochores. In Curr Biol.

Menssen, A., Epanchintsev, A., Lodygin, D., Rezaei, N., Jung, P., Verdoodt, B., Diebold, J., and Hermeking, H. (2007). c-MYC delays prometaphase by direct transactivation of MAD2 and BubR1: identification of mechanisms underlying c-MYC-induced DNA damage and chromosomal instability. In Cell Cycle, pp. 339-352.

Meraldi, P., Draviam, V.M., and Sorger, P.K. (2004). Timing and checkpoints in the regulation of mitotic progression. Dev Cell *7*, 45-60.

Michel, L., Diaz-Rodriguez, E., Narayan, G., Hernando, E., Murty, V.V.V.S., and Benezra, R. (2004). Complete loss of the tumor suppressor MAD2 causes premature cyclin B degradation and mitotic failure in human somatic cells. In Proc Natl Acad Sci USA, pp. 4459-4464.

Michel, L.S., Liberal, V., Chatterjee, A., Kirchwegger, R., Pasche, B., Gerald, W., Dobles, M., Sorger, P.K., Murty, V.V., and Benezra, R. (2001). MAD2 haplo-insufficiency causes premature anaphase and chromosome instability in mammalian cells. In Nature, pp. 355-359.

Moyle, M.W., Kim, T., Hattersley, N., Espeut, J., Cheerambathur, D.K., Oegema, K., and Desai, A. (2014). A Bub1-Mad1 interaction targets the Mad1-Mad2 complex to unattached kinetochores to initiate the spindle checkpoint. J Cell Biol *204*, 647-657.

Nelson, C.R., Hwang, T., Chen, P.-H., and Bhalla, N. (2015). TRIP13PCH-2 promotes Mad2 localization to unattached kinetochores in the spindle checkpoint response. In J Cell Biol, pp. 503-516.

Nijenhuis, W., Vallardi, G., Teixeira, A., Kops, G.J., and Saurin, A.T. (2014). Negative feedback at kinetochores underlies a responsive spindle checkpoint signal. Nat Cell Biol *16*, 1257-1264.

Nilsson, J., Yekezare, M., Minshull, J., and Pines, J. (2008). The APC/C maintains the spindle assembly checkpoint by targeting Cdc20 for destruction. In Nat Cell Biol, pp. 1411-1420.

Notta, F., Chan-Seng-Yue, M., Lemire, M., Li, Y., Wilson, G.W., Connor, A.A., Denroche, R.E., Liang, S.B., Brown, A.M., Kim, J.C.*, et al.* (2016). A renewed model of pancreatic cancer evolution based on genomic rearrangement patterns. Nature.

Nurse, P. (1990). Universal control mechanism regulating onset of M-phase. Nature *344*, 503-508.

Overlack, K., Primorac, I., Vleugel, M., Krenn, V., Maffini, S., Hoffmann, I., Kops, G.J., and Musacchio, A. (2015). A molecular basis for the differential roles of Bub1 and BubR1 in the spindle assembly checkpoint. Elife *4*, e05269.

Pei, L., and Melmed, S. (1997). Isolation and characterization of a pituitary tumor-transforming gene (PTTG). Mol Endocrinol *11*, 433-441.

Pfleger, C.M., Lee, E., and Kirschner, M.W. (2001). Substrate recognition by the Cdc20 and Cdh1 components of the anaphase-promoting complex. Genes Dev *15*, 2396-2407.

Pinsky, B.A., Nelson, C.R., and Biggins, S. (2009). Protein phosphatase 1 regulates exit from the spindle checkpoint in budding yeast. Curr Biol *19*, 1182-1187.

Primorac, I., Weir, J.R., Chiroli, E., Gross, F., Hoffmann, I., van Gerwen, S., Ciliberto, A., and Musacchio, A. (2013). Bub3 reads phosphorylated MELT repeats to promote spindle assembly checkpoint signaling. Elife *2*, e01030.

Rieder, C.L., Cole, R.W., Khodjakov, A., and Sluder, G. (1995). The checkpoint delaying anaphase in response to chromosome monoorientation is mediated by an inhibitory signal produced by unattached kinetochores. J Cell Biol *130*, 941-948.

Rodriguez-Bravo, V., Maciejowski, J., Corona, J., Buch, H.K., Collin, P., Kanemaki, M.T., Shah, J.V., and Jallepalli, P.V. (2014). Nuclear pores protect genome integrity by assembling a premitotic and mad1-dependent anaphase inhibitor. In Cell, pp. 1017-1031.

Roig, I., Dowdle, J.A., Toth, A., de Rooij, D.G., Jasin, M., and Keeney, S. (2010). Mouse TRIP13/PCH2 is required for recombination and normal higher-order chromosome structure during meiosis. In PLoS Genet.

Rosenberg, S.C., and Corbett, K.D. (2015). The multifaceted roles of the HORMA domain in cellular signaling. J Cell Biol *211*, 745-755.

Rowald, K., Mantovan, M., Passos, J., Buccitelli, C., Mardin, B.R., Korbel, J.O., Jechlinger, M., and Sotillo, R. (2016). Negative Selection and Chromosome Instability Induced by Mad2 Overexpression Delay Breast Cancer but Facilitate Oncogene-Independent Outgrowth. Cell Rep *15*, 2679-2691.

Rual, J.-F., Venkatesan, K., Hao, T., Hirozane-Kishikawa, T., Dricot, A., Li, N., Berriz, G.F., Gibbons, F.D., Dreze, M., Ayivi-Guedehoussou, N.*, et al.* (2005). Towards a proteome-scale map of the human protein-protein interaction network. In Nature, pp. 1173-1178.

San-Segundo, P.A., and Roeder, G.S. (1999). Pch2 links chromatin silencing to meiotic checkpoint control. In Cell, pp. 313-324.

Santaguida, S., Tighe, A., D'Alise, A.M., Taylor, S.S., and Musacchio, A. (2010). Dissecting the role of MPS1 in chromosome biorientation and the spindle checkpoint through the small molecule inhibitor reversine. In J Cell Biol, pp. 73-87.

Schvartzman, J.-M., Duijf, P.H.G., Sotillo, R., Coker, C., and Benezra, R. (2011). Mad2 Is a Critical Mediator of the Chromosome Instability Observed upon Rb and p53 Pathway Inhibition. In Cancer Cell, pp. 701-714.

Schvartzman, J.-M., Sotillo, R., and Benezra, R. (2010). Mitotic chromosomal instability and cancer: mouse modelling of the human disease. In Nat Rev Cancer, pp. 102-115.

Schwab, M., Neutzner, M., Mocker, D., and Seufert, W. (2001). Yeast Hct1 recognizes the mitotic cyclin Clb2 and other substrates of the ubiquitin ligase APC. EMBO J *20*, 5165-5175.

Schweizer, N., Ferrás, C., Kern, D.M., Logarinho, E., Cheeseman, I.M., and Maiato, H. (2013). Spindle assembly checkpoint robustness requires Tpr-mediated regulation of Mad1/Mad2 proteostasis. In J Cell Biol.

Shepperd, L.A., Meadows, J.C., Sochaj, A.M., Lancaster, T.C., Zou, J., Buttrick, G.J., Rappsilber, J., Hardwick, K.G., and Millar, J.B. (2012). Phosphodependent recruitment of Bub1 and Bub3 to Spc7/KNL1 by Mph1 kinase maintains the spindle checkpoint. Curr Biol *22*, 891-899.

Silió, V., McAinsh, A.D., and Millar, J.B. (2015). KNL1-Bubs and RZZ Provide Two Separable Pathways for Checkpoint Activation at Human Kinetochores. In Dev Cell, pp. 600-613.

Sotillo, R., Hernando, E., Díaz-Rodríguez, E., Teruya-Feldstein, J., Cordón-Cardo, C., Lowe, S.W., and Benezra, R. (2007). Mad2 overexpression promotes aneuploidy and tumorigenesis in mice. In Cancer Cell, pp. 9-23.

Sotillo, R., Schvartzman, J.-M., Socci, N.D., and Benezra, R. (2010). Mad2-induced chromosome instability leads to lung tumour relapse after oncogene withdrawal. In Nature, pp. 436-440.

Stelzl, U., Worm, U., Lalowski, M., Haenig, C., Brembeck, F.H., Goehler, H., Stroedicke, M., Zenkner, M., Schoenherr, A., Koeppen, S*., et al.* (2005). A human protein-protein interaction network: a resource for annotating the proteome. In Cell, pp. 957-968.

Stephens, P.J., Greenman, C.D., Fu, B., Yang, F., Bignell, G.R., Mudie, L.J., Pleasance, E.D., Lau, K.W., Beare, D., Stebbings, L.A*., et al.* (2011). Massive genomic rearrangement acquired in a single catastrophic event during cancer development. In Cell, pp. 27-40.

Sudakin, V., Chan, G.K., and Yen, T.J. (2001). Checkpoint inhibition of the APC/C in HeLa cells is mediated by a complex of BUBR1, BUB3, CDC20, and MAD2. In J Cell Biol, pp. 925-936.

Suijkerbuijk, S.J.E., Vleugel, M., Teixeira, A., and Kops, G.J.P.L. (2012). Integration of Kinase and Phosphatase Activities by BUBR1 Ensures Formation of Stable Kinetochore-Microtubule Attachments. In Dev Cell, pp. 745-755.

Suzuki, H., Kaizuka, T., Mizushima, N., and Noda, N.N. (2015). Structure of the Atg101-Atg13 complex reveals essential roles of Atg101 in autophagy initiation. In Nat Struct Mol Biol.

Tang, Z., Bharadwaj, R., Li, B., and Yu, H. (2001). Mad2-Independent inhibition of APCCdc20 by the mitotic checkpoint protein BubR1. Dev Cell *1*, 227-237.

Teichner, A., Eytan, E., Sitry-Shevah, D., Miniowitz-Shemtov, S., Dumin, E., Gromis, J., and Hershko, A. (2011). p31comet promotes disassembly of the mitotic checkpoint complex in an ATP-dependent process. In Proc Natl Acad Sci USA.

Tighe, A., Johnson, V.L., Albertella, M., and Taylor, S.S. (2001). Aneuploid colon cancer cells have a robust spindle checkpoint. In EMBO Rep, pp. 609-614.

Tipton, A.R., Tipton, M., Yen, T., and Liu, S.-T. (2011). Closed MAD2 (C-MAD2) is selectively incorporated into the mitotic checkpoint complex (MCC). In Cell Cycle.

Tipton, A.R., Wang, K., Oladimeji, P., Sufi, S., Gu, Z., and Liu, S.-T. (2012). Identification of novel mitosis regulators through data mining with human centromere/kinetochore proteins as group queries. In BMC Cell Biol, pp. 15.

Uhlmann, F., Lottspeich, F., and Nasmyth, K. (1999). Sister-chromatid separation at anaphase onset is promoted by cleavage of the cohesin subunit Scc1. Nature *400*, 37-42.

Uzunova, K., Dye, B.T., Schutz, H., Ladurner, R., Petzold, G., Toyoda, Y., Jarvis, M.A., Brown, N.G., Poser, I., Novatchkova, M.*, et al.* (2012). APC15 mediates CDC20 autoubiquitylation by APC/C(MCC) and disassembly of the mitotic checkpoint complex. In Nat Struct Mol Biol.

Vanoosthuyse, V., and Hardwick, K.G. (2009). A novel protein phosphatase 1-dependent spindle checkpoint silencing mechanism. Curr Biol *19*, 1176-1181.
Varetti, G., Guida, C., Santaguida, S., Chiroli, E., and Musacchio, A. (2011). Homeostatic control of mitotic arrest. In Mol Cell, pp. 710-720.

Vigneron, S., Prieto, S., Bernis, C., Labbe, J.C., Castro, A., and Lorca, T. (2004). Kinetochore localization of spindle checkpoint proteins: who controls whom? Mol Biol Cell *15*, 4584-4596.

Vogel, C., Kienitz, A., Hofmann, I., Müller, R., and Bastians, H. (2004). Crosstalk of the mitotic spindle assembly checkpoint with p53 to prevent polyploidy. In Oncogene, pp. 6845-6853.

Wang, K., Sturt-Gillespie, B., Hittle, J.C., Macdonald, D., Chan, G.K., Yen, T.J., and Liu, S.-T. (2014). Thyroid Hormone Receptor Interacting Protein 13 (TRIP13) AAA-ATPase is a Novel Mitotic Checkpoint Silencing Protein. In J Biol Chem.

Weaver, B.A.A., Silk, A.D., Montagna, C., Verdier-Pinard, P., and Cleveland, D.W. (2007). Aneuploidy acts both oncogenically and as a tumor suppressor. In Cancer Cell, pp. 25-36.

Wei, R.R., Al-Bassam, J., and Harrison, S.C. (2007). The Ndc80/HEC1 complex is a contact point for kinetochore-microtubule attachment. Nat Struct Mol Biol *14*, 54-59.

Westhorpe, F.G., Tighe, A., Lara-Gonzalez, P., and Taylor, S.S. (2011). p31comet-mediated extraction of Mad2 from the MCC promotes efficient mitotic exit. In J Cell Sci.

Williams, B.R., Prabhu, V.R., Hunter, K.E., Glazier, C.M., Whittaker, C.A., Housman, D.E., and Amon, A. (2008). Aneuploidy affects proliferation and spontaneous immortalization in mammalian cells. In Science, pp. 703-709.

Wojcik, E., Basto, R., Serr, M., Scaerou, F., Karess, R., and Hays, T. (2001). Kinetochore dynein: its dynamics and role in the transport of the Rough deal checkpoint protein. Nat Cell Biol *3*, 1001-1007.

Wojtasz, L., Daniel, K., Roig, I., Bolcun-Filas, E., Xu, H., Boonsanay, V., Eckmann, C.R., Cooke, H.J., Jasin, M., Keeney, S.*, et al.* (2009). Mouse HORMAD1 and HORMAD2, two conserved meiotic chromosomal proteins, are depleted from synapsed chromosome axes with the help of TRIP13 AAA-ATPase. In PLoS Genet, pp. e1000702.

Xia, G., Luo, X., Habu, T., Rizo, J., Matsumoto, T., and Yu, H. (2004). Conformation-specific binding of p31(comet) antagonizes the function of Mad2 in the spindle checkpoint. In EMBO J, pp. 3133-3143.

Xu, G., Chapman, J.R., Brandsma, I., Yuan, J., Mistrik, M., Bouwman, P., Bartkova, J., Gogola, E., Warmerdam, D., Barazas, M.*, et al.* (2015). REV7 counteracts DNA double-strand break resection and affects PARP inhibition. In Nature, pp. 541-544.

Yamagishi, Y., Yang, C.H., Tanno, Y., and Watanabe, Y. (2012). MPS1/Mph1 phosphorylates the kinetochore protein KNL1/Spc7 to recruit SAC components. Nat Cell Biol *14*, 746-752.

Yamaguchi, M., VanderLinden, R., Weissmann, F., Qiao, R., Dube, P., Brown, N.G., Haselbach, D., Zhang, W., Sidhu, S.S., Peters, J.-M*., et al.* (2016). Cryo-EM of Mitotic Checkpoint Complex-Bound APC/C Reveals Reciprocal and Conformational Regulation of Ubiquitin Ligation. In Mol Cell, pp. 593-607.

Yang, M., Li, B., Tomchick, D.R., Machius, M., Rizo, J., Yu, H., and Luo, X. (2007). p31comet blocks Mad2 activation through structural mimicry. In Cell, pp. 744-755.

Ye, Q., Rosenberg, S.C., Moeller, A., Speir, J.A., Su, T.Y., and Corbett, K.D. (2015). TRIP13 is a protein-remodeling AAA+ ATPase that catalyzes MAD2 conformation switching. In Elife.

Yim, E.-K., and Park, J.-S. (2005). The role of HPV E6 and E7 oncoproteins in HPV-associated cervical carcinogenesis. In Cancer Res Treat, pp. 319-324.

Zhang, C.Z., Spektor, A., Cornils, H., Francis, J.M., Jackson, E.K., Liu, S., Meyerson, M., and Pellman, D. (2015a). Chromothripsis from DNA damage in micronuclei. Nature *522*, 179-184.

Zhang, G., Lischetti, T., Hayward, D.G., and Nilsson, J. (2015b). Distinct domains in Bub1 localize RZZ and BubR1 to kinetochores to regulate the checkpoint. Nat Commun *6*, 7162.

Zhou, H.-J., Wang, J., Yao, B., Wong, S., Djakovic, S., Kumar, B., Rice, J., Valle, E., Soriano, F., Menon, M.-K*., et al.* (2015). Discovery of a First-in-Class, Potent, Selective, and Orally Bioavailable Inhibitor of the p97 AAA ATPase (CB-5083). In J Med Chem, pp. 9480-9497.

Zhu, T., Dou, Z., Qin, B., Jin, C., Wang, X., Xu, L., Wang, Z., Zhu, L., Liu, F., Gao, X*., et al.* (2013). Phosphorylation of Microtubule-binding Protein Hec1 by Mitotic Kinase Aurora B Specifies Spindle Checkpoint Kinase Mps1 Signaling at the Kinetochore. In J Biol Chem, pp. 36149-36159.

Zou, H., McGarry, T.J., Bernal, T., and Kirschner, M.W. (1999). Identification of a vertebrate sister-chromatid separation inhibitor involved in transformation and tumorigenesis. Science *285*, 418-422.